DIELECTRIC RECOVERY OF SHORT A-C. ARCS BETWEEN LOW-BOILING-POINT ELECTRODES

Thesis by

Thomas Everett Browne, Jr.

In Partial Fulfillment of the Requirements

for the Degree of Doctor of Philosophy

California Institute of Technology,

Pasadena, California,

1936.

TABLE OF CONTENTS

TABLE OF CONTENTS, Continued

SUMMARY

The re-ignition characteristics (variation of re-ignition voltage with time after current zero) of short alternating-current arcs between plane brass electrodes in air were studied by observing the average re-ignition voltages on the screen of a cathode-ray oscilloscope and controlling the rates of rise of voltage by varying the shunting capacitance and hence the natural period of oscillation of the reactors used to limit the current. The shape of these characteristics and the effects on them of varying the electrode separation, air pressure, and current strength were determined.

The results show that short arc spaces recover dielectric strength in two distinct stages. The first stage agrees in shape and magnitude with a previously developed theory that all voltage is concentrated across a partially deionized space charge layer which increases its breakdown voltage with diminishing density of ionization in the field-free space. The second stage appears to follow complete deionization by the electric field due to displacement of the field-free region by the space charge layer, its magnitude and shape appearing to be due simply to increase in gas density due to cooling. Temperatures calculated from this second stage and ion densities determined from the first stage by means of the space charge equation and an extrapolation of the temperature

curve are consistent with recent measurements of arc values by other methods. Analysis of the decrease with time of the apparent ion density shows that diffusion alone is adequate to explain the results and that volume recombination is not. The effects on the characteristics of variations in the parameters investigated are found to be in accord with previous results and with the theory, if deionization mainly by diffusion be assumed.

DIELECTRIC RECOVERY OF SHORT A-C. ARCS BETWEEN LOW-BOILING-POINT ELECTRODES

I. INTRODUCTION

It has long been known [1] that short alternating-current arcs between electrodes of such low-boiling-point materials as brass, zinc, or cadmium are much more difficult to maintain than are arcs between electrodes of the more commonly used high-boiling-point materials, such as copper, iron, or carbon. In fact, the earliest investigator [1] of this effect designated the former class of materials as "non-arcing metals". Such metals were employed as electrodes in the multigap type of lightning arrester which made use of their "non-arcing" property to interrupt the flow of power current following a discharge.

More recent investigations of short metal-electrode A-C. arcs[2,3,4] have shown more exactly the magnitude of this effect

---

(1) Wurts, "Lightning Arresters", Trans. A.I.E.E. 9, p. 102 (1892).

(2) Todd and Browne, "Extinction of Short A-C. Arcs between Brass Electrodes" and "Restriking ofShort A-C. Arcs", Physical Review, 36, pp. 726-737 (1930).

(3) Browne, "Extinction of Short A-C. Arcs", Trans. A.I.E.E., 50, p. 1461 (1931).

(4) Slepian and STrom, "Arcs in Low-Voltage A-C. Networks", Trans. A.I.E.E., 50, p. 847 (1931).

and its dependence on the boiling temperature of the electrode surfaces and upon electrode separation. Within limits, the "non-arcing" property was found to increase as the arc length and the electrode boiling temperature diminished. The purpose of this investigation has been to explore this effect more in detail in hope of further clarifying both it and the general theory of the re-ignition or extinction of a short A-C. arc. Specifically, the effects on the "arc re-ignition characteristic" (curve of re-ignition voltage vs. time after current zero) of varying such conditions as electrode separation, arc current, and gas pressure have been investigated.

The engineer is generally interested in this subject from a negative standpoint, desiring to know how arcs, usually at atmospheric pressure, may be prevented from re-igniting, since in engineering experience arcs usually occur during the opening of a circuit by a switch or as a result of insulation failure or flash-over. As pointed out some years ago by Slepian(5), the re-ignition or extinction of an A-C. arc following a moment of zero current depends upon the outcome of "a kind of race" between two apposing quantities: (1) the voltage applied to the arc terminals by the circuit, and (2), the "dielectric strength" of the arc space, or voltage required to re-ignite the arc. Both are functions of time after current zero. The recovery of voltage across the arc

---

(5) Slepian, "Extinction of an A-C. Arc", Trans. A.I.E.E., 47, p. 1398 (1928).

terminals depends mainly upon the characteristics of the circuit and so can, at least in simple cases, be calculated by well-known principles. The dielectric recovery of the arc space, however, cannot be accurately predicted even in principle, depending as it does upon relatively complex phenomena associated with the arc itself. Consequently the obtaining of further empirical knowledge of arc re-ignition characteristics seems to be desirable from a practical as well as from a theoretical point of view.

II. THEORY

1. Arc Re-ignition. An alternating-current arc differs from a direct-current arc in that it essentially ceases to exist, or "goes out", twice during each cycle as the current passes through its zero value. Following each current zero, then, the arc must be re-ignited with current flow reversed, the electrode formerly the anode becoming the cathode and vice versa. In arcs with thermionic cathodes, both electrodes seem to be hot enough for adequate thermionic emission and remain so during the very brief current-zero period. Therefore, the voltage required to re-ignite the arc in the new direction is little if any greater than its normal burning voltage(2). Arcs between electrodes of such refractory materials as carbon and tungsten are of this type. With most other electrodes, however, the temperature of the cathode surface is limited by boiling of the electrode material (or in special cases by motion of the arc terminals) to a value far too low for appreciable thermionic emission. For these arcs some mechanism other than thermionic emission must therefore be responsible for the production of the electrons at the cathode. The commonly accepted theory is that the electrons are pulled out of the cathode by the action of a very high field of the order of 10^6 volts per centimeter or more resulting from a very dense space charge sheath of positive ions(6). An alternative

---

(6) Langmuir, "Positive Ion Currents in the Positive Column of the Mercury Arc", G. E. Review, 26, p. 735 (1923).

theory is that the high energy input into the gas layer adjacent to the cathode surface results in thermal ionization of this layer, all of the electrons coming from the "cathode spot" originating here and all of the current to the cathode being carried by positive ions(7). Either of these two theories of the "cold cathode" of an arc requires a very high current density and therefore a high density of ionization at and of energy input to the cathode layer. Consequently, by either theory the requisite conditions for the existence of an arc cathode must disappear with extreme rapidity upon cessation of the sustaining current. In any case, they should not be present initially at the incoming cathode, which was the anode just before current zero. In the absence, then, of thermionic emission or of other extraneous ionizing agents, the re-ignition of an A-C. arc between closely spaced electrodes must be entirely similar to the ordinary breakdown of a spark gap, except that in this case the gas between the electrodes is already considerably ionized as a result of the previous half-cycle of arcing. The re-ignition of an A-C. arc was first analysed in this way by Slepian(5), who proceeded on this basis to derive an approximate expression for the arc re-ignition voltage as a function of time. The theory described below is essentially his.

2. Space Charge Formation. The spark breakdown of an initially ionized gas between plane parallel electrodes differs

---

(7) Slepian, "Theory of Current Transference at the Cathode of an Arc", Phys. Rev. 27, p. 407 (1926).

markedly from the breakdown of a normal unionized gas chiefly because of the extreme distortion of the electric field by the presence of the ions. The gas initially contains almost equal numbers per cm.^{3} of positive and negative ions, the negative ions being mainly electrons at the temperature existing in the arc core at atmospheric pressure. Thus, there is no initial net charge density, or "space charge", so long as there is no applied voltage. When a potential difference appears between the electrodes the ions move under the influence of the resulting electric field. Because of their very much smaller mass (thousands of times) the motion of the electrons is so much more rapid than that of the positive ions that the motion of the latter may be completely neglected during the first few micro-seconds under consideration, at least as a first approximation. At the new cathode the electrons are repelled, leaving behind a region occupied only by the relatively stationary positive ions, and, therefore, being now a region of net positive charge. Because of this space charge a high, non-uniform gradient, obtainable by integration of Poisson's equation, exists in the space, having a maximum value at the cathode surface and a minimum value at the outer boundary of the space charge region. The electrons will continue to move, causing the space charge boundary to recede from the cathode, until all of the applied voltage is impressed across the "space charge sheath" and the gradient at its far boundary is

therefore reduced to zero. Calculation of the thickness of this sheath in terms of the applied voltage and the density of positive charge is a simple electrostatic problem. Only slightly less simple is the calculation for steady-state conditions, considering also the motion of the positive ions. Within the space charge region the ions move with a velocity proportional to the field (assuming its thickness to be large compared with the ionic mean free path) from its outer boundary to the cathode surface. Since the field outside of the region is zero, ions reach the outer boundary only by diffusion, at a rate given by :

$$\gamma = \frac{1}{4} n \bar{c} \qquad (1)$$

where γ is the number crossing a square centimeter of the surface per second, n is the ion density just outside the region, and $\bar{c}$ is the average velocity of thermal agitation of the ions. The current density flowing across the sheath is thus:

$$i = \frac{1}{4} n e \bar{c} \qquad (2)$$

where e is the electronic charge, assuming singly charged ions. The equation for the thickness of the space charge sheath under these conditions is:

$$i = \frac{9}{32 \pi} k \frac{V^2}{d^3} \qquad (3)$$

as first derived by Aston(8).

In this equation V is the potential difference applied, k is the ion mobility (ratio of ion velocity to field strength), and

---

(8) Aston, "Experiments on the Length of the Cathode Dark Space with Varying Current Densities and Pressures in Different Gases", Proc. Royal Soc. 79 A, p. 85, (1907).

d is the resulting thickness of the sheath. Eliminating i between equations (2) and (3) gives:

$$d = \frac{1}{2}\left(\frac{9\ k}{\pi\ e\ \bar{c}}\right)^{\frac{1}{3}} \frac{V^{\frac{2}{3}}}{n^{\frac{1}{3}}} \qquad (4)$$

for the sheath thickness in terms of applied potential difference and ion density. Changing to practical units and taking the electronic charge $e = 1.59 \times 10^{-19}$ coulombs, this becomes approximately:

$$d = 136\left(\frac{k}{\bar{c}}\right)^{\frac{1}{3}} \frac{V^{\frac{2}{3}}}{n^{\frac{1}{3}}} \text{ cm} \qquad (4a)$$

3. Dielectric Strength of Space Charge Sheath. For arc re-ignition to occur, this space charge layer of thickness d must be broken down by ionization by collision. This will happen if and when the applied voltage V becomes equal to the breakdown voltage or dielectric strength of the resulting space charge layer. Since a certain minimum voltage, of the order of the cathode drop in a normal glow, is required for spark breakdown of a gap, however short, the cathode layer will be able to withstand voltages up to this minimum value as soon as it is formed. Since practically all of the voltage applied across the arc electrodes is known to appear across this cathode layer[9,10], at least this minimum breakdown potential (of the order of 200 or 300 volts)

---

(9) Dow, Attwood, and Timoshenko, "Probe Measurements and Potential Distribution in Copper A-C. Arcs", Trans. A.I.E.E. 52, p. 926 (1933).

(10) Timoshenko, "Die Lichtbogenwiederzündung als Durchschlag in stark ionisierten Gasen", Zeit. für Phys., 84, p. 783 (1933).

will be required to re-ignite the arc as soon after a current zero as it is possible for any practical circuit to apply appreciable voltage to the arc terminals. Recovery of further dielectric strength will take place as de-ionization results in growth of the space charge layer to thicknesses everywhere greater than the minimum sparking distance. Because of the relation between sheath thickness d and applied voltage (equation (4a)), the actual breakdown voltage, or dielectric strength, of an ionized gas can be found only by eliminating d between (4a) and an equation giving sparking voltage as a function of d. This latter functional relation is known empirically[11,12] for atmospheric air and some other gases in the absence of space charge. The presence of the space charge in the cathode layer will so distort the electric field, however, that the actual sparking voltages will be much less, at least above the minimum point, than those given by such curves. They will also increase less rapidly with increase in d[11]. Because of this situation, it would be clearly impossible to predict accurately the breakdown voltage of the arc space, even if the ion density and temperature at the sheath boundary and ion mobility within the sheath were accurately known. Incidentally,

---

(11) Slepian and Mason, "Electric Discharges in Gases - III", Elect. Eng. 53, p. 512, (April, 1934).

(12) Schumann, "Elektrische Durchbruchfeldstarke von Gasen" (Springer).

the ion mobility is not a constant at the existing field strengths but may be expected to vary as $X^{-\frac{1}{2}}$, where X is the field strength. Also, where the mean free path is an appreciable fraction of the sheath thickness, as it may become for very high ion densities, the concept of mobility loses much of its meaning and the accuracy with which equations (3) and (4) can be applied is still further impaired. Consequently, only very rough calculations on the basis of this theory would seem to be justified.

4. Conditions Affecting Dielectric Strength. A frequently used rough approximation to the sparking potential - distance curve for air at atmospheric pressure and ordinary temperatures is the relation:-

$$V = 30{,}000 \; d \quad \text{volts} \qquad (5)$$

which assumes a constant sparking gradient of 30,000 volts per centimeter. This is much too low for ordinary air at distances much less than a centimeter but may be nearer to the true value for short spaces containing space charge. Because of its simplicity it is useful for approximate estimates of dielectric strength of the arc space, which alone are justified by the present status of the theory. To account for the reduced density resulting from the higher-than-normal temperature of the arc gases, equation (5) must be modified by the application of Paschen's law to the form:-

$$V = 30{,}000 \; d \; \frac{T_o}{T} \quad \text{volts,} \qquad (6)$$

where $T_o = 273^\circ$ K and T is the absolute temperature of the arc

gases. Then, eliminating d between equations (6) and (4a) gives for the breakdown voltage:-

$$V = \frac{6.8 \times 10^{19}\ k}{\bar{c}} \cdot \frac{1}{n} \cdot \left(\frac{T_o}{T}\right)^3 \qquad (7)$$

This equation reveals the role of deionization (decrease in n) in dielectric recovery and also indicates the importance of temperature of the gas. (Since both k and $\bar{c}$ vary as $T^{\frac{1}{2}}$ at constant pressure $k/\bar{c}$ is independent of temperature.)

To take into account changes in pressure, both equations (6) and (7) must be further modified. By Paschen's law, (6) becomes:-

$$V = 30{,}000\ d\ \frac{T_o}{T}\ p \quad \text{volts,} \qquad (6a)$$

where p is the pressure in atmospheres. Since the ion mobility, k, varies as $p^{-\frac{1}{2}}$ at constant temperature, (7) becomes:-

$$V = \frac{6.8 \times 10^{19}\ k_o}{\bar{c}_o} \cdot \frac{1}{n} \cdot \left(\frac{T_o}{T}\right)^3 \cdot p^{\frac{5}{2}} \quad \text{volts,} \qquad (7a)$$

where k_o and $\bar{c}_o$ are now the values of mobility and average thermal velocity at one atmosphere and 0° C.

5. Rate of Dielectric Recovery. In any practical case the quantity in equation (7a) which may be expected to vary most rapidly with time is n, the density of positive ions in the field-free region just outside of the cathode layer. Here deionization will be taking place by diffusion to the boundaries of the "plasma" region and by direct recombination. Previous calculations on

deionization by diffusion in the short arc space appeared to show it to be far too slow alone to account for the observed rates of dielectric recovery and the effect on these of electrode separation(2). Recombination has been shown to be important, however(5). For equal densities of positive and negative ions the rate of recombination is given by:-

$$\frac{dn}{dt} = - \alpha n^2 \qquad (8)$$

where n is the density of ions of one sign and α is the coefficient of recombination. Integration gives:-

$$\frac{1}{n} = \alpha t + \frac{1}{n_o} \qquad (9)$$

where n_o, the initial ion density, is very large as it is in the arc space at current zero, $\frac{1}{n_o}$ may be neglected in comparison with αt when the time t becomes appreciable and equation (9) becomes simply:-

$$\frac{1}{n} = \alpha t \qquad (10)$$

According to both experiment and theory α should vary approximately as the inverse cube of the temperature near atmospheric pressure and directly as the pressure(11). Hence, equation (10) becomes:-

$$\frac{1}{n} = \alpha_o \left(\frac{T_o}{T}\right)^3 p\, t \qquad (11)$$

---

(11) Thomson, "Conduction of Electricity Through Gases", I, p. 35 and p. 52 (Cambridge, 3rd. Edition.)

where α_o is the recombination coefficient for the gas under consideration at 0° C. and atmospheric pressure. Substitution in equation (7a) gives:-

$$V = \frac{6.8 \times 10^{19} \; k_o \; \alpha_o}{\bar{c}_o} \cdot \left(\frac{T_o}{T} \right)^6 \cdot p^{\frac{7}{2}} \cdot t \text{ volts} \qquad (12)$$

for the complete dielectric recovery equation according to the above assumptions. The great importance of gas temperature in dielectric recovery of the arc space is now clearly revealed. Since the initially very hot (several thousand degrees) arc gases may be expected to cool rapidly during the current zero period, the actual shape of the dielectric recovery curve should be concave upward rather than straight as indicated by equation (12). Also, the dependence upon temperature should be even greater than in (12) at the higher temperatures, because of the diminishing probability of electron attachment to form negative ions, an essential element in the recombination process, at very high temperatures. Another reason for upward concavity of the dielectric recovery curve which may be operative at the shorter times is the departure of the actual sparking voltage-vs.-distance relation from equation (6a) when d is near the minimum sparking distance. This will result in the curve passing not through the origin as shown by equation (12) but through a value of a few hundred volts at zero time.

It should be noted that equation (12) applies only for the assumed condition of two distinct regions between the electrodes:

the space charge sheath and the field-free plasma region, the latter constituting the source of ions for the former. Eventually the sheath will grow until it completely displaces the plasma, thus eliminating its own ion source. When this occurs the electric field will very quickly sweep away all of the remaining positive ions, leaving the arc space completely deionized. From this point on d is fixed and so further dielectric recovery will take place at a slower rate due only to the increase in density of the gas with diminishing temperature, as shown by equation (6). At this point loss of the field-distorting space charge may produce an actual discontinuity in the dielectric recovery curve as well as a sudden change in both slope and curvature. Beyond this point the dielectric strength of the arc space should approach asymptotically the normal sparking voltage of the gap. The time of occurrence of the transition point will depend, of course, on both the electrode separation and the rate of deionization.

6. Phenomena at the Anode. In the above approximate treatment of dielectric recovery it has been assumed that all of the applied voltage is consumed by the space charge sheath at the incoming cathode, no drop occurring in the plasma region or at the anode. The only measurements of potential distribution in the arc space during the reignition period so far made[9,10] essentially confirm this assumption for a 15-cm. 25-ampere copper-electrode arc in air. In these measurements no drop in potential was ever detected in the inter-electrode region and the anode drop did not exceed

about 20 volts. Under different conditions, however, it is conceivable that the anode drop just preceding breakdown of the arc space might become large enough to add appreciably to the total breakdown voltage. The anode drop can also be negative, subtracting from the total re-ignition voltage. According to Langmuir's theory of probes the magnitude and sign of the anode drop will depend on the relative magnitudes of the diffusion, or "random" electron current in the plasma and the current being carried by the discharge. Thus, if the electron density and temperature next to the anode is high and the "Townsend" current preceding breakdown small, the anode drop should be negative. If the conditions are opposite it should be positive. In the absence of information to the contrary it is probably justified to assume that the anode drop, whether positive or negative, will be small compared with the voltage drop at the cathode during the re-ignition period.

7. Ionizing Activity. In this discussion it has been assumed that the normal ionizing agents in the arc suddenly stop their activity with cessation of the arc current. In the positive column where ions are believed to be produced thermally(12) this should not be strictly true since some finite time is required for cooling of the gas. Recent studies have shown this "time of relaxation" in the arc to be of the order .001 second(13). This is the time required

---

(12) Compton, "Theory of the Electric Arc.", Phy. Rev. 21, p.266 (1923).

(13) Suits, "High Pressure Arcs", G.E. Review 39, p. 194, (1936).

for cessation of the ionizing activity after a sudden stopping of the current. In the A-C. arc, however, the current may be decreasing so rapidly just before current zero that equilibrium conditions do not exist. The result may be that the last few tenths of an ampere may be carried by virtue of the ions previously formed without the necessity of any further ionizing activity, if the ion density is diminishing by recombination no faster than is the current. Therefore, it seems likely that at current zero the production of ions in the arc may have already practically stopped and the assumption of no ionizing activity during the zero-current period other than that due to the electric field is justified.

III. EXPERIMENTAL PROCEDURE

1. Method. All of the experiments to be described in this thesis were made with continuously burning A-C. arcs between plane brass electrodes in air at atmospheric and lower pressures. The current was limited by means of almost pure reactance to values of 12.5, 25, and 50 amperes r.m.s., respectively, in a circuit essentially the same as that of Figure 1. The voltage at which re-ignition occurred was measured directly on the fluorescent screen of a cathode-ray oscilloscope of the Braun, or sealed glass tube type (R.C.A. 904). The natural period of oscillation of the circuit and hence the time after current zero at which re-ignition occurred was controlled by varying C (Figure 1). The time corresponding to the measured re-ignition voltage was calculated by means of an equation given by Attwood, Dow, and Kransnick,(14):-

$$e = E - E_m \cos (w t + \theta) \qquad (13)$$

in which E is the peak value of the applied A-C. voltage, w is 2π times the natural frequency of the circuit, given by:-

$$w = \frac{1}{\sqrt{L C}} \quad , \text{ and}$$

E_m is the maximum amplitude of the voltage oscillation about E, given by $E_m = E - e_m$, where e_m is the "negative maximum" of the oscillation, measured from the zero axis. θ is the phase angle by which the negative maximum lags behind the moment of zero current.

---

(14) Attwood, Dow, and Kransnick, "Reignition of Metallic A-C. Arcs in Air", Trans. A.I.E.E., 50, p. 949 (1931).

It is given by:-

$$\theta = \tan^{-1} \sqrt{\left(\frac{E - e_m}{E - E_1}\right)^2 - 1}$$

where E_1 is the value of the arc voltage at cufrent zero. A typical re-ignition transient is represented in Figure 2, in which the above quantities are labelled. Because of the very short time involved, the applied circuit voltage remains practically constant at its maximum value, E. As the arc current i_a (shown by the heavy dotted line) approaches zero at its normal rate it eventually reaches a value at which the arc is no longer stable. At this point the arc suddenly fails and the current drops immediately to zero. From here on until re-ignition occurs the arc space conducts practically no current and so the voltage is determined entirely by the circuit constants and the initial conditions of the oscillation. These initial conditions are the initial voltage, E_1, and the value of the arc current just preceding arc failure, I_1. Since the current in the inductance cannot change suddenly, it continues to flow, not now into the arc, but into the capacitance C, causing the voltage across the capacitance and inductance in parallel to rise from the value it has at $t = 0$, $E - E_1$, to the value $E_m = E - e_m$ at $t = t_m$. The amplitude of the oscillation, E_m, and consequently the negative maximum voltage, e_m, will thus be determined by the magnitude of I_1. I_1 is generally of the order of 0.1 ampere, but depends to some extent on the circuit constants and probably also on the arc conditions. It is subject to large random variations

from one half-cycle to the next. Following re-ignition at $t = t_s$ the discharge carrying current in the new direction usually takes the form of a glow, at least in the case of the low-current arcs studied, changing discontinuously to an arc again when the current reaches a value, also subject to large random variations, sufficient to maintain a stable arc. The two types of discharge are, of course, identified by their characteristics voltage drops, practically all of which occur at the cathode. The cathode drop of a normal glow is of the order of two or three hundred volts, while that of an arc is only ten or twenty volts.

To calculate the duration of the current zero period, t_s, equation (13) can be solved for t and the re-ignition voltage e_s substituted for e. In terms of measured quantities this is:-

$$t_s = \sqrt{L\,C}\left(\cos^{-1}\frac{E - e_s}{E - e_m} + \tan^{-1}\sqrt{\left(\frac{E - e_m}{E - E_1}\right)^2 - 1}\right) \qquad (14)$$

If L is expressed in henries and C in micro-microfarads, t_s is given conveniently in micro-seconds. For very small values of C, the absolute value of e_m tends to become greater than the normal glow voltage. When this occurs arc failure generally results in transition to a "negative glow" before the current finally drops to zero, giving the situation represented in Figure 3. For this case the initial voltage E_1 is identical with the negative peak e_m and so the arc tangent term in equation (14) drops out, leaving the simpler form:-

$$t_s = \sqrt{L\,C}\ \cos^{-1}\frac{E - e_s}{E - e_m} \qquad (14a)$$

In representing the results of the experiments the values of re-ignition voltage e_s were plotted against the corresponding calculated values of t_s. For each arc condition a series of such points was determined for values of the parallel capacitance C varying from only the distributed capacitance of the reactors and leads to the largest value (usually) at which the arc could be maintained. The curve determined by these points was taken to represent the recovery of dielectric strength by the arc space with time after current zero.

IV. RESULTS

Figures 15 through 36 represent the results of 527 tests. Results for a 25-ampere arc are shown in Figures 15 through 26, for a 12.5-ampere arc in Figures 27 through 34, and for a 50-ampere arc in Figures 35 and 36. Curves were obtained at 25 amperes for electrode separations of 0.45 mm., 1.0 mm., 2.05 mm., and 4.13 mm., for pressures of 1, 1/2, and 1/4 atmosphere in most cases and for 1/8 atmosphere in one case. The actual measured pressures were 739-748, 370, 185, and 92 millimeters of mercury. The 12.5-ampere arc was investigated only at one atmosphere and 1/2 atmosphere. Two recovery curves were obtained at 50 amperes: one at one atmosphere and one millimeter and one at 1/2 atmosphere and 2.05 millimeters. Only the first 200 microseconds were investigated as beyond this time the re-ignition voltage generally became very erratic and frequently so high that the arc was unstable in the 690-volt circuit. The distributed capacitance of the circuit (about 150 micro-microfarads) placed a lower limit on the times which could be studied of from 3 to 10 microseconds, depending on the voltage and current settings.

1. General Discussion. With a few exceptions, the curves are divided into two distinct regions, the first region concave and the second convex upward or nearly straight. The curves of Figures 35 and 36 are clear-cut examples of this. In other cases, such as Figures 15, 16, and 17, the situation is not so clear, but

the otherwise anomalous occurrence of different re-ignition voltages existing simultaneously can be readily explained by assuming that the dielectric recovery was of the same type in these cases also. The apparent overlapping of the two portions of the curve in Figures such as 20, 23, or 24 is believed to be due to random variations in the time at which the actual dielectric recovery broke sharply upward, as shown by the dotted lines representing limiting cases. In such regions two distinct groupings of the re-ignition voltage values were observed on the oscilloscope screen. In some cases it was apparent that these double values were associated with the occurrence or the non-occurrence of a "negative" glow before current zero, the two values falling on the same smooth curve when this was taken into account. In other cases, however, double values occurred in the complete absence of a negative glow and of such disparity that they could not possibly lie on the same continuous curve. Intermediate values may have been of frequent occurrence, but as they were not grouped closely they were not observed as "points". The frequently occurring breaks at the upper ends of the lower branches of the curves, as in Figure 16, were interpreted as indicating that the individual recovery curves, varying from one cycle to the next, turned up sharply at or prior to these breaks, their slopes becoming equal to or greater than those of the applied voltage curves. (See Figure 11.)

2. Agreement with Theory - Upper Region. The characteristic division of the curves into two regions with a point of discontinuity between agrees perfectly with the prediction of the theory already described. The first concave-upward portion should represent dielectric recovery due to the space charge growth associated with deionization, as given by equation (7a) or (12). The second flatter portion should, then, represent dielectric recovery of the arc space according to equation (6a), due to increasing density of the now completely deionized gas as it cools. Assuming this to be the case, the temperatures indicated by the observed dielectric strengths in this second region were calculated (see Appendix D) and plotted as functions of time in Figures 15, 16, 17, 23, 26, 35, and 36. The temperature curves of Figures 15, 16, and 17 are re-plotted to the same scale in Figure 37 to show the effect of electrode separation on the apparent cooling. For the shorter arcs the values of temperature thus obtained are entirely reasonable and the shape of the cooling curves, nearly exponential, is just what would be expected. The assumption upon which the temperature calculation is based, complete deionization, evidently does not hold for most of the curve of Figure 17 for 2.05 mm. separation, the values so obtained becoming improbably high at the shorter values of time. Inspection of Figure 17 shows, moreover, that there is a "hump" in the dielectric recovery curve beginning in the vicinity of 130 microseconds (time decreasing), apparently indicating a gradual

transition between the two types of recovery. It is suggested that this gradualness of the transition may be due to the existence of thermal ionization of the gas at these high temperatures. The dotted extrapolation of the 2.05 mm. curve shows the variation of the actual gas temperature as estimated by comparison with the other curves. This dotted curve, as well as those for the shorter arcs, is consistent also with the value of temperature, 4050° K, observed by Suits[13] for a D-C. arc between copper electrodes.

3. Analysis of Lower Region. The lower, or first portions of the dielectric recovery curves are of particular interest from both a theoretical and a practical viewpoint. From the standpoint of circuit interruption, the first few microseconds are of greatest importance because they are of importance in the interruption of the most difficult circuits: those having the highest voltage recovery rates. Also, as further analysis of the results will show, this first deionization period tends to become longer as the arc current is increased, and again it is the high-current cases which generally present the most practical difficulty. Furthermore, high-current short circuits usually have high recovery rates associated with them. Hence, in cases of practical interest to switch designers it is this first type of dielectric recovery which is generally of interest. From the theoretical standpoint, it is this first portion of the curves which may throw some light on the deionizing processes in the arc space.

The curve of Figure 35 was chosen for detailed analysis because of its clear portrayal of the general type of recovery and because its conditions (atmospheric pressure, 1 mm. separation, 50 amperes) most nearly approach those of practical interest. The temperature curve calculated for the upper portion was extrapolated as shown to give an estimate of the gas temperature during the first 43 micro-seconds. Both curves are re-plotted for this region to an expanded scale in Figure 38. On the basis of these curves of breakdown voltage and temperature and the curve given by Slepian and Mason[11], derived by them from Schumann[12] of sparking voltage vs. pressure-times-separation (see Figure 57 and Appendix E) for plane electrodes in air already used in the temperature calculations, the space charge sheath thickness required to withstand the observed voltages was calculated and plotted in Figure 38. This rises smoothly at an increasing rate from a value only a little greater than the minimum sparking distance at 5 micro-seconds to the electrode separation of 1 mm. at the transition time, 43 microseconds. From the sheath thickness and the re-ignition voltage the average sparking gradient in the sheath can be obtained. By writing equation (6) in the more general form:

$$V = X\ d \qquad (6b)$$

and combining it with equation (4a) modified to:

$$d = 136 \left(\frac{k_o}{c_o}\right)^{\frac{1}{3}} \frac{V^{\frac{2}{3}}}{X^{\frac{1}{6}}\ n^{\frac{1}{3}}} \qquad (4b)$$

to take into account the effect of the average gradient, X, on the average ion mobility, k, and evaluating k_o and $\bar{c}_o$ by kinetic theory, an expression for the ion density:

$$n = \frac{20{,}200\ X^{\frac{3}{2}}}{d} \quad , \qquad (7b)$$

was obtained. Values of n given by this expression are also plotted in Figure 38. Again, these values seem quite consistent with the steady-state value, 4×10^{13} ions per $cm.^3$, derived by Suits(13) for a D-C. copper-electrode arc, when it is considered that the dynamic situation in the A-C. arc is such that the ion density should begin to diminish long before current zero is actually reached. In fact, it is believed that these measurements consitute an independent determination of both the temperature and the ion density in the arc just after current zero, permitting by extrapolation a reasonably reliable estimate of at least the order of magnitude of these quantities before current zero. The approximations involved in the theory upon which the calculations are based may cause an uncertainty in the results of two or three times at the most, but not, it is believed, in their order of magnitude.

4. Nature of the Deionizing Processes. If the essential correctness of the ion density curve is accepted, these results make possible for the first time a detailed quantitative check of the theories of deionization in the arc space, since both the magnitude and the rate of decrease of the ion density are given by the curve. The results of calculations (Appendix F) using equation (8)

and the assumption that α varies inversely as the cube of the temperature indicate that recombination, the process assumed in Slepian's theory described above and hence the basis of equation (12), is inadequate alone to account for the deionization occurring in this case. Further calculations, based on a simplified picture of the process in the plasma region, indicate that diffusion is of the right order of magnitude to account for the observed rate of deionization. Also, the shape of the deionization curve, approximately exponential like the cooling curve, indicates that the rate of deionization falls off as the first power of the ion density, as it should for diffusion, rather than as the sedond power as it would if recombination were the chief deionizing process. For the diffusion process, shrinkage of the plasma region as it approaches the vanishing point at transition should cause a sudden acceleration of the deionization and hence the dielectric recovery near this point. Such a behavior, shown by the dotted variation of the dielectric recovery curve between 30 and 43 microseconds, is clearly as consistent with the available experimental data shown in Figure 35 as is the curve originally drawn. It is also more consistent with the curves postulated to explain the double-valued re-ignition voltages of such Figures as 15 and 16.

5. Effect of Arc Length. Probably the most striking characteristic of short A-C. arcs between low-boiling-point electrodes is the superiority for circuit interruption of very short arcs over somewhat

longer arcs. This means, of course, that, roughly speaking, dielectric recovery is more rapid for the shorter arcs than for the longer. Figures 39, 40, and 41 show this effect in detail. Here groups of curves for different electrode separations but other conditions the same are re-plotted for direct comparison. It is clearly shown that the effect is almost entirely confined to that portion of the dielectric recovery which is due to deionization of the arc space, the subsequent rate of recovery due to cooling being very little affected. An exception to this last statement may be noted in the case of the 0.45 mm. arc at 12.5 amperes and 1 atmosphere, and at 25 amperes and 1/2 atmosphere, where the second type of recovery begins so quickly that the cooling is still very rapid (see Figure 37 and others). The effect on the initial recovery rate is certainly very striking. For arc lengths of only 2.05 mm. the initial recovery rate is reduced to the same order of magnitude as the subsequent recovery rate so that the transition becomes less sharp, and at 4.13 mm. complete deionization apparently does not occur at all during the first 200 microseconds. The peculiar break and "doubling up" of the 25-ampere, 1-atmosphere, 4.16 mm. curve is believed to be due to changes in motion of the arc terminals over the electrodes, to be discussed later, rather than to the type of transition postulated for the other curves. Evidently, from the standpoint of circuit interruption, there is an optimum arc length, depending on the

current, pressure, and circuit recovery rate. For high currents, high recovery rates, and atmospheric pressure, the best separation for brass electrodes seems to be extremely small, probably even less than 0.45 mm.. In other cases, however, it is noticeable that when the separation becomes too small the reduction in the ultimate sparking voltage begins to offset the increase in rate of initial recovery due to deionization. This situation has been observed also in previous work with short arcs(3), particularly for electrode materials other than brass.

From the preceding discussion of deionizing processes (paragraph 4 of this section) it seems clear that this effect of electrode separation must be primarily upon the rate of loss of ions to the electrodes by diffusion. To the extent to which recombination may be important, the effect is also on the coefficient of recombination through the effect on cooling (Figure 37). There is also a direct effect of cooling on the gas density and hence on the dielectric strength. In addition to direct diffusion of both heat and ions to the electrodes, cooling and deionization may also result from evolution of vapor from the boiling surfaces of the electrodes, the cooling being due to the inmixing of zinc vapor from the comparatively low-boiling-temperature brass and the direct deionization to dilution and to the speeding up of diffusion by the gas blast. Although this vapor blast may not exist beyond current zero, its importance in deionization is strongly suggested by the large effect of electrode boiling temperature on dielectric recovery shown by previous work(3).

6. Effect of Pressure. Figures 42 through 45 show the effect of pressure on dielectric recovery for the 25-ampere arc with four electrode separations. In general, the effect on the initial recovery is opposite to the effect on the later recovery. The effect after deionization is simply upon the density of the gas between the electrodes. If the temperature were the same, the dielectric strength in this region would be almost directly proportional to the pressure. The fact that it is not indicates that the temperatures are different, being higher at the higher pressures as may be seen by comparison of Figures 16 and 23. This is to be expected, of course, since the initial arc temperature is undoubtedly lower at the lower pressures and the rate of cooling is proportional to the mean free path and therefore inversely proportional to the gas density.

The opposite effect of pressure on the initial recovery is another indication that deionization is chiefly by diffusion rather than by recombination. Examination of equation (7a) shows that, since the temperature is observed to vary nearly as the square root of the pressure, the dielectric strength of the space charge sheath should vary directly with the pressure and inversely as the ion density. Since the early dielectric recovery rate actually tends to diminish slightly with increase in pressure (See especially Figures 44 and 45, neglecting the latter portion of the curve for 1/8th atmosphere in 45.), the conclusion is that deionization, again like

cooling, must be more rapid at the lower pressures where the mean free path and hence the diffusion rate is comparatively high. If recombination were important, equation (12) shows that the dielectric recovery by the sheath should vary as the square root of the pressure (again taking account of the observed effect of pressure on temperature). Because of the exponential relation between 1/n and the coefficient of diffusion, further consideration of equation (7a) shows that for deionization by diffusion the early recovery rate should be almost independent of pressure initially but as deionization proceeds it should begin to vary inversely as a higher and higher power of the pressure. This is, in fact, exactly the behavior of the curves of Figure 45! The upper portion of the 1/8-atmosphere curve in this figure must be neglected because it clearly represents dielectric recovery after complete loss of ionization at about 67 microseconds. (See Figure 26.)

7. Comparison of Curves for Constant $p\ell$. According to the law of similitude for sparking the upper portion of the dielectric recovery curves should be independent of electrode separation as long as the pressure is varied so as to keep the product of pressure and separation constant. This presumes, of course, that the temperature also remains the same, the pressure actually representing the gas density. The curves for the 25-ampere arc are compared on this basis in Figures 46 through 49, for values of $p\ell$ of 0.25, 0.5, 1, and 2. The two 50-ampere curves for $p\ell = 1$ are shown in Figure 50.

The disparity between the curves for constant $p\ell$ indicates that the temperature of the gas did not remain constant but increased with the arc length. The closest agreement is for the smallest value of $p\ell$, the difference between the curves increasing with this value. For the 50-ampere arc the agreement is very close even at $p\ell = 1$. It is noticeable in these cases that both the initial rate and the subsequent dielectric recovery decrease with increasing arc length, suggesting that the effect is of the same kind for the two parts. The effect on the initial rate of recovery is considerably greater, however, than the effect on the later recovery. In fact, the initial recovery rate seems to vary almost directly as the pressure for the 25-ampere arc.

A simple consideration of the theory leads to the conclusion that both cooling and diffusion of ions should be independent of either pressure or electrode separation alone at constant $p\ell$, at least at constant temperature, since the mean free path and hence both the diffusion coefficient and the heat conductivity vary with the arc length. This assumes diffusion in only one dimension, however, completely neglecting lateral diffusion of heat and of ions to the surrounding cooler gas beyond the arc boundary. It is significant that the similitude principle holds most closely for the larger currents and the smaller values of $p\ell$ where the cross-section of the arc is largest relative to the electrode separation and hence the conditions for only one-dimensional diffusion are most closely

met. For the longer and thinner arcs it is probable that lateral diffusion is almost as important as direct diffusion to the electrodes, the shape of the mass of hot ionized gas being more nearly spherical than in the assumed shape of a thin flat cylinder. Thus, the volume of the space to be cooled and deionized by diffusion may vary roughly as the cube of electrode separation rather than as the first power as assumed. This affords one possible rough explanation of why the initial dielectric recovery rate decreases as the electrode separation is increased, in spite of the proportionate decrease in pressure. Another possible and more exact explanation follows from the discussion in paragraph 5 of the effect of pressure. There it was noted by examination of equation (7a) that if the gas temperature be assumed to vary as the square root of the pressure, the breakdown voltage of the space charge sheath should vary directly with the pressure and inversely as the ion density. With the further assumption, then, that n remains about the same, the slope of the initial recovery curves should vary directly as the pressure, as they do almost exactly in Figures 47, 48, and 49. Perhaps the actual situation is that the assumptions of the last explanation, varying temperature and constant ion density, are not exactly true but that under some conditions the first-mentioned effect of lateral diffusion adds to the second direct effect of pressure sufficiently to make up for the lack of exactness of the

second-case assumptions. Certainly, the curves show that the temperature does increase as some fractional power of the pressure and the opposite effect of pressure and of separation on deionization may very well result in ion density remaining about the same from one curve to the next. As for the effect of a possible vapor blast from the electrodes, it should also be unchanged with $p\ell$ constant since its relative penetration into the arc space would be proportional to the mean free path. Finally, it should be mentioned that one obvious difficulty in attempting to apply the principle of similitude to the arc space is that ionization in the arc is not believed to be simply ionization by collision, which is the basis of the similitude principle, but rather thermal ionization. This latter requires a certain minimum temperature which must be maintained by a sufficient energy and therefore current density. Hence the variation of current density with the square of the pressure as required by the principle of similitude probably does not hold at all in the arc up to current zero, resulting in different initial conditions for deionization even with $p\ell$ constant.

8. Effect of Current Strength. Figures 51 through 56 show the effect of different current magnitudes with other conditions the same, the first four figures being for atmospheric pressure with different arc lengths and the last two for 1/2 atmosphere pressure and two different lengths. The lower curves for the higher currents drawn in Figures 52, 53, and 54 were taken from the results of

previous work[2,3,4]. Since they are for odd lengths, 1.6 and 3.2 mm., they are not directly comparable with the curves of any figure and so two of them are repeated in both Figure 52 and Figure 53. Also, the 1200-ampere curve is for copper electrodes rather than brass. There is a definite effect in all cases of increasing current lowering both the initial recovery rate and the subsequent sparking voltage. This is further evidence that diffusion and cooling cannot be treated strictly as one-dimensional processes, since in the absence of lateral diffusion current magnitude should make no difference, provided that the current density remains the same. Where lateral diffusion is important, however, the varying ratio of surface to area should produce just the effect observed, the diffusion being relatively more rapid for the smaller current, smaller cross-section arcs. The sloping volt-ampere characteristic of arcs of such small currents as used here indicates the presence of this effect before current zero, and incidentally also that current is carried in the smaller-current arcs with lower ion densities than in the higher-current arcs. This last indirect effect of lateral diffusion on initial ion density also helps to explain the observed variation of the curves. At the very high currents it is apparent that complete deionization of the arc space did not occur during the first 200 microseconds. The limited amount of data on which the 1200-ampere curve (obtained by an indirect method) was based indicated that it begins to curve upward after about 300 microseconds[4]. The

practically horizontal portion shown undoubtedly represents the minimum sparking potential in copper vapor under the conditions existing just after current zero. The intercept of the 300-ampere curves on the zero-time axis is also probably near to the minimum sparking potential in the vapor from brass. It is characteristic of all the curves that they tend to approach a common value if extrapolated to or somewhat beyond the time of current zero. This common value is of the order of magnitude of the minimum sparking potential and undoubtedly does correspond to this value under the test conditions. As mentioned previously, there may be an appreciable positive or negative drop at the anode included.

V. CONCLUSIONS

From the foregoing consideration of the results it may be concluded that:-

(a) Slepian's theory that dielectric recovery by the arc space after current zero is due to the formation of a space charge sheath at the cathode which must be broken down like an ordinary spark gap, this gap increasing with deionization of the space, is applicable, at least for low-boiling-point electrodes.

(b) The chief deionizing process for short arcs is not recombination, as assumed by Slepian, but diffusion.

(c) Recent determinations of arc temperatures (4000-6000° K.) and densities of ionization (10^{13}) at atmospheric pressure are verified, at least as to order of magnitude. It is further shown that cooling to a few hundred degrees Centigrade and complete deionization of short arc spaces between brass electrodes may occur within the first 10 to 100 microseconds after current zero for currents of 50 amperes or less.

The "non-arcing" effect of low-boiling-point electrodes is still not fully explained. In view of past results and of conclusion (b) it seems probable that the effect of the electrode surface temperature on the rate of cooling of the arc gases just before and after current zero may be critical, the gas temperature

falling immediately to values too low for thermal ionization with low-temperature electrodes but not with electrodes boiling at the higher temperatures. More investigation of this point is needed. For this purpose it is suggested that further experiments of the type described here be performed with arcs between electrodes of other materials than brass.

VI. ACKNOWLEDGMENT

The writer wishes to express his gratitude to the Electrical Engineering faculty of the California Institute of Technology for their cooperation in this work, to Mr. H. T. Holtom for his aid in developing the measuring equipment, to Mr. Takeji Onaka for his untiring assistance in conducting the experiments and making the calculations, and to Mr. L. T. Rader and Miss Esther Gilbert for their invaluable help with the preparation of this thesis.

APPENDIX A.

Apparatus

The actual circuit used, though similar in principle to that of Figure 1, is shown more completely in Figure 4. The peculiar transformer combination was necessary to obtain the desired voltage (690) from an ungrounded source with theequipment available. The 3 kva. group actually consisted of three pairs of 1 kva. distribution transformers in parallel. The transformer terminal voltage was measured through a 20-1 potential transformer. Two inductively-coupled air-core reactors were used as shown for 25 and 50 amperes and a third was added to obtain 12.5 amperes. Some of the tests were made at 460 volts with the inductance correspondingly reduced. The reactors (three identical sections) were constructed of No. 7 copper wire wound in 19 layers of 19 turns each. The turns were separated only by the double cotton covering and the layers by 1/4-inch wooden strips laid axially at frequent intervals. This construction was adopted to minimize distributed capacitance and gave very good results, the measured capacitance of the single coils being only 18 micro-microfarads. Each coil had a resistance of 0.63 ohm and an inductance of approximately 0.0334 henry, giving a reactance of 10.5 ohms at 50 cycles. With all three coils in series and as closely coupled magnetically as possible, the 50-cycle reactance was 54.7 ohms and the distributed capacitance 35 micro-

microfarads. The reactance could be adjusted by changing taps and by varying the magnetic coupling between coils. Figures 5 and 6 are views, respectively, of one coil alone and of all the coils mounted for use, the transformers being shown below in Figure 6.

To avoid trouble due to themagnetic field of the reactors, the arc electrodes and the oscilloscope were located about 15 feet away from the coils on a line perpendicular to their axis. The electrodes are shown mounted in the arcing structure in Figure 7. They were flat brass blocks, 5 cm. square by 1.27 cm. thick initially, being planed down between groups of tests to restore their surfaces. The lower electrode was pierced at its center by a small hole (0.9 mm. diameter) through which a somewhat smaller tungsten wire could be projected to make and break contact with the upper electrode and so start the arc. In the final tests the re-ignition voltage was measured only with the upper unpierced electrode as the cathode. Between tests the electrodes were cleaned with both a file and emery cloth. They were replaced as soon as they became noticeably pitted by the arc. The electrode holders were mounted on a drilled glass plate fitted to a bell-jar cover and the whole connected to a vacuum pump and closed-tube mercury manometer for controlling and measuring the pressure. The arc igniter electrode already mentioned was operated through a flexible bellows (Silfon) seal. A general view of the apparatus in use is shown in Figure 8.

The voltage divider had to be of the resistance-capacitance type in order to match the impedance of the oscilloscope for all frequencies from 50 to 50,000 cycles per second. All six sections were identical, consisting of 600,000 ohm carbon-rod resistors in parallel with small adjustable mica "trimming" condensers of between 50 and 100 micro-microfarads capacitance. The resistors were adjusted by filing so as to have equal D-C. resistances and the condensers were subsequently adjusted to give the proper voltage ratios at 50,000 cycles. Equality of capacitance of corresponding sections was checked by inserting the condensers into a tuned circuit. As shown, the maximum divider ratio of three could be changed to two by closing the switches S_5 and to unity by connecting the oscilloscope leads directly to the arc terminals. The symmetrical arrangement of the divider about ground was found to be necessary to eliminate spurious deflections due to ground currents flowing through unsymmetrical capacitances to ground of other parts of the circuit. It was also necessary to balance the rest of the circuit insofar as possible with respect to ground to eliminate distortion of the electrostatic field between the oscilloscope deflecting plates which occurred for high-frequency oscillations if one plate were much closer to ground potential than the other. Most of the capacitance to ground existed in the supply transformers, of course.

The oscilloscope tube was equipped with only one pair of deflecting plates, deflection in the other direction being produced by an electro-magnetic field. In these experiments the field coils were connected to the 50-cycle supply voltage through a phase

shifting transformer. This could be so adjusted that the beam would cross the center of the screen as the arc current reached its zero value and the re-ignition transient to be observed took place. As the field strength was such that the beam appeared on the screen only during a very small portion of the cycle when the sweep current was near zero, its speed across the screen was practically constant, giving a linear time scale. By applying a voltage of the same frequency as, but 90° out of phase with, the sweep current to the control grid of the tube, the beam could be cut off on its return sweep, thus showing the re-ignition transient for only one polarity at a time. Oscillograms could be taken by photographing the screen with an ordinary camera. The camera used had an f 4.5 lens and an extensible bellows for close-up focusing. Wratten Hypersensitive Panchromatic plates were found to give best results with high-speed transients, but Portrait Panchromatic films could also be used. A certain amount of background fogging was necessary to obtain maximum sensitivity with these plates or films. It was also necessary to use voltages as high as 6000 on the beam (the rated voltage of the tube was 4600) to obtain really satisfactory photographs of the highest speed transients. Representative oscillograms are shown in Figures 9, 12, 13, and 14. The timing oscillation was produced by a Western Electric oscillator and fed into the circuit by magnetic coupling to the reactors, the frequency being nearly the natural frequency of the circuit when unshunted.

The condensers used for controlling the natural frequency of the circuit were of two types. The smaller sizes were mica insulated in molded composition and the larger sizes were ordinary "telephone" condensers of rolled paper. The smaller sizes were measured at high frequencies (10 to 50 kilocycles) in a tuned circuit, using a General Radio variable standard condenser, and the larger sizes were measured with a simple capacitance bridge. Most of the condensers were of such voltage ratings that they had to be used in groups of two equal condensers in series. Practically any desired value of capacitance could be obtained by series-parallel combinations.

APPENDIX B.

Experimental Technique

Much time was spent in developing the method of testing to the point where the results obtained were sufficiently consistent and reproducible for the plotting of satisfactory curves. As shown by previous work[2,10,14], apparently inherent variability is one of the chief characteristics of the behavior of A-C. arcs, particularly of the re-ignition voltage. However, with proper care in maintaining the electrode surfaces, etc. the re-ignition voltage values were found to be very consistent in many cases and reasonably so for all of the tests. Variations in magnitude were "averaged out" in these experiments by observing on the oscilloscope screen the repeated re-ignition of the continuously running arc for several seconds and locating the average value of the re-striking voltage by eye. For this purpose a sliding index was used. The uncertainty in location of this average was usually quite small for the shorter times but became considerable as the duration of the current-zero period approached the maximum value at which the arc could be maintained. The re-ignition values were usually very clearly "bunched" in a small region with relatively few high and low values occurring occasionally. The frequency of occurrence of the low values generally exceeded that of the high values. In no sense, however, were the recorded values maximum re-ignition voltages. Rather, they were the

maximum consistently repeated values. Frequently, low values were found to be due to the arc momentarily jumping out from between the plane faces of the electrodes, thus increasing its effective length. It was found that generally higher and more consistent values were obtained when the upper unpierced electrode was the incoming cathode than when the reverse was the case. Whenever the arc stood still or wandered only very slowly, a common condition at the higher pressures and larger separations, the re-ignition voltage diminished rapidly with continued arcing, making necessary brevity of the tests and frequent replacement of the electrodes. To detect this effect, points obtained just before changing electrodes were usually checked with the fresh electrodes. The largest variations observed were those of e_m, the coordinate of the negative peak of the oscillation when there was no negative glow. Values of E_1, the last arc voltage, and of e_m for the negative glow case were more consistent. Readings of the average value of each of these quantities were taken in the same way as described for e_s, the re-ignition voltage. Readings of time could not be obtained directly on the oscilloscope screen because of the large variation in the starting point of the transients due to variation in I_1, the arc failure current. This is illustfated by Oscillogram H-3, Figure 9, which shows several successive transients.

Since variations in beam current incident to focusing the spot as well as variations in line voltage caused changes in the

oscilloscope deflection sensitivity, it was necessary to calibrate the oscilloscope before each reading. This was done by measuring the deflection corresponding to the peak applied voltage at the same time that the voltage was read. The short-circuit current (current with arc shorted out) was also read and adjusted if necessary by varying the reactance. At the same time the transformer terminal voltage was measured with the current flowing. The peak of this latter voltage was the value actually applied to the oscillating circuit at arc failure and was assumed to remain practically constant during the current-zero period because of the relatively large distributed capacitance of the transformers and therefore their long natural period. Consequently, it was the value actually used as E in formula (14) or (14a). The r.m.s. value was, of course, also the voltage used in calculating L by the relation:-

$$L = \frac{\mathcal{E}}{2\pi \cdot 50\ I} \qquad (15)$$

where $\mathcal{E}$ and I are, respectively, the r.m.s. "short-circuit" voltage and current. The oscilloscope deflection was found to be approximately linear except at very small values. As the deflections corresponding to E_1 came within this non-linear range, E_1 was actually measured by a D-C. voltmeter connected to a voltage source which could be adjusted to give a steady deflection equal to that produced by E_1. e_m was measured similarly when its value fell within the range of this D-C. calibrating voltage. A divider

ratio of unity was used to obtain maximum deflection in measuring these smaller voltage values or any other values when possible. As the zero position of the electron beam tended to shift continuously as well as with any adjustment, it was checked before each reading and the millimeter scale shifted if necessary.

APPENDIX C.

Errors and Accuracy of the Method

Readings of deflections on the oscilloscope screen were probably accurate to within one millimeter for the larger deflections of two to five centimeters, giving an accuracy of two to five percent. Smaller deflections, except where variations were large, were determined to within perhaps 0.2 mm. but the total deflection was frequently so small that the accuracy was only about ten percent. Errors resulting from non-linearity of the oscilloscope deflection amounted to only one or two percent at the larger deflections but to very much more, perhaps ten or twenty percent, at the smallest deflections used. Readings of circuit voltage, made with an ordinary portable iron-vane voltmeter and a large standard potential transformer should have been accurate to within less than one percent. Similar accuracy can be expected for readings of current and for the values of inductance calculated from them. The actual values of current in the arc, however, were as much as five percent less than the values actually measured with the arc short-circuited because of the arc voltage thus neglected. Measurements of capacitance of the condensers were made with an estimated accuracy of two to five percent. The distributed capacitance of the circuit, calculated from the inductance and observed resonant frequency of the circuit unshunted and with small shunting capacitance was only roughly

known. It was assumed to be 150 micro-microfarads for the balanced circuit and 230 micro-microfarads for the circuit before it was balanced, these being approximate mean values of several rather widely divergent determinations. Electrode separation was determined by closing the gap on "feeler gauges" consisting of strips of copper or brass sheet previously measured with micrometer calipers. It was probably subject to variations of not more than five percent. The gas pressure was measured with the mercury manometer to well within 0.5 mm. of mercury, giving an accuracy of from 0.1% to 0.5%. For pressures less than atmospheric, the pressure read after each test was generally from 1% to 3% higher than the initial pressure recorded because of heating of the gas within the bell jar by the arc. Momentary increases of several times this amount were noticed while the arc was running. Failure to correct for the temperature of the mercury caused an error of not more than 0.5%.

Somewhat larger errors are probably to be expected in the calculation of time by means of the simple equations (14) and (14a). These equations presume constants lumped as in Figure 1, with no series resistance and no conductance in parallel with the arc. They also assume the oscillation frequency to be large compared to the supply frequency, which was always the case. The more complete equation for e, taking series resistance R into account, is(14):-

$$e = E - \varepsilon^{-\frac{R}{2L}t}\left\{(E-E_1)\cos w\,t + \frac{1}{w\,C}\left[-I_1 + \frac{R}{2L}\,C\,(E-E_1)\right]\sin w\,t\right\} \quad (15)$$

where in this case

$$w = \sqrt{\frac{1}{L\,C} - \frac{R^2}{4\,L^2}}$$

Calculations using typical constants and R = 5 ohms, a value somewhat greater than that given by rough measurements on the test circuit, showed that the effect of this resistance was truly negligible. Similarly, the equation considering shunting conductance alone is:-

$$e = E - \varepsilon^{-\frac{t}{2RC}}\left\{(E-E_1)\cos w\,t + \frac{1}{w\,C}\left[-I_1 + \frac{E-E_1}{2R}\right]\sin w\,t\right\} \qquad (16)$$

where now

$$w = \sqrt{\frac{1}{L\,C} - \frac{1}{4\,R^2\,C^2}}$$

Again, calculations with typical circuit constants and R = 2×10^6 ohms, which was somewhat less than the measured leakage resistance through the circuit insulation and the voltage divider when set for a 2-1 ratio, showed the decrement due to this leakage also to be entirely negligible during the first cycle of the oscillation. However, oscillograms such as H-3, Figure 9, did not verify this result. The complete oscillation upon extinction of the arc is re-plotted in Figure 10. Here it is shown that an exponential envelope can be accurately fitted to the curve. When plotted on semi-logarithmic paper this envelope becomes a straight line whose slope indicates a leakage resistance of only about 85,000 ohms! Other similar oscillograms gave resistances of the same order.

Since the measured value of parallel resistance is so much higher than this, this damping must have been due mainly to current leakage through the arc space, probably in the form of a "Townsend discharge". From Figure 10 it was concluded that the effect of this "arc leakage" was too great to be neglected in the time calculations and so a great deal of work was done on equation (16) in an effort to evolve a practicable method of using it for the time calculations. The equation of the form of (16) found to represent the oscillation of Figure 10 most closely is:-

$$e = 620 - 1070\ \varepsilon^{-\frac{t}{39.45}} \cos (0.157\ t - 0.937) \qquad (17)$$

where t is in micro-seconds. It is shown dotted in Figure 10. With such values as in (17), equation (16) defied all efforts to achieve a workable form by making permissible approximations. The chief difficulty lay in determining I_1 from measureable quantities, a trial-and-error solution seeming to be the only one possible.

The situation was relieved, however, by further oscillographic measurements made to determine the actual error resulting from the use of equation (14) or (14a) in calculating current-zero-to-re-ignition times. Figure 11 shows the results. The points marked by circles were calculated from measurements made in the usual way and those marked by crosses were taken from measurements made on oscillograms such as P-2, O-1, and P-1

(Figures 12, 13, and 14, respectively). The short dotted lines represent sections of the assumed voltage rise curves upon which the calculations (according to (14) and (14a)) were based. The points from the oscillograms fall considerably closer to these lines than might be expected from the foregoing considerations. The two closely parallel lines are for the cases where the negative glow did and did not occur. The oscillogram points fall very close to the proper one of these lines in each case, the only one noticeably off being that taken from the transient in P-2 which exhibits an abnormally large value of $-e_m$. In the case of oscillogram P-1, the agreement is not so good, but this was the region in which the arc was unstable and showed large variations in re-ignition voltage. One apparent reason for this is that the voltage rise curve was very nearly tangent to the dielectric recovery curve in this region. Point 1 was calculated from the measurements taken on the oscilloscope screen while point 2 was calculated similarly except that a larger value of $-e_m$ (corresponding to P-1) was used. The dotted curve was calculated from the equation:-

$$e = 937 - 1097 \cos (0.0196\ t - 0.522) \text{ volts,} \qquad (18)$$

determined to fit the transient of P-1 as closely as possible without damping. Comparison of this curve and the curve for P-1 reveals the reason for the enigma presented by the rapid

damping shown in H-3 contrasted with the close agreement in the case of points from P-2 and O-1, the latter indicating negligible damping. The transient of P-1 follows the undamped curve calculated from equation (18) (of the form of (14)) very closely for the first 100 microseconds and then begins to fall below it at a rapidly increasing rate. This sudden falling off of the actual voltage rise curve suggests that appreciable leakage current begins to flow through the arc space only at and above some 600 or 800 volts, increasing rapidly at voltages above this value. This is just the expected characteristic of a Townsend discharge, which cannot even approximately be represented by a constant value of resistance. Clearly, then, the resistance value calculated from the damping of the oscillation of H-3 was only an average value resulting mainly from current leakage occurring near the peaks of the oscillation alone. Careful examination of the shape of the curve of Figure 10 seems to bear out this idea. The conclusion is that the damping of extinction transients gives no measure of the effective damping of the normal voltage transients preceding re-ignition, the greater portions of which remain at voltages too low for the Townsend discharge to occur. It is believed, therefore, that the evidence of Figure 11 provides sufficient justification for the use of the equations (14) and (14a), neglecting the effect of leakage current entirely.

From the above considerations it appears that an accuracy of around 5% in voltage and 10% in time is to be expected for the

dielectric recovery curves obtained in these experiments. The error in the time calculations is such that the time values plotted are probably somewhat too short. Because of the small average slope of these curves, however, it is believed that this error is comparatively unimportant. In general, an idea of the overall precision of the method is given by the closeness with which the points fall on definite smooth curves of the shape predicted by theory.

APPENDIX D.

Temperature Calculation

The temperature of the arc gases after deionization was calculated as follows:-

The value of $p\ell$ corresponding to each chosen value of re-ignition voltage was determined from Figure 57. The dotted portion is an extrapolation from the curve given by Slepian and Mason(11). The apparent pressure is then given by:-

$$p = \frac{p\ell}{\ell} \qquad (18)$$

Since this is really a value proportional to the density of the gas, the gas density is:-

$$\Delta = \frac{p}{p_o} \cdot \Delta_o \qquad (19)$$

where p_o is the actual measured pressure and Δ_o is the density at p_o and the temperature, T_o, at which p_o was measured. (T_o was taken to be 273° K. in these calculations, probably about 10% too low.) By the perfect gas law, then, the temperature of the gas is:-

$$T = T_o \cdot \frac{\Delta_o}{\Delta} = 273 \cdot \frac{p_o}{p} \qquad (20)$$

in degrees Kelvin. On the Centigrade scale it is 273° less than this. Since the arc space was not in thermal equilibrium and therefore not at constant temperature, the value of T so calculated represents only a kind of average temperature along the breakdown path. The maximum temperature between the electrodes may have been considerably greater than this value.

APPENDIX E.

Calculations of Sheath Thickness and Ion Density

Using values of T obtained from the extrapolation of the curve calculated as in Appendix D for the second recovery period, values of the space charge sheath thickness, d, were calculated from values of $p\ell$ corresponding in Figure 57 to the re-ignition voltage values of the first recovery period by dividing $p\ell$ by the value of p corresponding to the density at the existing temperature. The value, p, was obtained by equation (19) written in the form:-

$$p = p_o \frac{273}{T} \qquad (19a)$$

According to the above, therefore:-

$$d = \frac{p\ell}{p} = \frac{p\ell \cdot T}{p_o \cdot 273} \qquad (21)$$

The average breakdown gradient is then given by equation (6b):-

$$V = X\ d$$

Knowing the values of d, V, and X, the ion density, n, can be obtained from equation (4a):-

$$d = 136 \left(\frac{k}{c}\right)^{\frac{1}{3}} \frac{V^{\frac{2}{3}}}{n^{\frac{1}{3}}}$$

if k_o and $\bar{c}_o$, the ion mobility and average thermal velocity are known.

The kinetic theory expression for $\bar{c}$ is:-

$$\bar{c} = 2\sqrt{\frac{2KT}{\pi m}} \qquad (22)$$

where K is Boltzmann's constant, 1.37×10^{-16} ergs per degree, and m is the mass of the ion. Assuming the ions to be singly-charged atoms of air (oxygen or nitrogen or both) and taking the molecular weight of air to be 29,

$$m = \frac{29}{2} \times 1.65 \times 10^{-24} = 2.39 \times 10^{-23} \text{ gram},$$

1.65×10^{-24} being the mass of a particle of unit molecular weight. The velocity can be expressed as:-

$$c = \bar{c}_o \left(\frac{T}{T_o}\right)^{\frac{1}{2}}, \qquad (23)$$

where $\bar{c}_o$ is the value of $\bar{c}$ at $T = T_o$.

By formula (22), then,

$$\bar{c}_o = 63{,}200 \text{ cm. per second.}$$

The kinetic theory expression for the mobility at high field strengths is:-

$$k = \sqrt{\frac{2 e \lambda}{\pi m X}} \qquad (24)$$

where λ is the ionic mean free path.

Because of the effect of temperature on density, λ is proportional to T at constant pressure and so the mobility also can be expressed as:-

$$k = k_o' \left(\frac{T}{T_o}\right)^{\frac{1}{2}} \qquad (25)$$

The effect of temperature thus cancels out in the expression $k/\bar{c}$ of equation (4a). Defining k_o as the ion mobility at standard conditions and at unit field strength leads to the relation:-

$$k = k_o \left(\frac{T}{T_o}\right)^{\frac{1}{2}} X^{-\frac{1}{2}} \qquad (26)$$

which in turn gives for (4a) the new form:-

$$d = 136 \left(\frac{k_o}{\overline{c}_o}\right)^{\frac{1}{3}} \frac{V^{\frac{2}{3}}}{X^{\frac{1}{6}}\ n^{\frac{1}{3}}} \qquad (4b)$$

The value of λ to use in calculating k_o is somewhat uncertain, but the value for nitrogen molecules under standard conditions, 0.6×10^{-5}, should be approximately right. Using this and other previously determined values gives:-

$$k_o = 505 \text{ cm. per second.}$$

per volt per cm. at 1 volt per cm.

Substituting these values in equation (4b) gives:-

$$d = 136 \sqrt[3]{\frac{505\ V^2}{63{,}200\ X^{\frac{1}{2}}\ n}} = \frac{27.2\ V^{\frac{2}{3}}}{X^{\frac{1}{6}}\ n^{\frac{1}{3}}} \qquad (27)$$

When solved for n this becomes:-

$$n = \frac{20{,}200\ X^{\frac{5}{2}}}{V} \qquad (27a)$$

which may be combined with (6b) to give:-

$$n = \frac{20{,}200\ X^{\frac{3}{2}}}{d} \qquad (7b).$$

APPENDIX F.

Investigation of Deionizing Processes

1. Recombination. To determine whether or not recombination alone is sufficient to explain the deionization curve of Figure 38, this process was assumed and the values of the recombination coefficient, α, required to fit the curve at each point were calculated. For recombination in a region containing equal numbers of positive and negative ions, α is defined by the equation:-

$$\frac{dn}{dt} = - \alpha n^2 \qquad (8)$$

α can be calculated directly from this equation, using measurements of $-\frac{dn}{dt}$ and corresponding values of n from the ion density curve of Figure 38. The results of this calculation are given in column 5 of the table. For comparison with usual values, extrapolations of these to 0° C. are given in column 6. This extrapolation was made by means of the equation:-

$$\alpha_o = \alpha \left(\frac{T}{T_o}\right)^3 \qquad (28)$$

using values of temperature from the dotted curve of Figure 38. Even the smallest value of α_o in column 6, that for 5 microseconds, is roughly 20 times the value ordinarily measured for air, 1.6×10^{-6}, and the required value of α_o increases with time by almost as much as ten times more at 43 microseconds.

Since the presence of metal vapor in the arc gases can hardly be expected to raise the coefficient of recombination, it seems clear that recombination is inadequate by at least one order of magnitude as an explanation of the observed rate of deionization.

2. Diffusion. A similar calculation was made assuming only one-dimensional diffusion to the electrode and to the sheath boundaries. To simplify the calculations, which would otherwise be long and tedious, the ion density distribution shown by the solid line in Figure 58 was assumed. A rough estimate of the actual ion distribution is given by the dotted curve labeled n'. The field-free, or plasma region of thickness ℓ-d was arbitrarily divided into four parts and all of the diffusion gradient assumed to exist across the outer fourths of the region. This assumed gradient was then:-

$$\frac{dn}{dx} = \pm \frac{4n}{\ell - d} \qquad (29)$$

The total number of ions per square centimeter of the arc cross-section diffusing away per second was then:-

$$\gamma = 2 D \frac{dn}{dx} = \frac{8 n}{\ell - d} D \qquad (30)$$

in terms of the diffusion coefficient, D. The relative rate of loss of ions in the plasma was:-

$$- \frac{dn}{dt} = \frac{\gamma}{\ell - d} = \frac{8 n}{(\ell - d)^2} D \qquad (31)$$

From this relation, D was calculated, using values from the curve of Figure 38 as before. Values of D are given in column 7 of the

table. For comparison, corresponding values of D_T, the kinetic theory diffusion coefficient, were calculated from the relation:-

$$D_T = \frac{1}{3}\lambda \bar{c} = \frac{1}{3}\lambda_o \bar{c}_o \left(\frac{T}{T_o}\right)^{\frac{3}{2}} \qquad (32)$$

and entered in column 8.

The values used were:-

$\lambda_o = 10^{-5}$ cm.

$\bar{c}_o = 63{,}000$ cm. per sec.

$T_o = 273^\circ$ K.

and T determined from Figure 38.

The ratios of values of D apparently required to the kinetic theory values at the estimated temperatures are given in column 9. The two quantities are clearly always of the same order of magnitude, which is as good agreement as could be expected from these very rough calculations. As pointed out in the discussion, the effect of diffusion laterally into the surrounding cooler gas would be in such a direction as to improve the agreement. The fact that the ratio D/D_T remains very nearly constant (between 4 and 7) during the first 30 microseconds, and could be made to remain so for the rest of the time by altering the dielectric recovery curve in a way which would be consistent with the data, is another point in favor of the diffusion theory.

APPENDIX F.

Table: Values from Figure 38.

1	2	3	4	5	6	7	8	9
t μsec.	V volts	n ions/cm.^{3} x 10-12	$-\frac{dn}{dt}$ x 10-16	α x 10^8	α_o x 10^5	D	D_T	D/D_T
5	370	4.37	25	1.31	3.08	50	10.2	4.9
10	393	3.27	22.6	2.115	4.32	57	9.5	4.8
15	425	2.06	18.6	4.38	7.93	31	8.9	4.8
20	475	1.33	12.6	7.12	11.5	58	8.5	6.8
25	540	0.826	7.68	11.26	16.1	43	8.0	5.4
30	610	0.557	4.87	15.67	19.8	28	7.5	3.7
35	710	0.343	2.6	22.04	25.4	11	7.1	1.6
40	840	0.226	1.067	20.9	21.8	11	6.8	1.6
43	940	0.184	0.88	26.0	25.5	0	6.6	0

APPENDIX G.

Motion of the Arc

Figures 59 through 70 are photographs of the electrodes after tests under various conditions. Both electrodes are shown, arranged as if opened out like a book, the lower electrode being on the left in every figure except No. 69. A centimeter scale is provided at the top, showing that the pictures are almost exactly natural size. In the titles below the pictures e_s is the re-ignition voltage and t_s the re-ignition time for the test after which each photograph was taken.

1. General Description. All the different types of arc trails commonly observed are shown. Their chief general characteristic is the spontaneous wandering of the arc over the electrode surfaces in almost every case. This wandering, sometimes slow and sometimes very fast, generally occurred in jumps, the arc terminals appearing to remain in one spot for one or more half-cycles. Many of the photographs show clear examples of spots in which the arc apparently remained for only one half-cycle. Perhaps the clearest is Figure 59, in which the small isolated spots show distinct differences between the corresponding ones on the two electrodes, suggesting that the arc remained at each only while it had one certain polarity and therefore for only one half-cycle. Both types of spots, distinctly different, can be observed on each electrode, the two types usually being side by side. Figures 59, 63, and 69 show trails upon which the arc moved only very

slowly while in the case of Figure 64 the arc remained stationary until blown by a current of air. The trail of Figure 63 is one of the few observed in which the motion of the arc appeared to be practically continuous, but definite spots can be observed near its end. Trails of very rapidly moving arcs are shown in Figures 60, 65, 66, and 68. These are characterized by the distinctness and the wide distribution of the spots over the electrode surfaces.

2. Effect of Arc and Circuit Conditions. The boundaries of the spots become less and less distinctly marked as the electrode separation is increased. As shown by comparison of Figures 59 through 64, the apparent spot size, or area burned by the arc, tends to increase rapidly with the arc length, other conditions being equal. This shows the need for caution in estimating the current density at the arc terminals from photographs of arc trails. Incidentally, all of the clear-cut spots in these photographs indicate current densities of many thousands of amperes per square centimeter, higher at the cathode (darker spots) than at the anode (lighter spots). This agrees with the essential requirement of Langmuir's high field theory of the arc cathode(15) Figures 59 and 60 show trails of the arc with all conditions

---

(15) Slepian and Haverstick, "Arcs with Small Cathode Current Density", Physical Review 33, p. 52 (1929).

identical except the speed of the circuit. They illustrate the always observed fact that the rate of wandering of the arc increased roughly with the length of the zero-current period, t_s. Figures 61 and 62 illustrate the differences which sometimes existed between arc trails with all conditions the same. Within certain ranges of conditions motion of the arc was very erratic, the arc sometimes moving rapidly and sometimes slowly or not at all. As in these two cases, the re-ignition voltage was generally somewhat and often very much higher when the arc was wandering rapidly than when it was almost or quite stationary. The attempt was made for the sake of uniformity to record only those measurements made with the arc wandering, but exceptions to this rule may sometimes have occurred where the motion was erratic. This is believed to be the explanation of the peculiar break in the recovery curve of Figure 18. The tendency of the arc to move also decreased with increase in the electrode separation, with pressure and with current strength. At the larger separations, pressures and currents, the arc would frequently wander readily when first struck but after several re-startings with the igniter electrode would burn steadily at the starting point without further wandering. The re-ignition voltage was observed to fall steadily with time in these cases, which was another reason for recording readings only with the arc wandering. In

general, very little difference was noticed between the arc trails at the different currents and pressures used. Trails of 12.5-ampere arcs are shown in Figures 66 and 67 and of 50-ampere arcs in Figures 69 and 70. One photograph of a trail at 1/4 atmosphere pressure is shown in Figure 68. The peculiar fine markings shown in Figure 67 seem to suggest that the arc terminals wandered in this case even while the current was flowing and not just between half-cycles as it usually appeared to do. It seems possible, also, that discrepancy between the current density in the positive column and at the cathode for these longer arcs may have resulted in the formation of several adjacent small cathode spots carrying the current from the relatively large positive column in parallel..

3. Explanation. The cause of this wandering seems reasonably clear. It is simply that re-ignition of the arc generally occurred at a point somewhat removed from the place last occupied by the arc. This may have been due to actual motion of the hot ionized gas region during the current zero period, or the re-ignition may have occurred first along a path to one side of the recently-conducting gas region. This last explanation appears to be the more probable for the cases of rapid motion while the first may easily apply to the cases of slow motion. The widespread distribution of the spots in figures like No. 60, seemingly with less than purely random clustering, lends support to the second

explanation for the fast moving arcs. The fact that rapid wandering occurs only for reignition of the second type, after complete deionization of the space has occurred, gives further support to this idea. The first possible explanation occurring to the writer of higher dielectric strength in the center than to one side of the old arc core is that cooling of the gas opposite the arc terminals may be accelerated by a vapor blast from them to such an extent that after deionization its density and therefore its dielectric strength may be higher than that of gas to one side which has recently passed through the arc core but has moved beyond the cooling influence of the vapor blast and so remains at a higher temperature than the gas nearer the arc terminals.

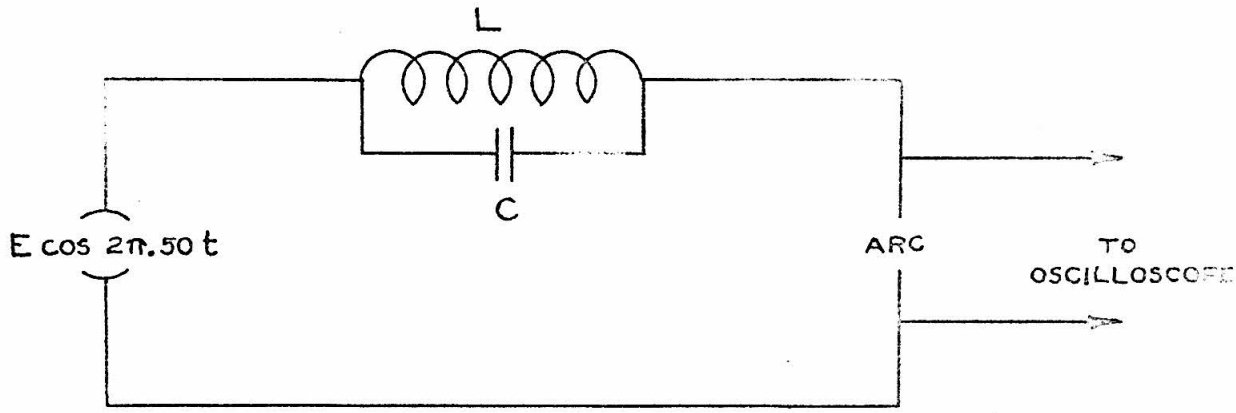

SCHEMATIC CIRCUIT DIAGRAM FIG. 1.

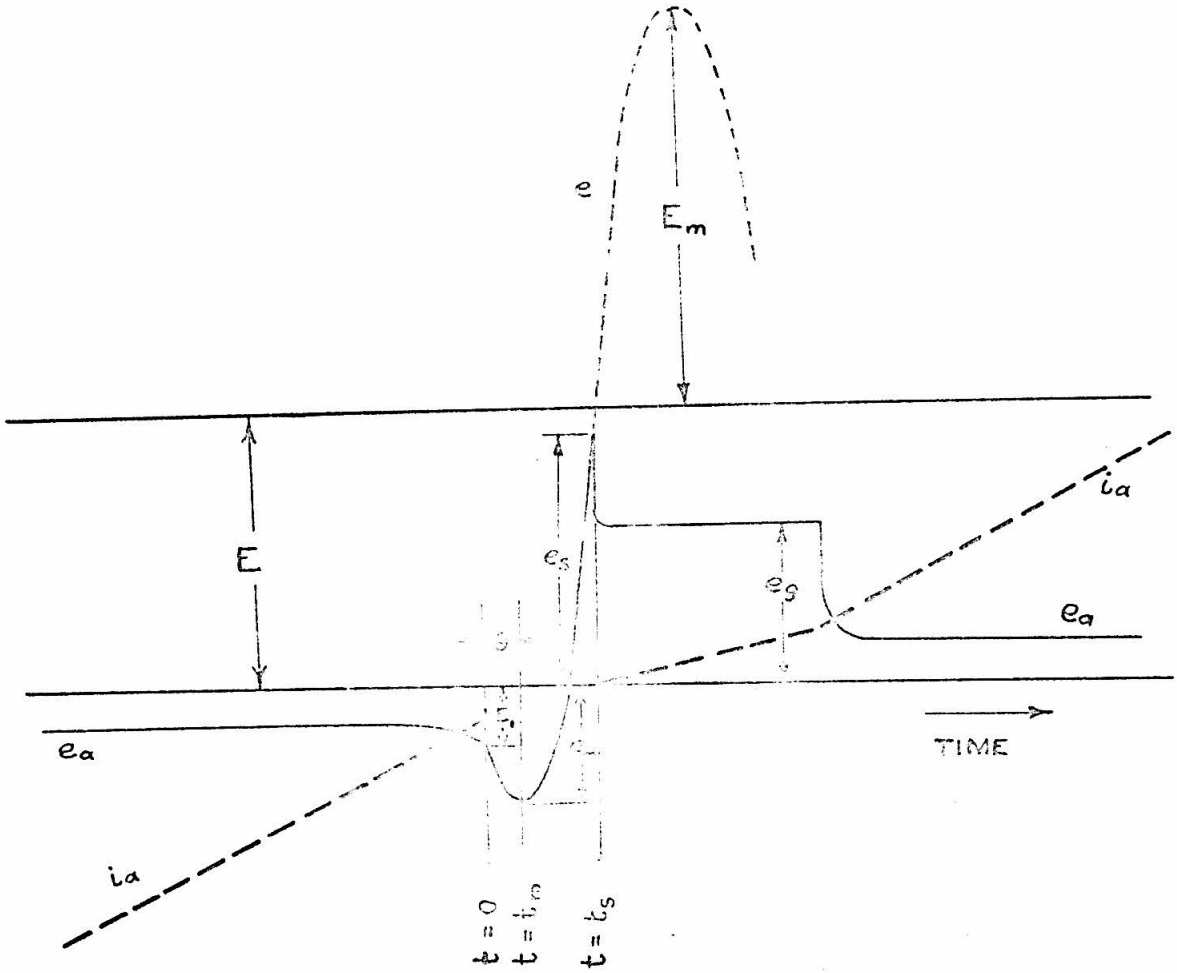

CURRENT AND VOLTAGE RELATIONS NEAR CURRENT ZERO FIG. 2.

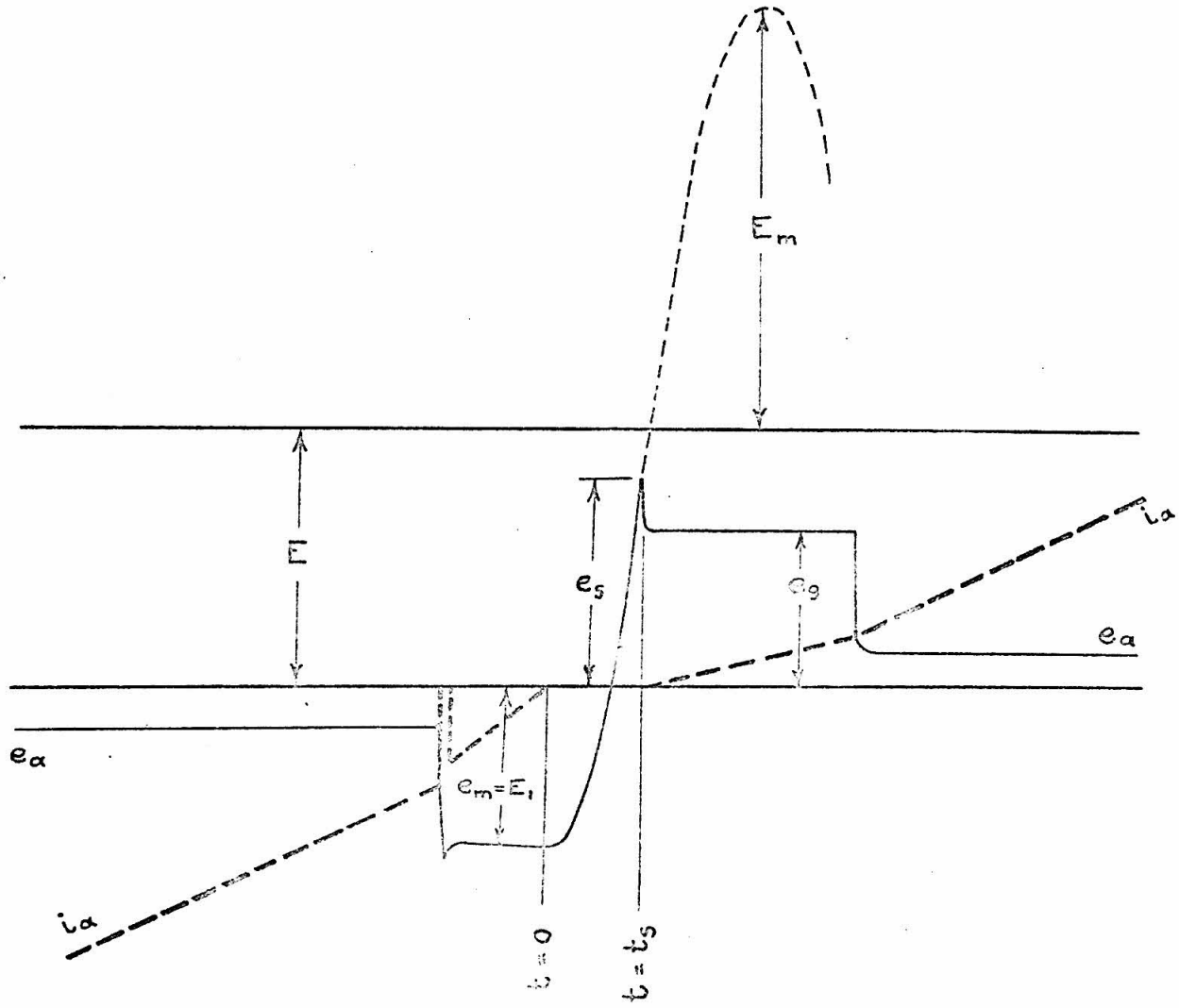

CURRENT AND VOLTAGE RELATIONS NEAR CURRENT ZERO - NEGATIVE GLOW CASE

FIG. 3.

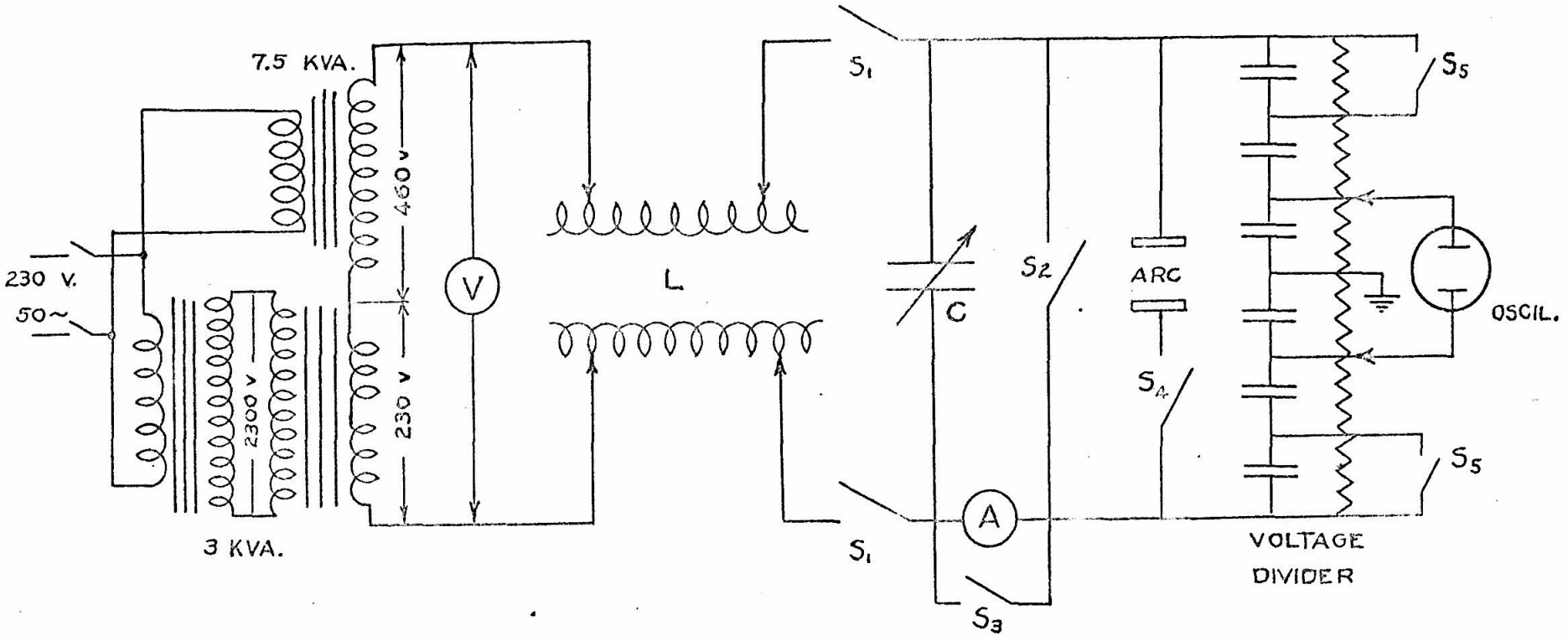

FIG. 4 - CIRCUIT DIAGRAM

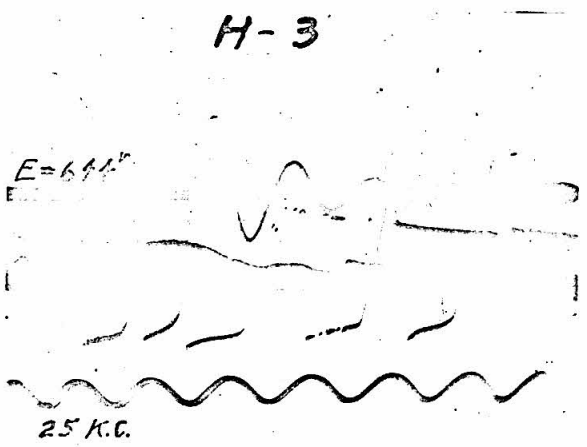

Figure 9. Oscillogram of Extinction Transient.

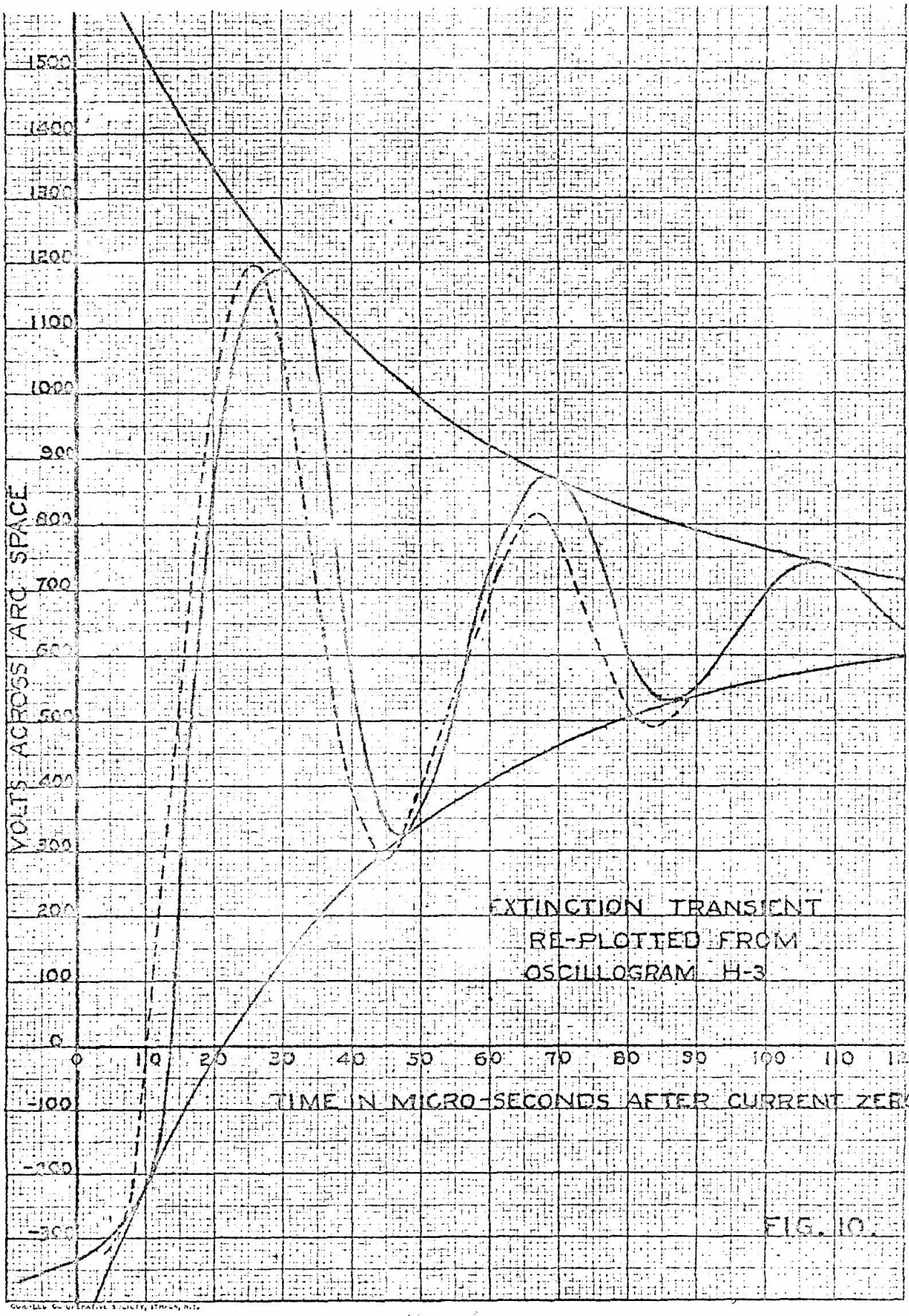

FIG. 10.

Curve No._____ Signature_____ Date_____

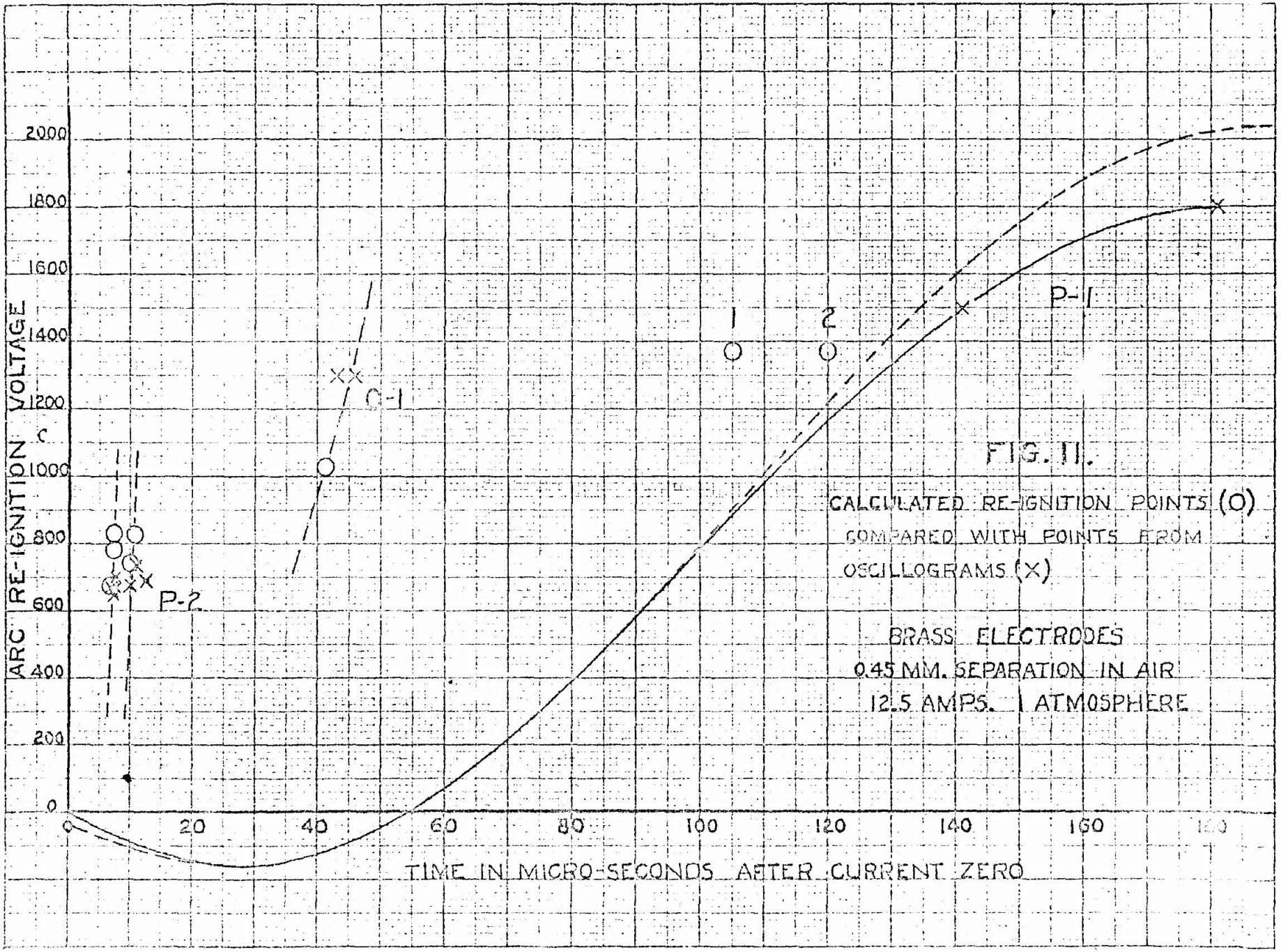
ARC RE-IGNITION VOLTAGE
2000
1800
1600
1400
1200
1000
800
600
400
200
0
0
20
40
60
80
100
120
140
160
TIME IN MICRO-SECONDS AFTER CURRENT ZERO
P-1
P-2
C-1
1
2
FIG. II.
CALCULATED RE-IGNITION POINTS (O)
COMPARED WITH POINTS FROM
OSCILLOGRAMS (X)
BRASS ELECTRODES
0.45 MM. SEPARATION IN AIR
12.5 AMPS. 1 ATMOSPHERE

Curve No. _____ Signature _____ Date _____

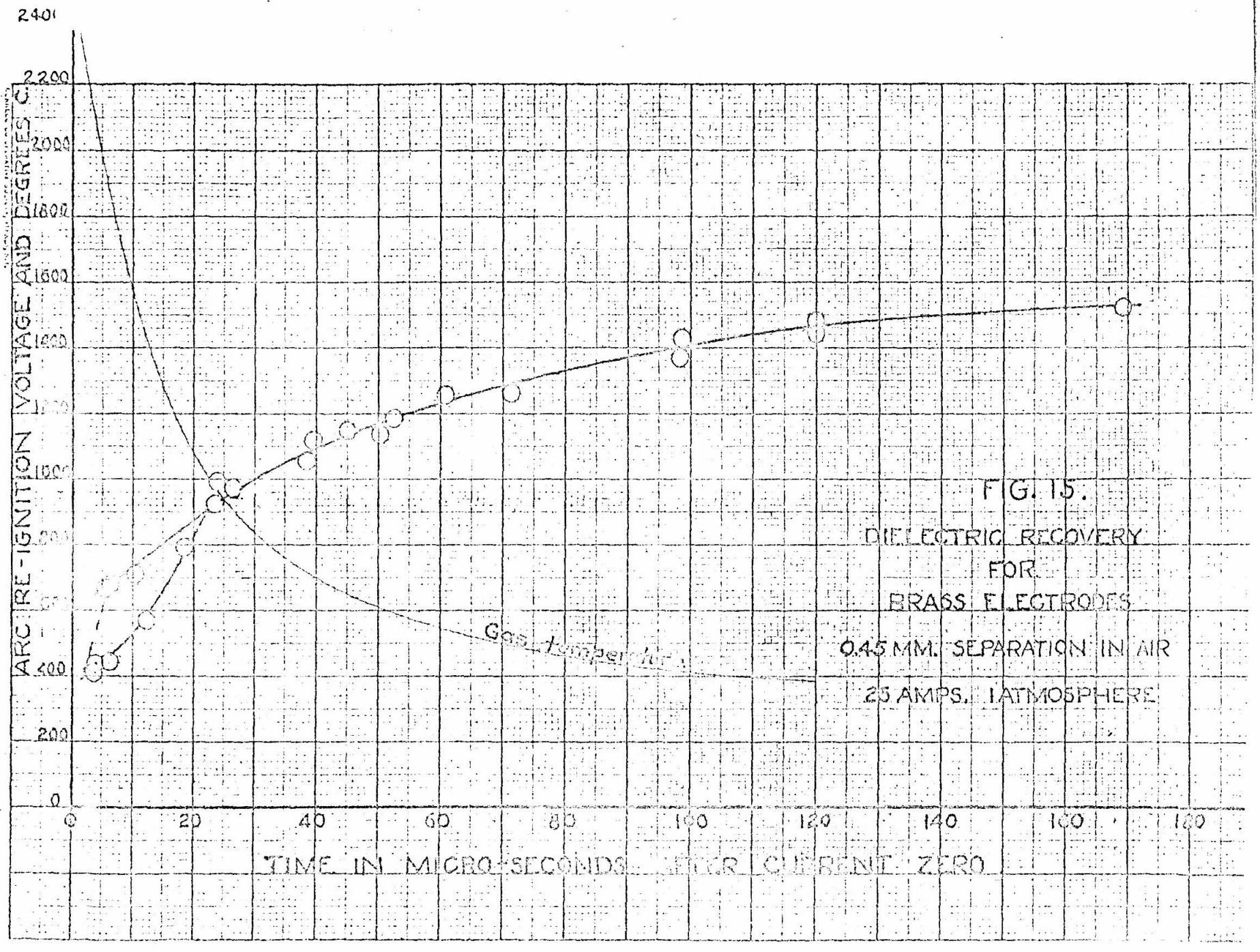

FIG. 15.

DIELECTRIC RECOVERY
FOR
BRASS ELECTRODES
0.45 MM. SEPARATION IN AIR
25 AMPS. 1 ATMOSPHERE

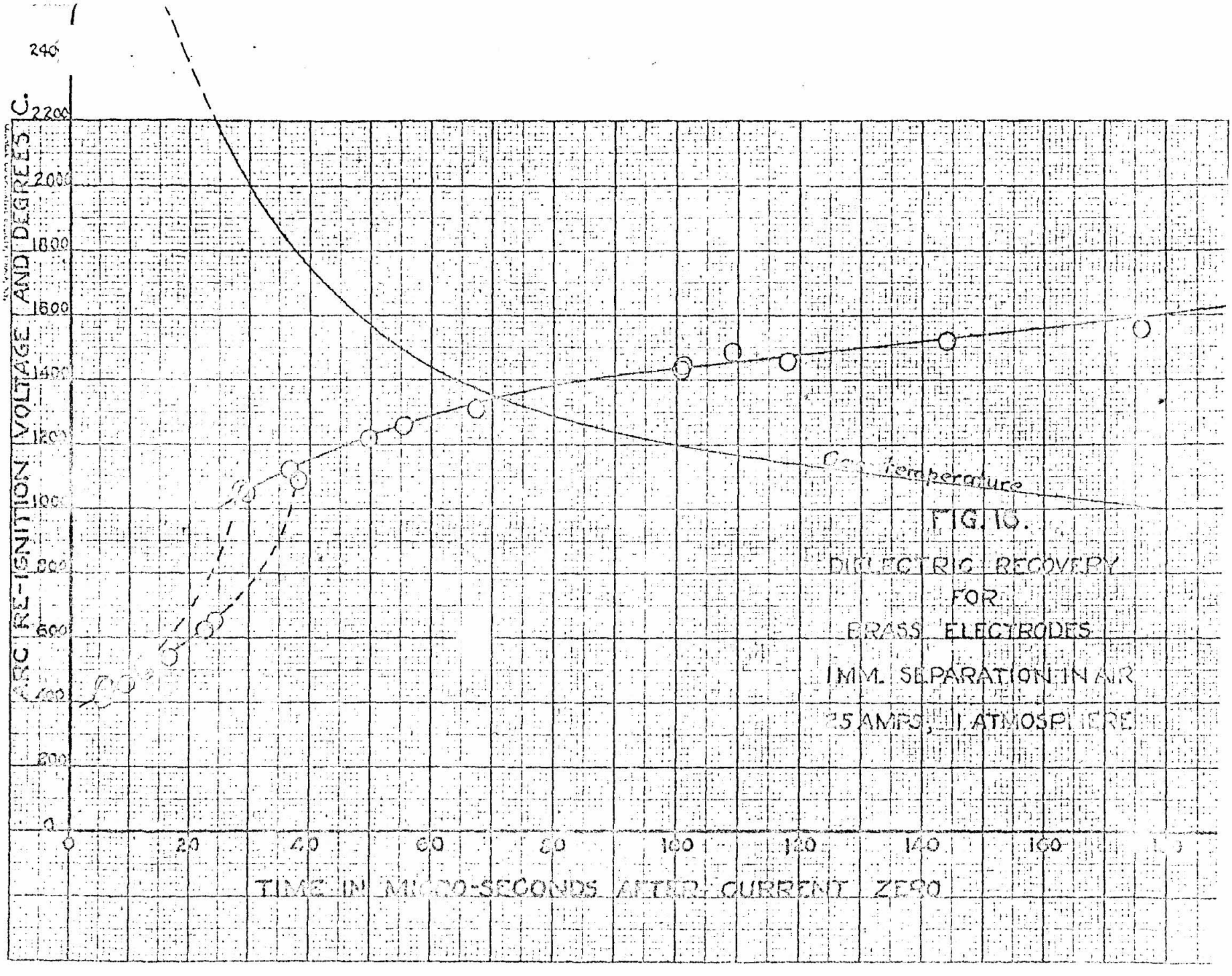

FIG. 10.

DIELECTRIC RECOVERY FOR BRASS ELECTRODES

1 MM. SEPARATION IN AIR

25 AMPS, 1 ATMOSPHERE

Curve No._____ Signature_____ Date_____

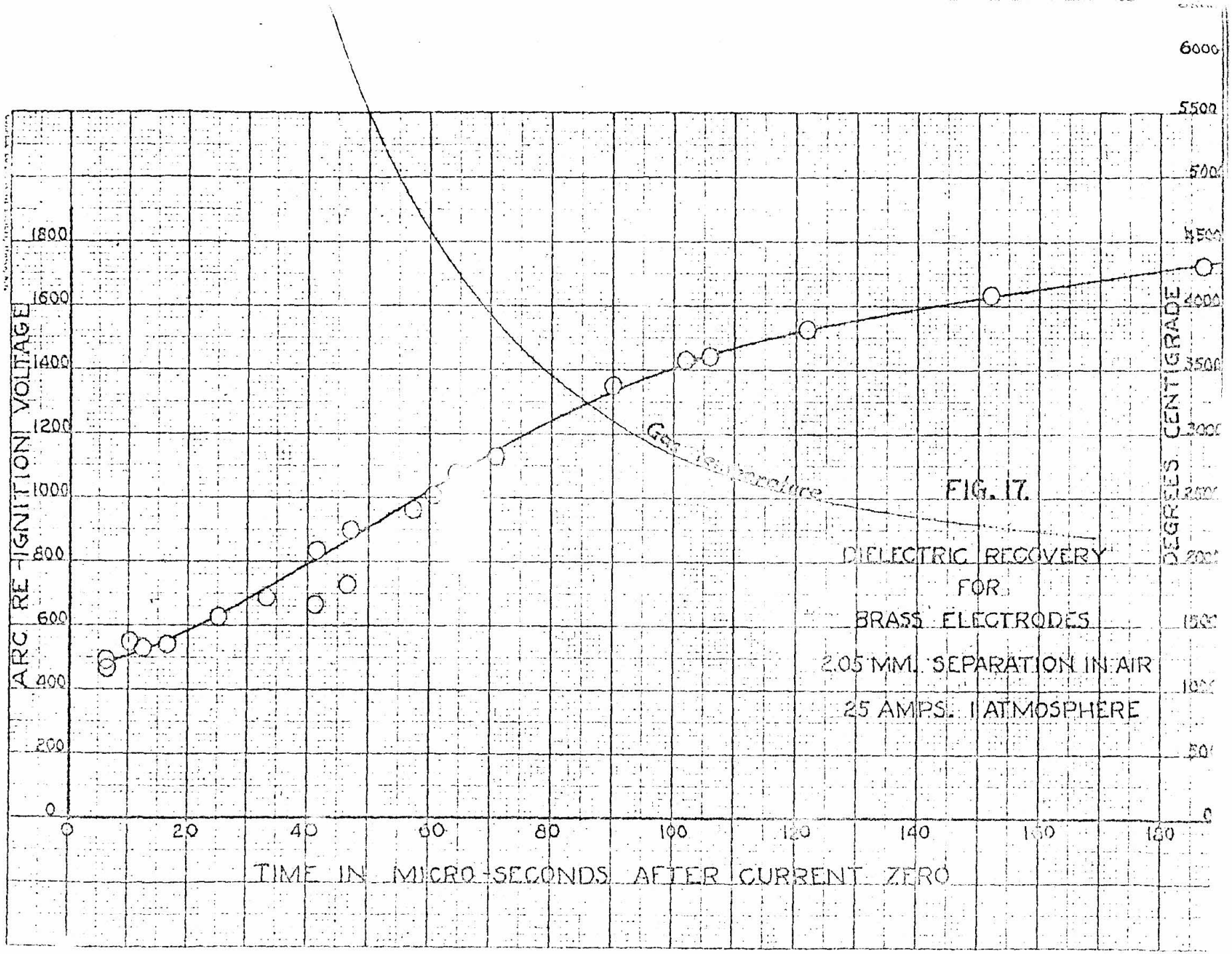

Curve No. _____ Signature _____ Date _____

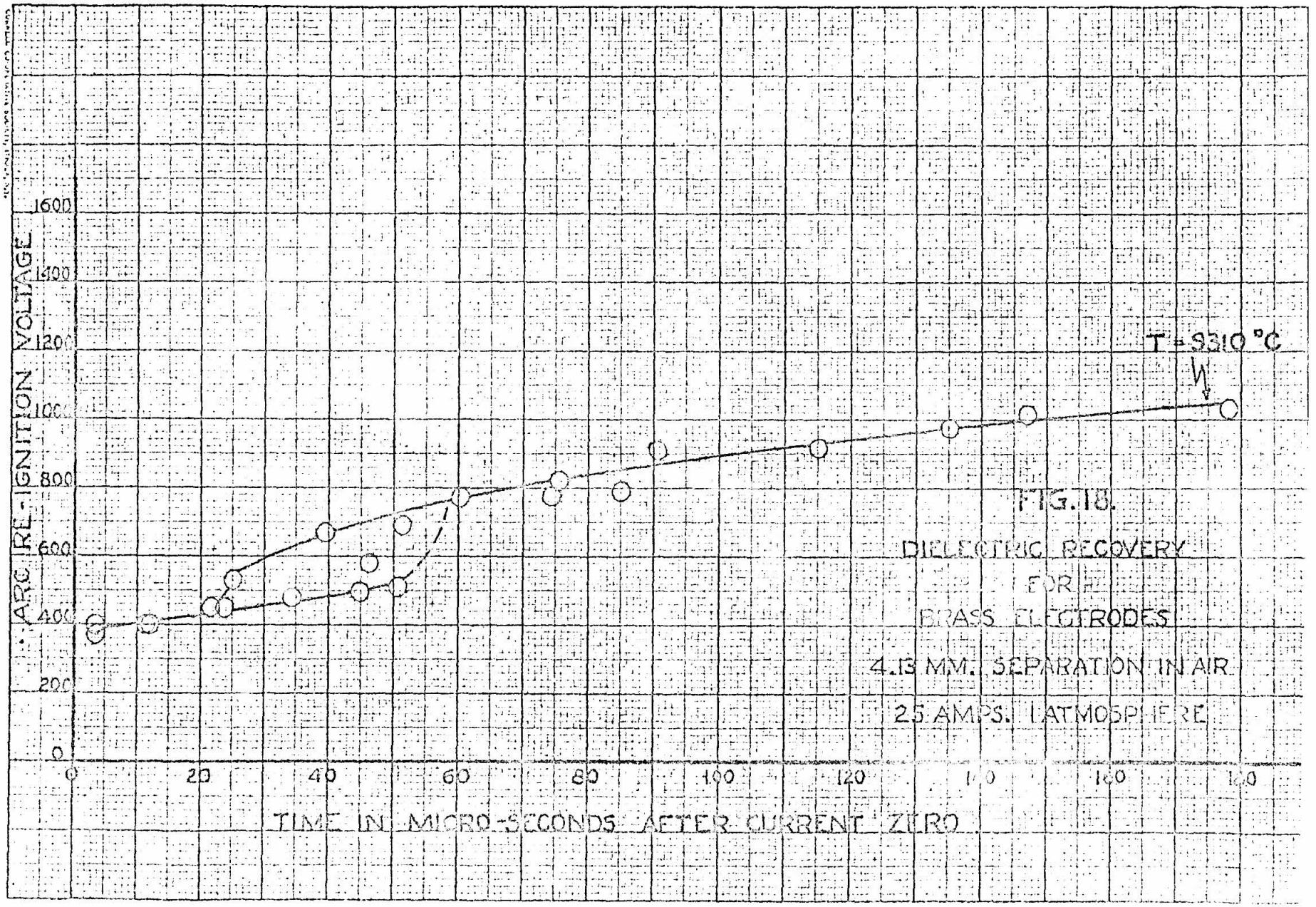

FIG. 18.

DIELECTRIC RECOVERY FOR BRASS ELECTRODES

4.13 MM. SEPARATION IN AIR

25 AMPS. ATMOSPHERE

Curve No. _____ Signature _____ Date _____

Curve No. _____ Signature _____ Date _____

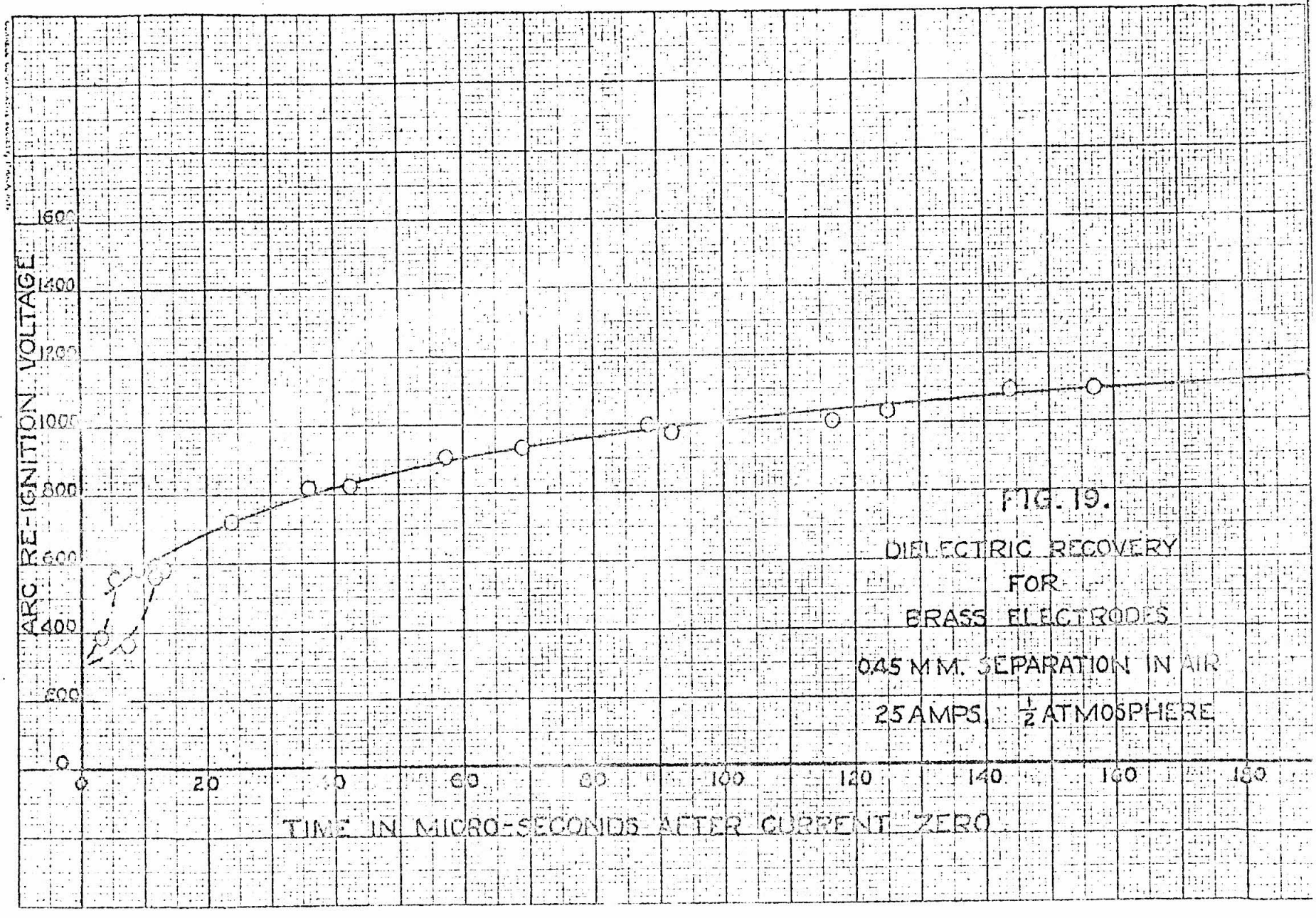

FIG. 19.

DIELECTRIC RECOVERY

FOR

BRASS ELECTRODES

.045 M.M. SEPARATION IN AIR

25 AMPS. $\frac{1}{2}$ ATMOSPHERE

Curve No. _____ Signature _____ Date _____

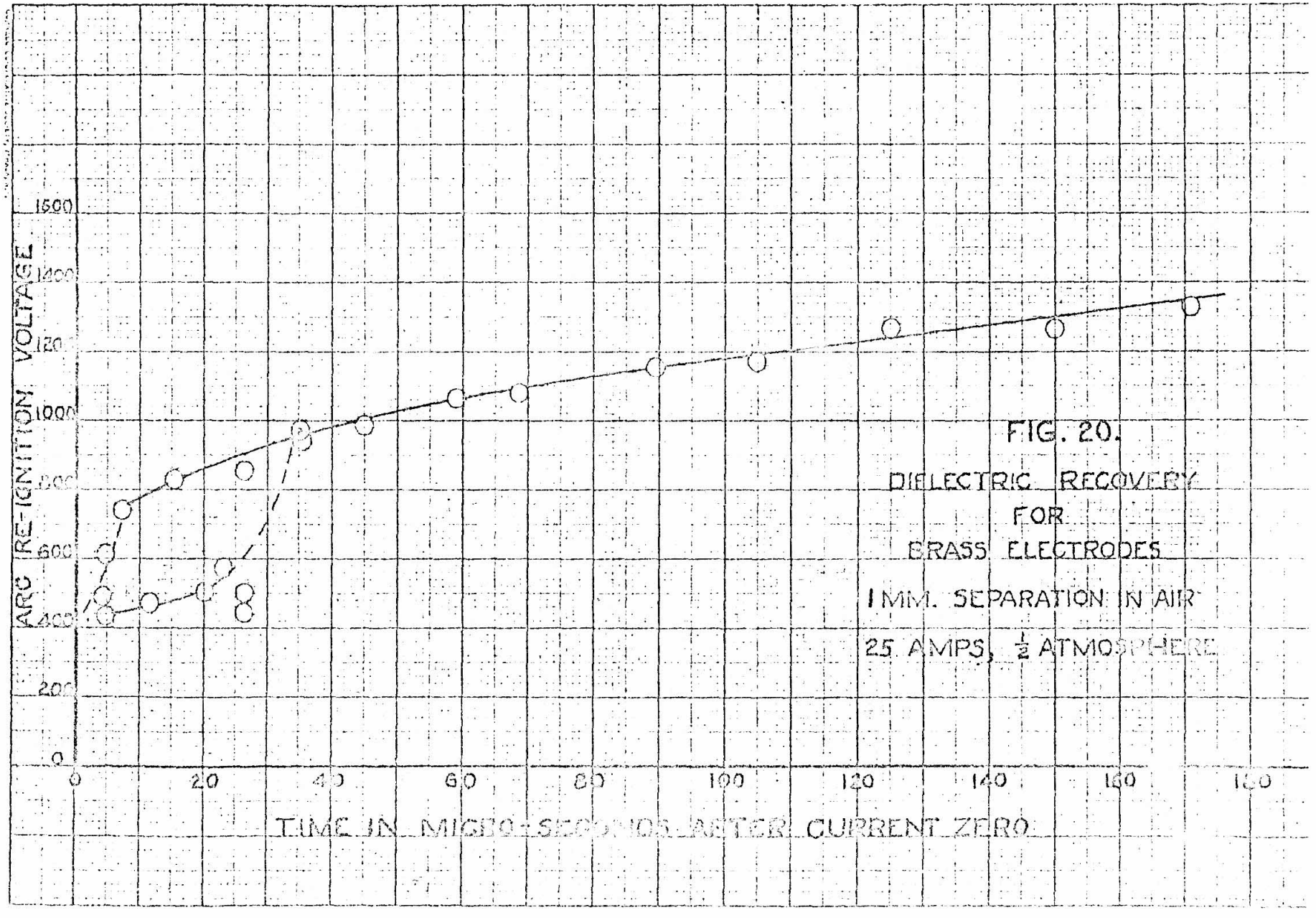

FIG. 20.

DIELECTRIC RECOVERY FOR BRASS ELECTRODES

1 MM. SEPARATION IN AIR

25 AMPS, $\frac{1}{2}$ ATMOSPHERE

Curve No. _____ Signature _____ Date _____

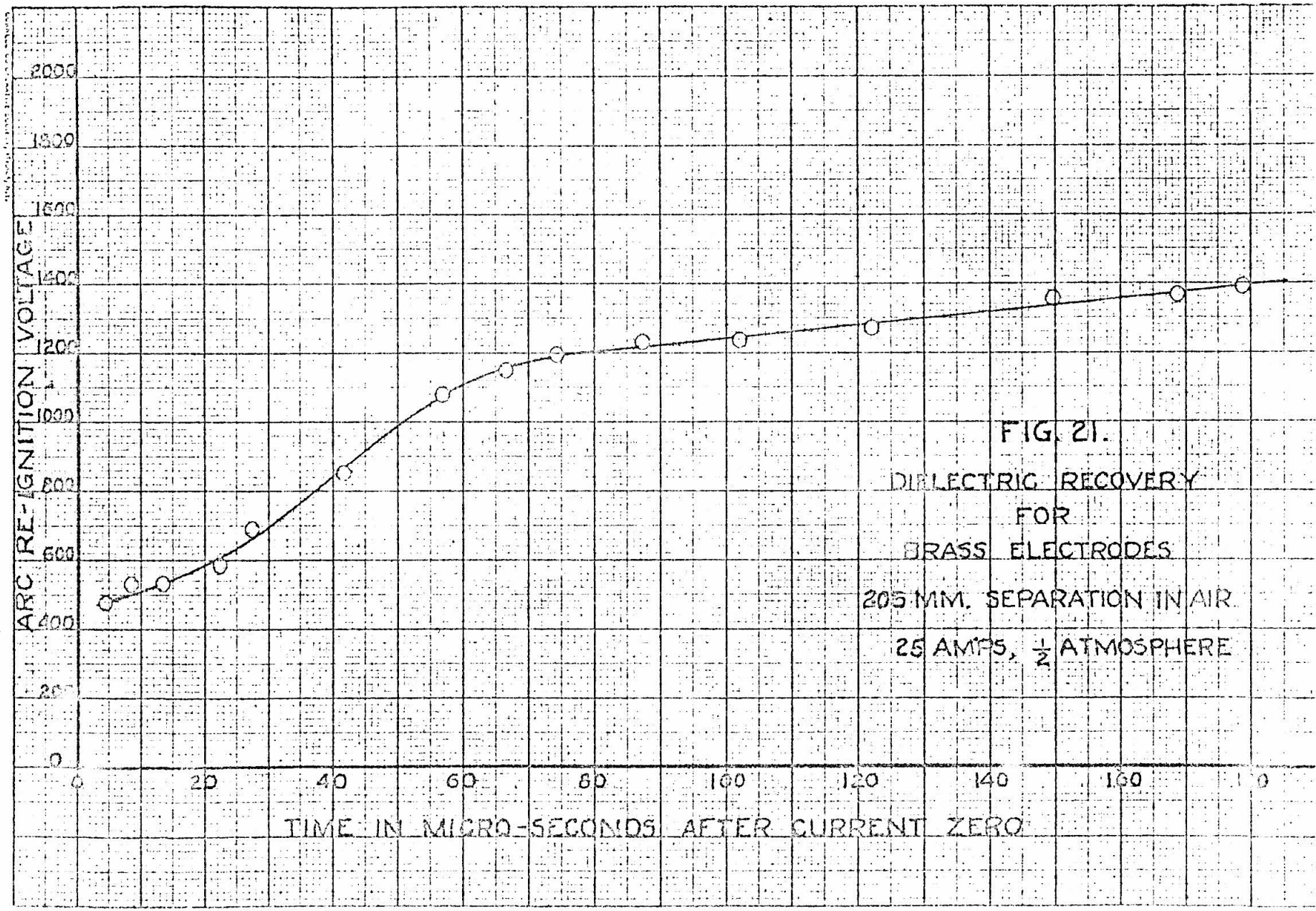

FIG. 21.

DIELECTRIC RECOVERY FOR BRASS ELECTRODES

2.05 MM. SEPARATION IN AIR

25 AMPS, $\frac{1}{2}$ ATMOSPHERE

Curve No. _____ Signature _____ Date _____

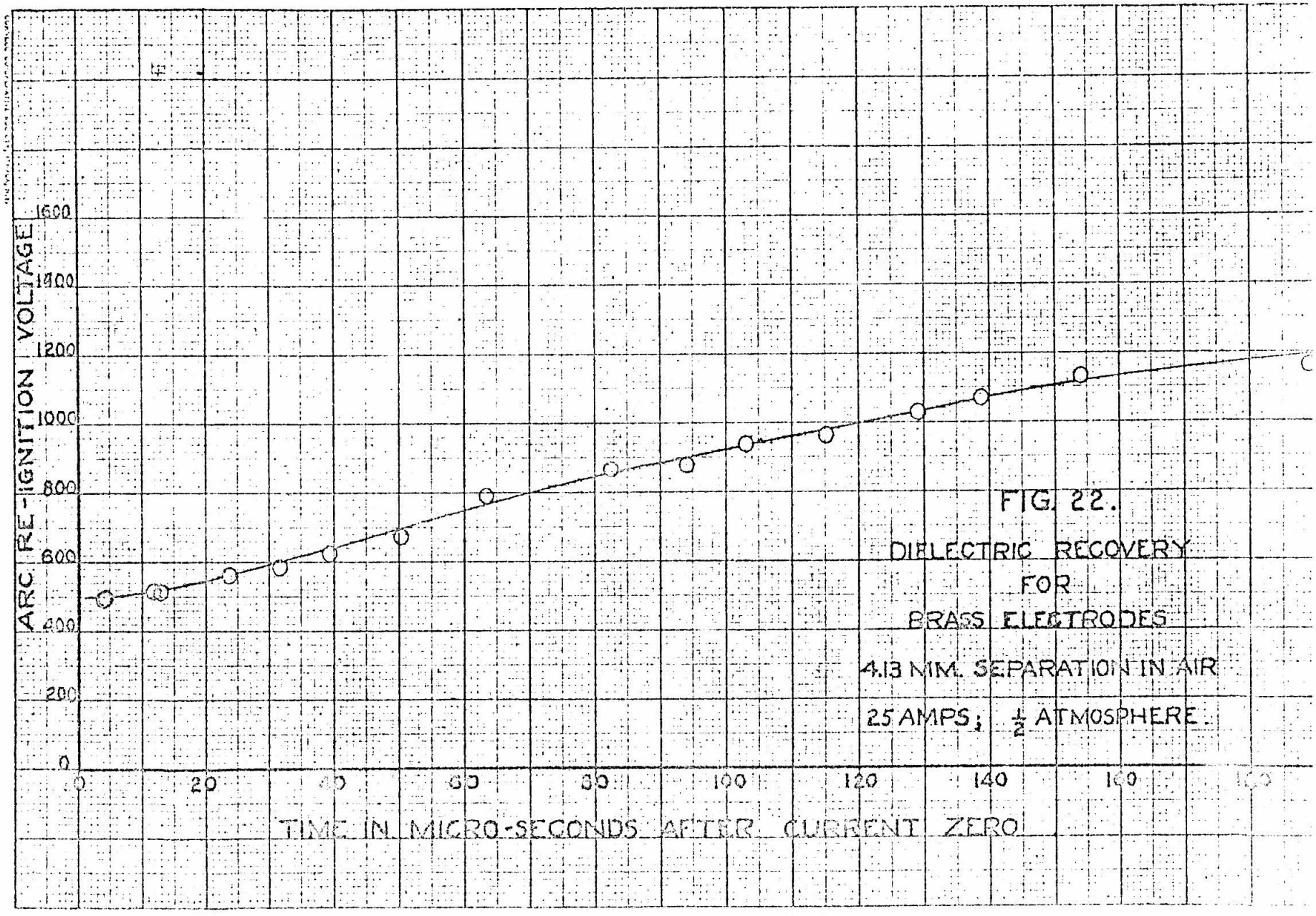

FIG. 22.

DIELECTRIC RECOVERY FOR BRASS ELECTRODES

4.13 MM. SEPARATION IN AIR

25 AMPS; $\frac{1}{2}$ ATMOSPHERE.

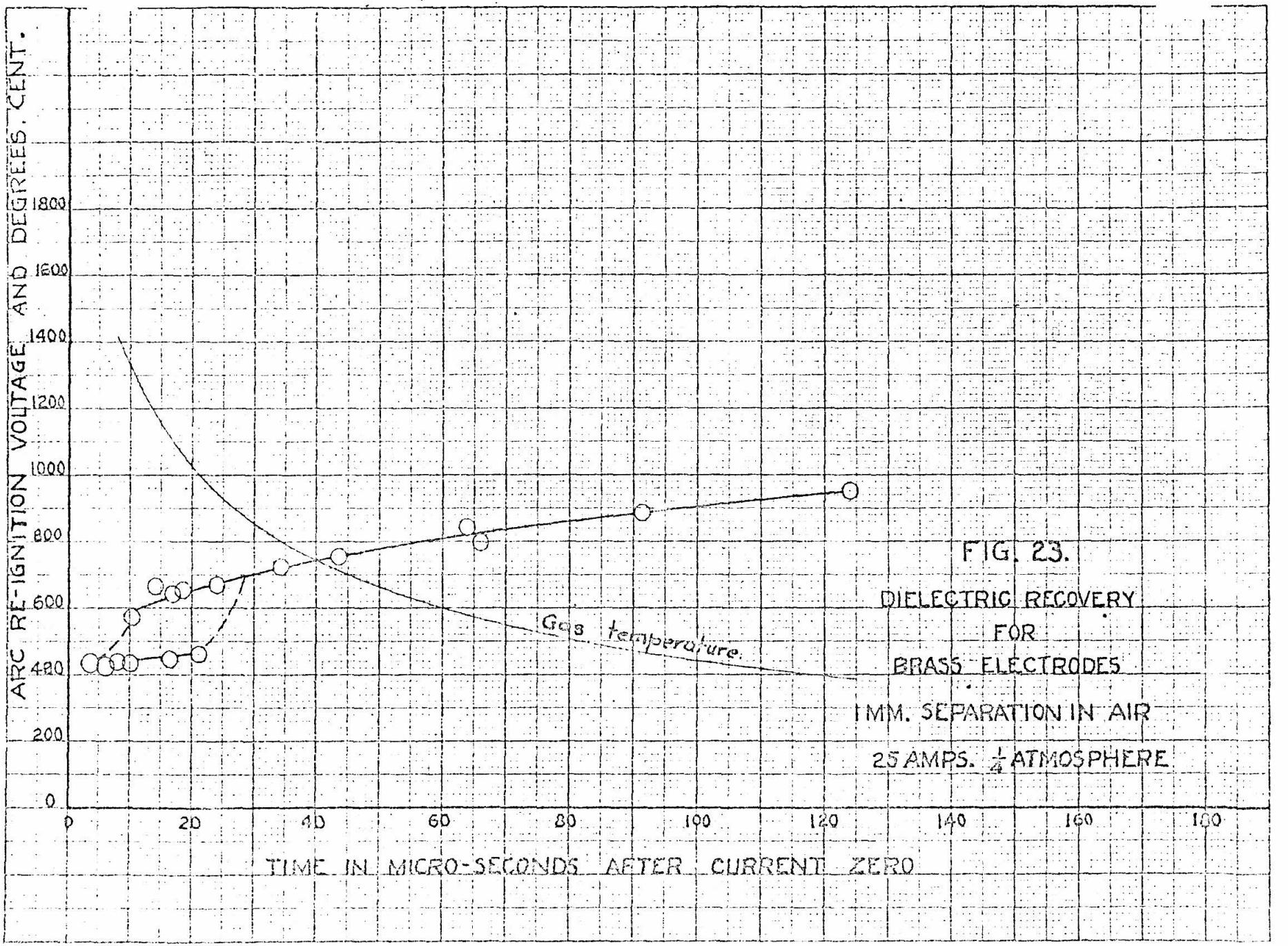

FIG. 23.

DIELECTRIC RECOVERY
FOR
BRASS ELECTRODES
1 MM. SEPARATION IN AIR
25 AMPS. $\frac{1}{4}$ ATMOSPHERE

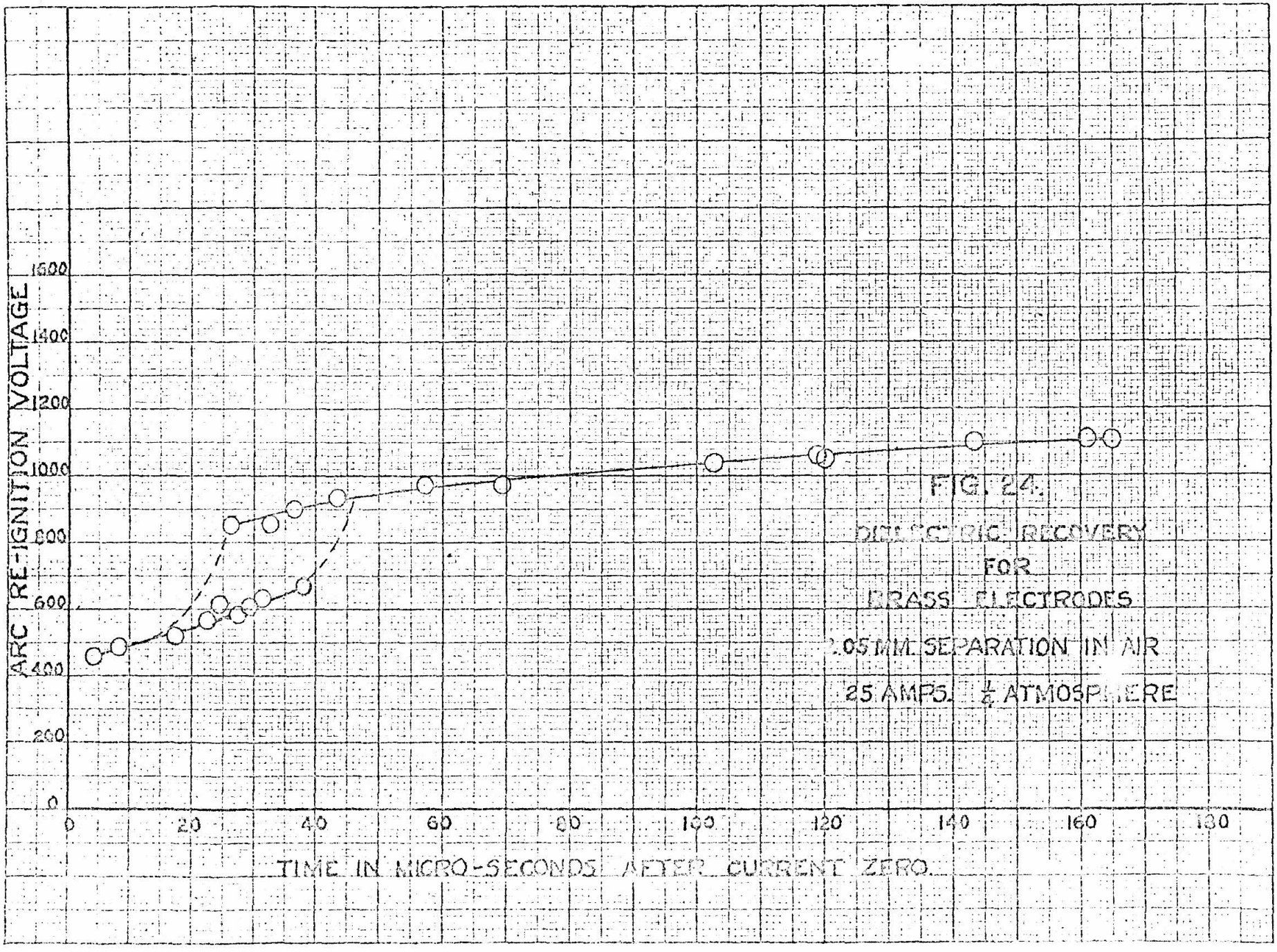

FIG. 24.

DIELECTRIC RECOVERY
FOR
BRASS ELECTRODES
.05 MM. SEPARATION IN AIR
25 AMPS. ½ ATMOSPHERE

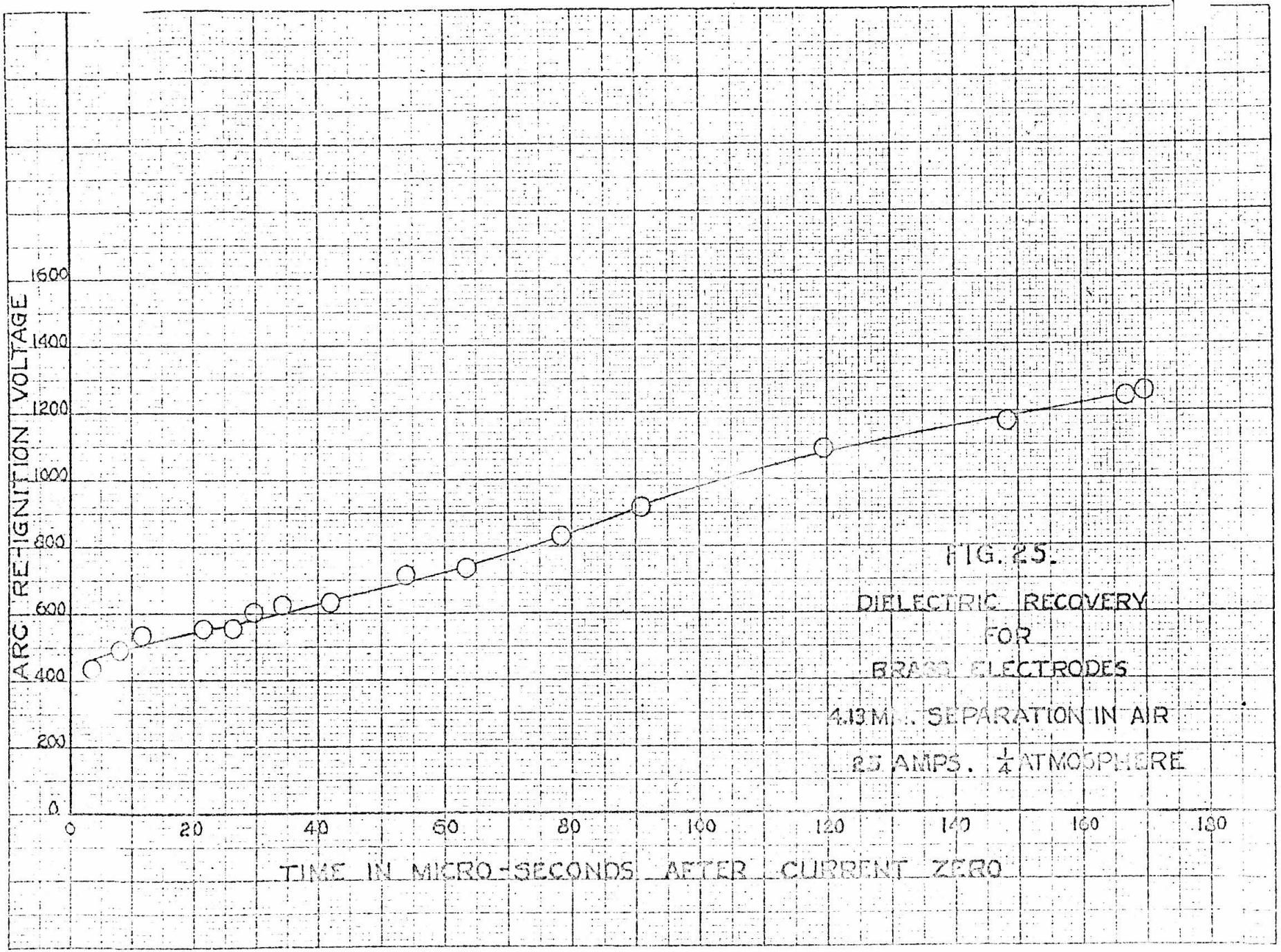
ARC RE-IGNITION VOLTAGE
1600
1400
1200
1000
800
600
400
200
0
0
20
40
60
80
100
120
140
160
180
TIME IN MICRO-SECONDS AFTER CURRENT ZERO
DIELECTRIC RECOVERY
FOR
BRASS ELECTRODES
4.13 M.M. SEPARATION IN AIR
25 AMPS. 1/4 ATMOSPHERE

FIG. 25.

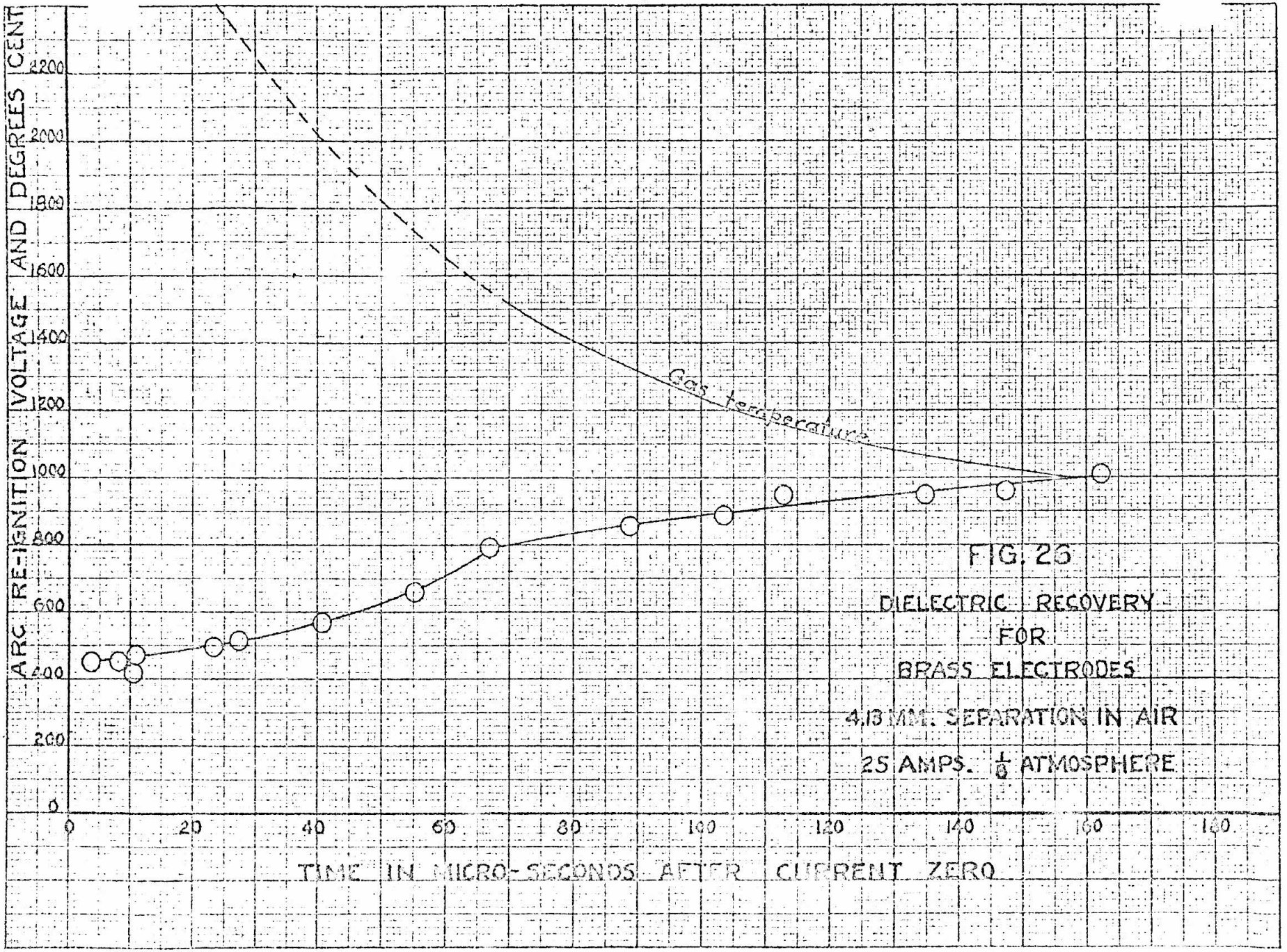

FIG. 26

DIELECTRIC RECOVERY FOR BRASS ELECTRODES 4.13 MM. SEPARATION IN AIR 25 AMPS. $\frac{1}{6}$ ATMOSPHERE

Curve No._____ Signature_____ Date_____

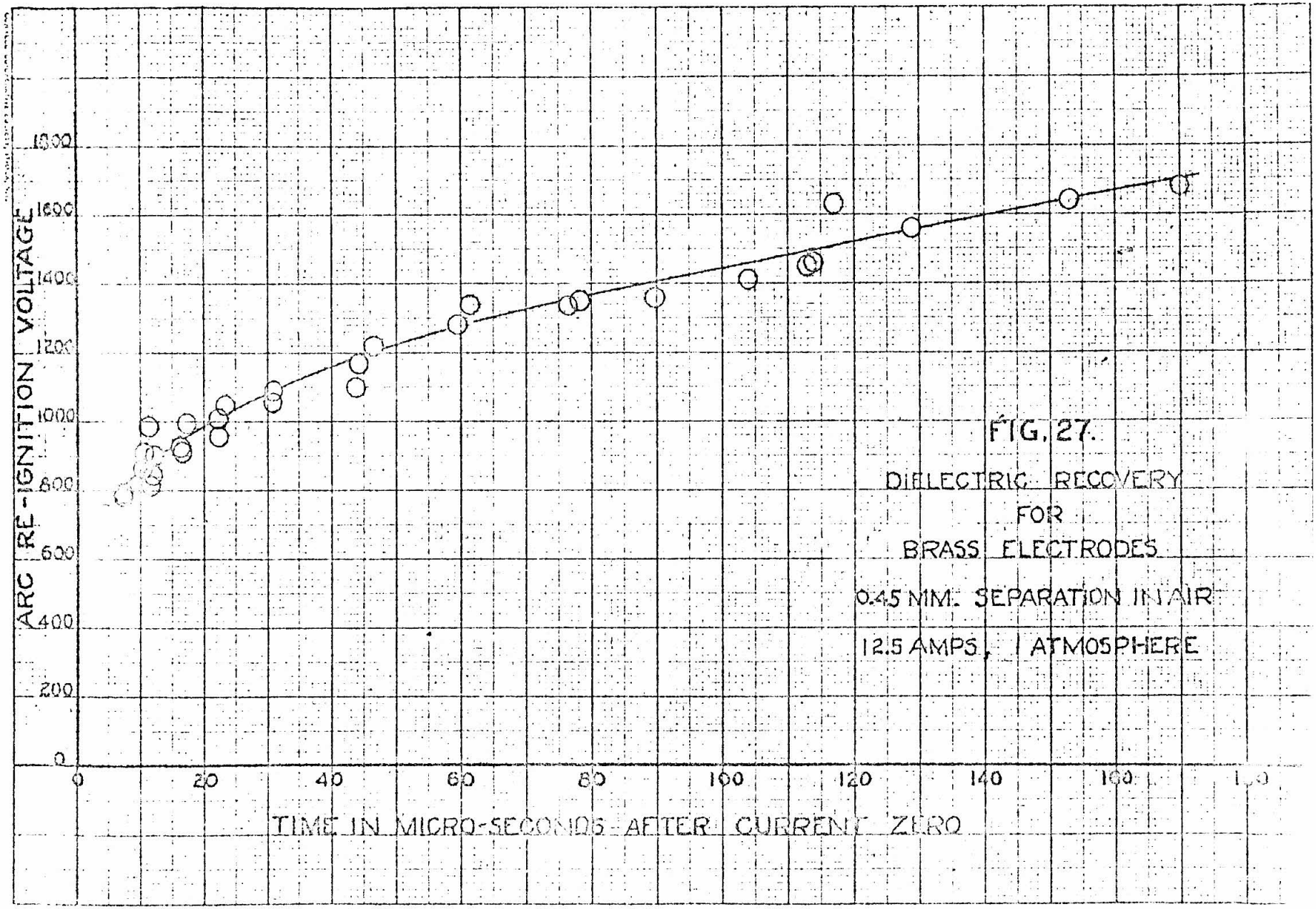

FIG. 27.

DIELECTRIC RECOVERY
FOR
BRASS ELECTRODES
0.45 MM. SEPARATION IN AIR
12.5 AMPS., 1 ATMOSPHERE

Curve No. _____ Signature _____ Date _____

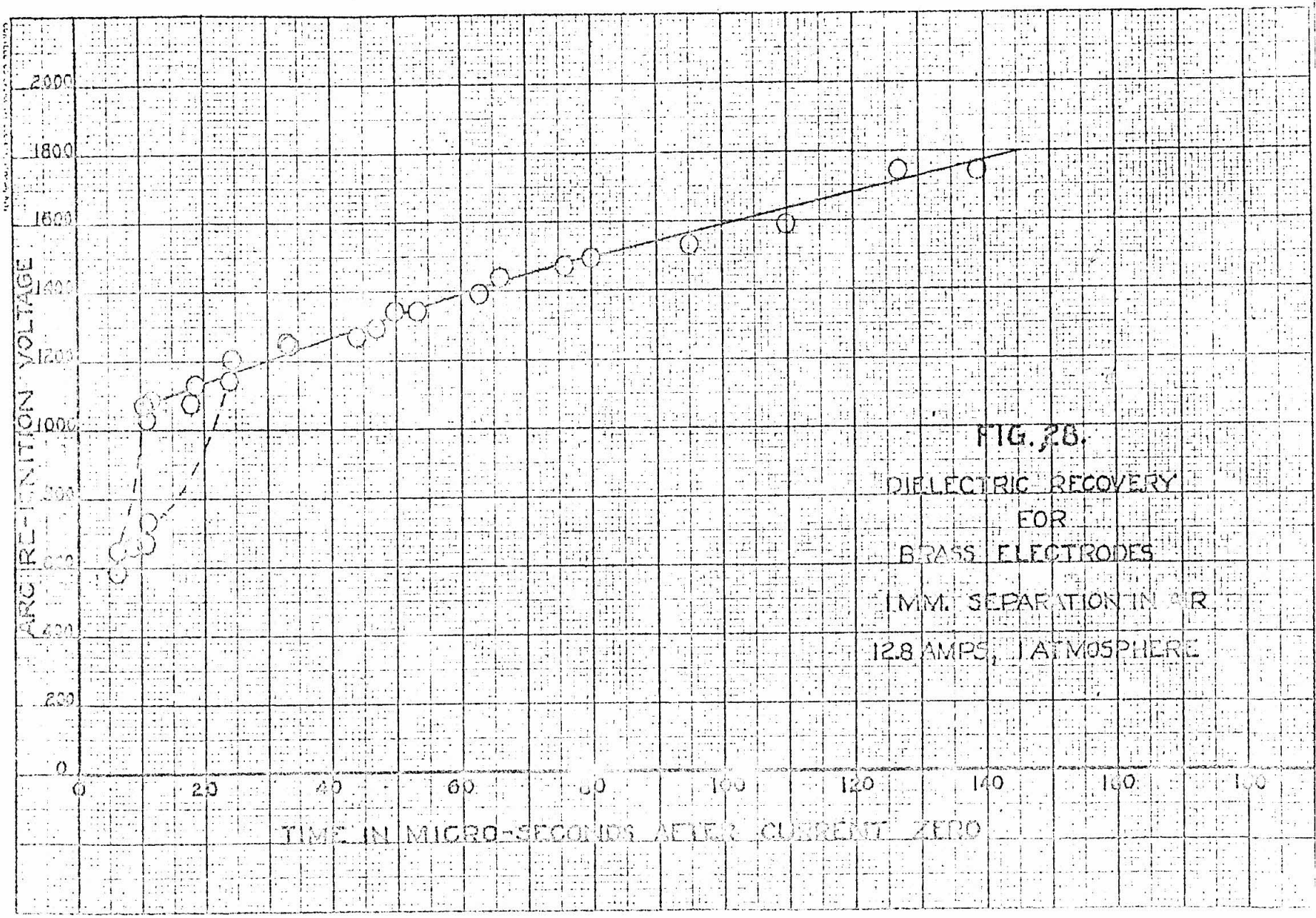

FIG. 28.

DIELECTRIC RECOVERY
FOR
BRASS ELECTRODES
1 M.M. SEPARATION IN AIR
12.8 AMPS, 1 ATMOSPHERE

Curve No._____ Signature_____ Date_____

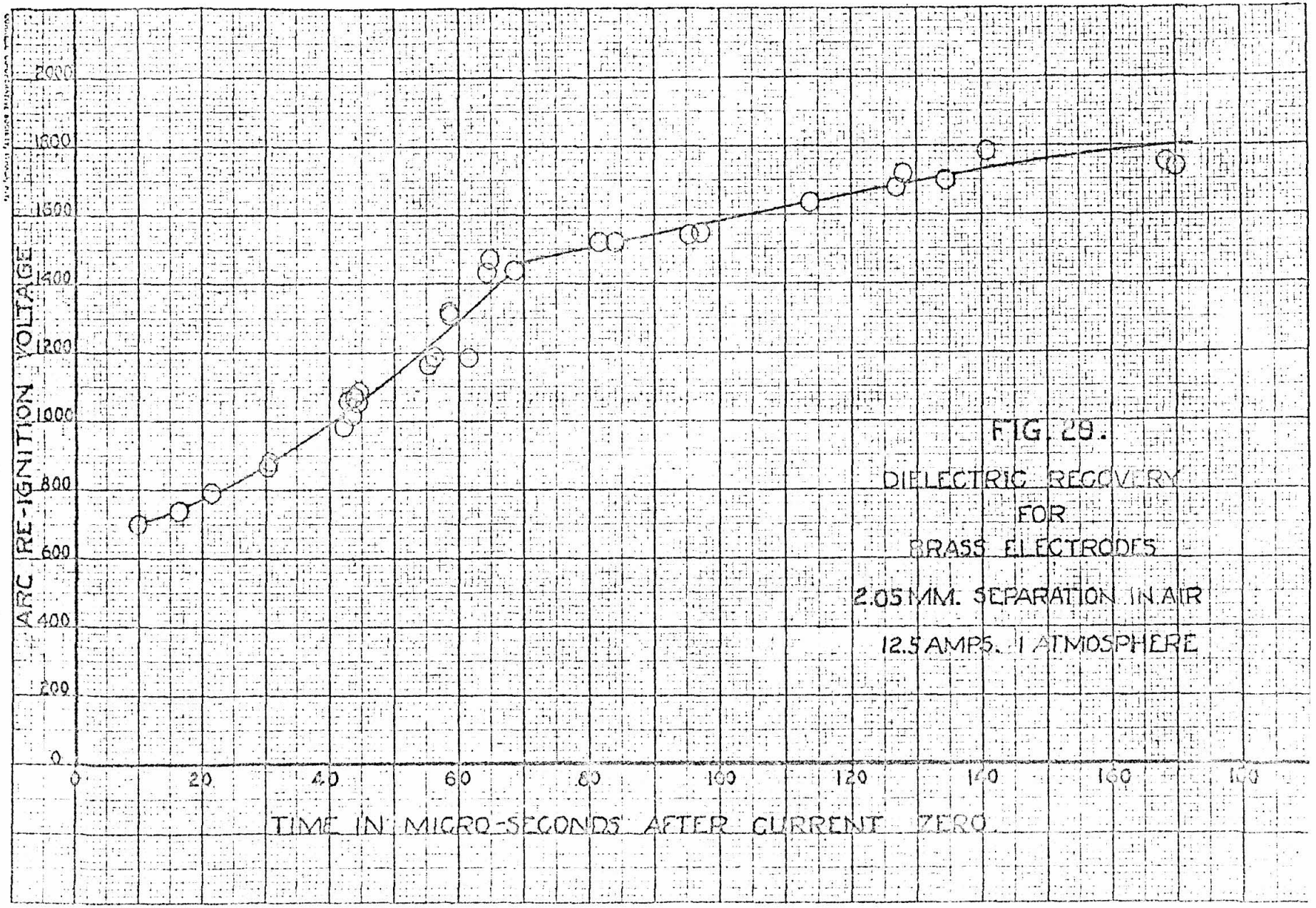

FIG. 29.

DIELECTRIC RECOVERY FOR BRASS ELECTRODES

2.05 MM. SEPARATION IN AIR

12.5 AMPS. 1 ATMOSPHERE

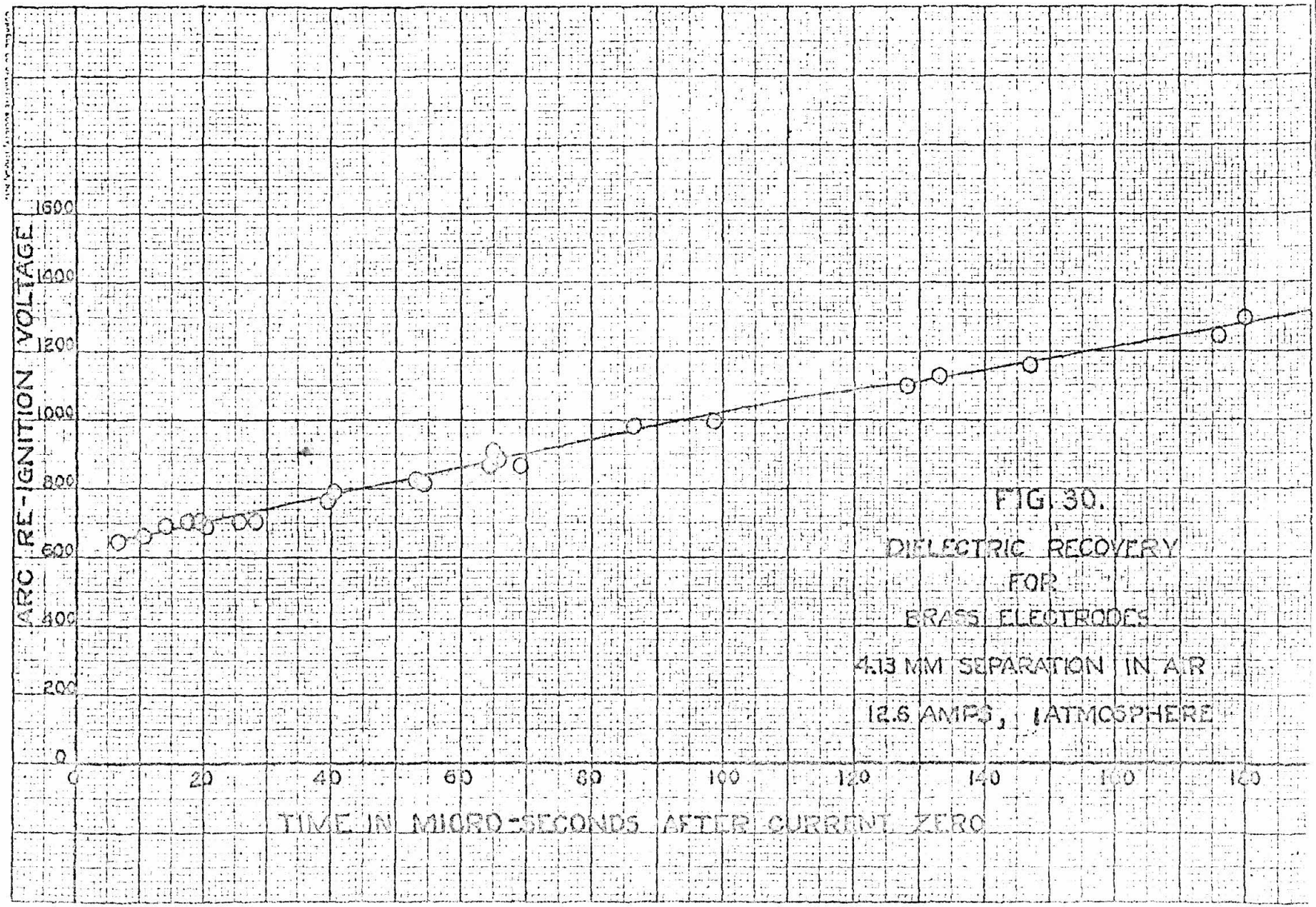

FIG. 30.

DIELECTRIC RECOVERY FOR BRASS ELECTRODES 4.13 MM SEPARATION IN AIR 12.6 AMPS., 1 ATMOSPHERE

Curve No. _____ Signature _____ Date _____

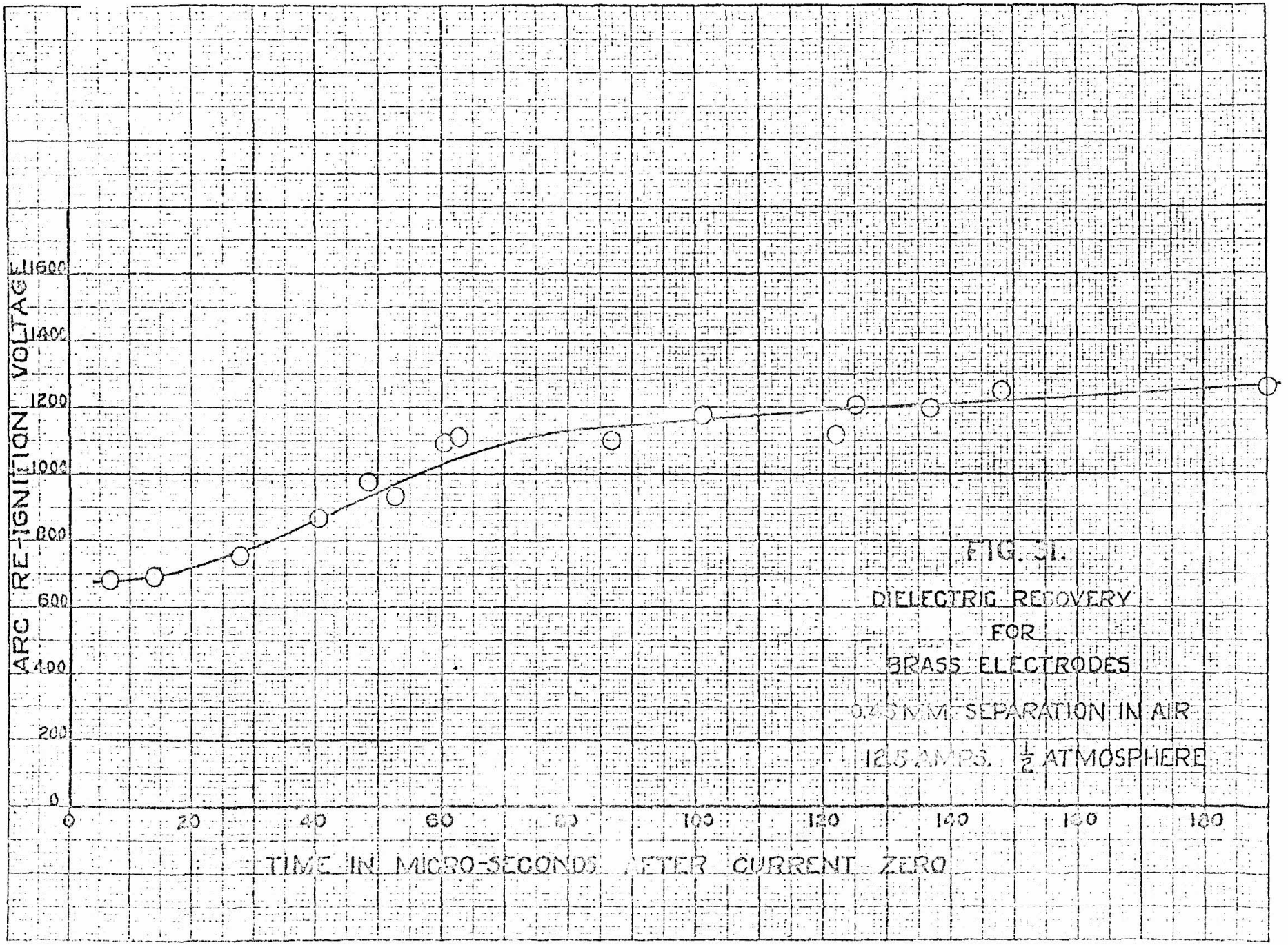

FIG. 31.

DIELECTRIC RECOVERY FOR BRASS ELECTRODES 0.45 M.M. SEPARATION IN AIR 12.5 AMPS. ½ ATMOSPHERE

Curve No.

Signature

Date

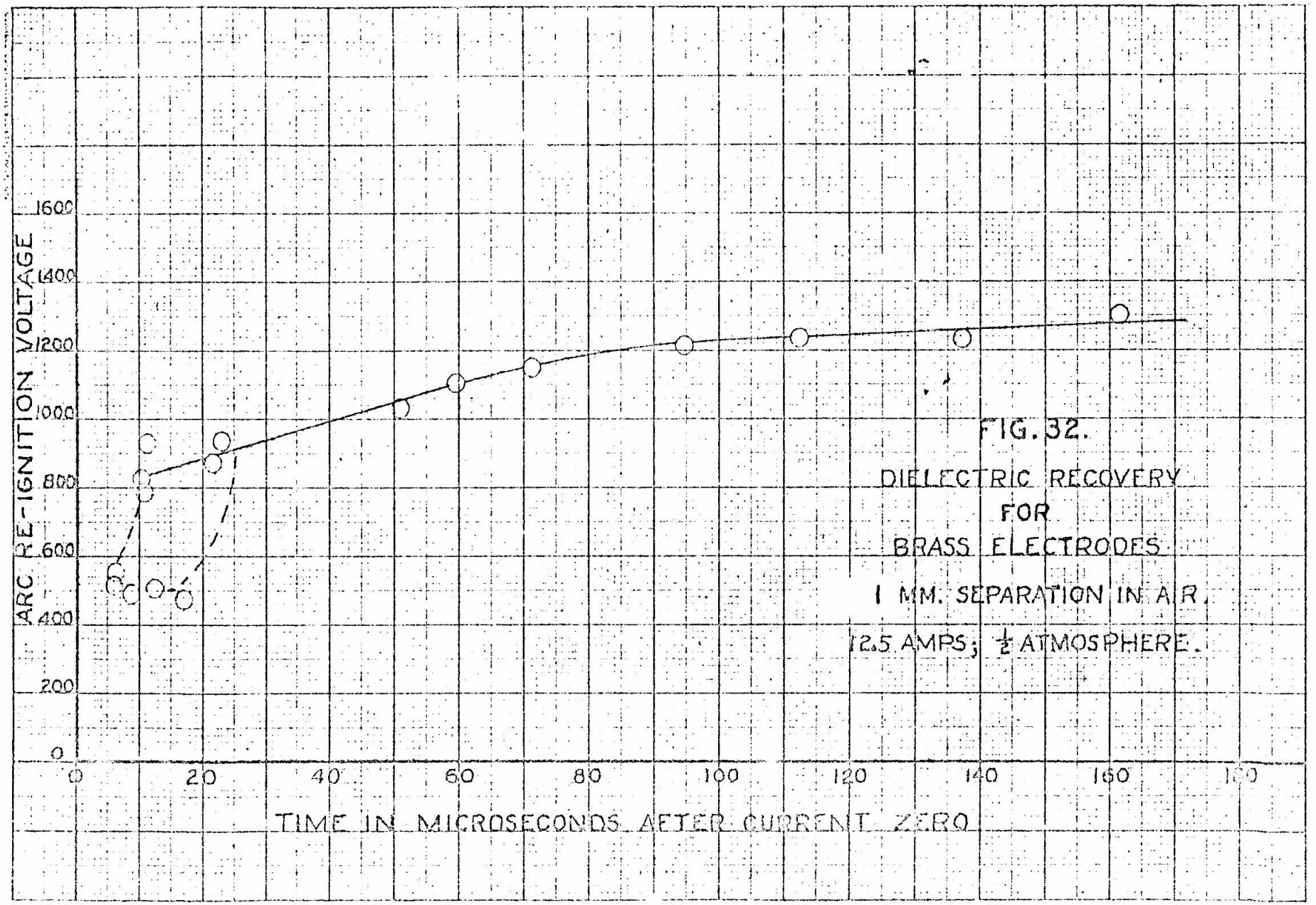

FIG. 32.

DIELECTRIC RECOVERY FOR BRASS ELECTRODES

1 MM. SEPARATION IN A.R.

12.5 AMPS; ½ ATMOSPHERE.

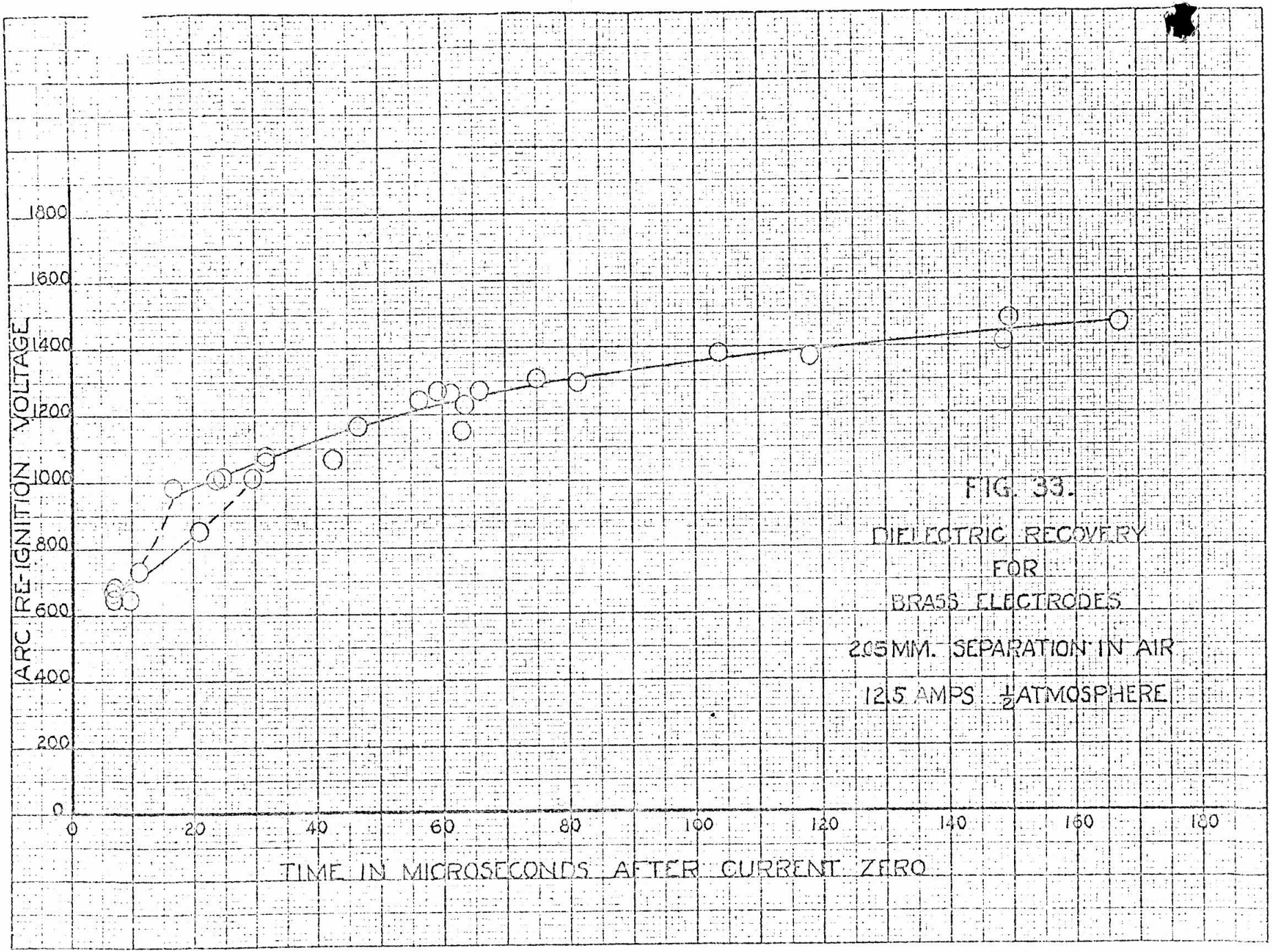

FIG. 33.

DIELECTRIC RECOVERY

FOR

BRASS ELECTRODES

2.05 MM. SEPARATION IN AIR

12.5 AMPS. $\frac{1}{2}$ ATMOSPHERE

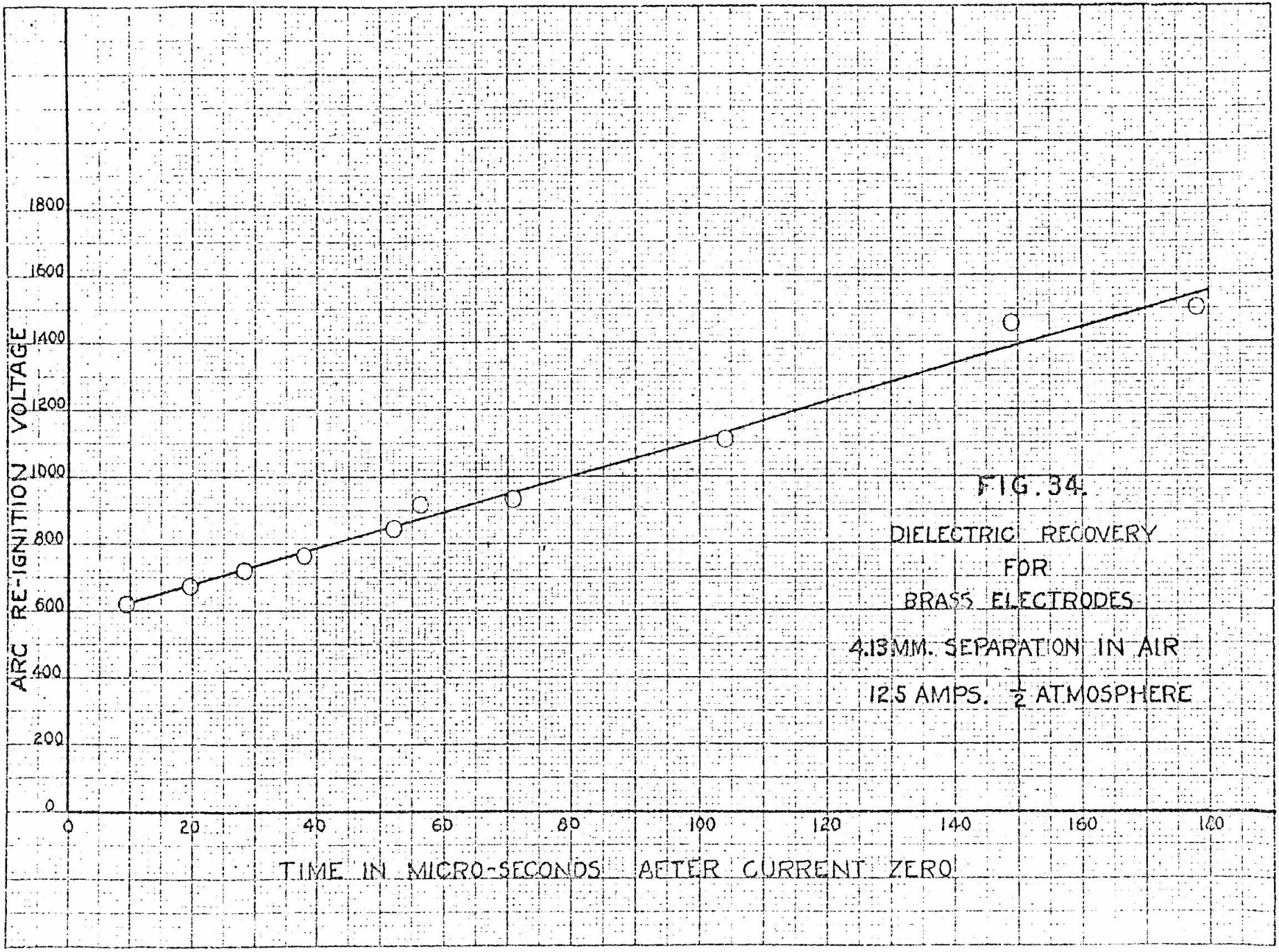

FIG. 34.

DIELECTRIC RECOVERY
FOR
BRASS ELECTRODES
4.13 MM. SEPARATION IN AIR
12.5 AMPS. ½ ATMOSPHERE

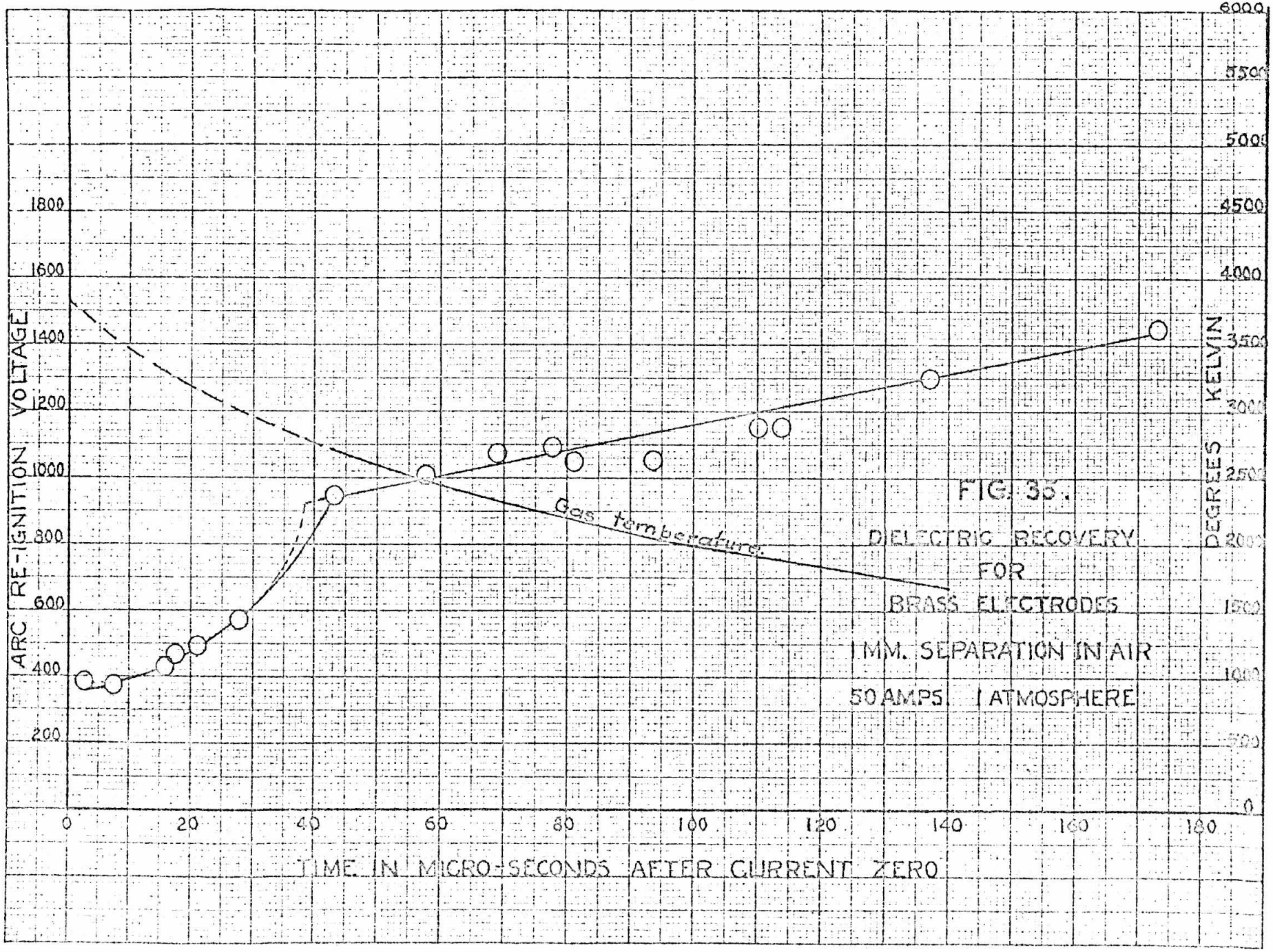

FIG. 35.

DIELECTRIC RECOVERY FOR BRASS ELECTRODES 1 MM. SEPARATION IN AIR 50 AMPS. 1 ATMOSPHERE

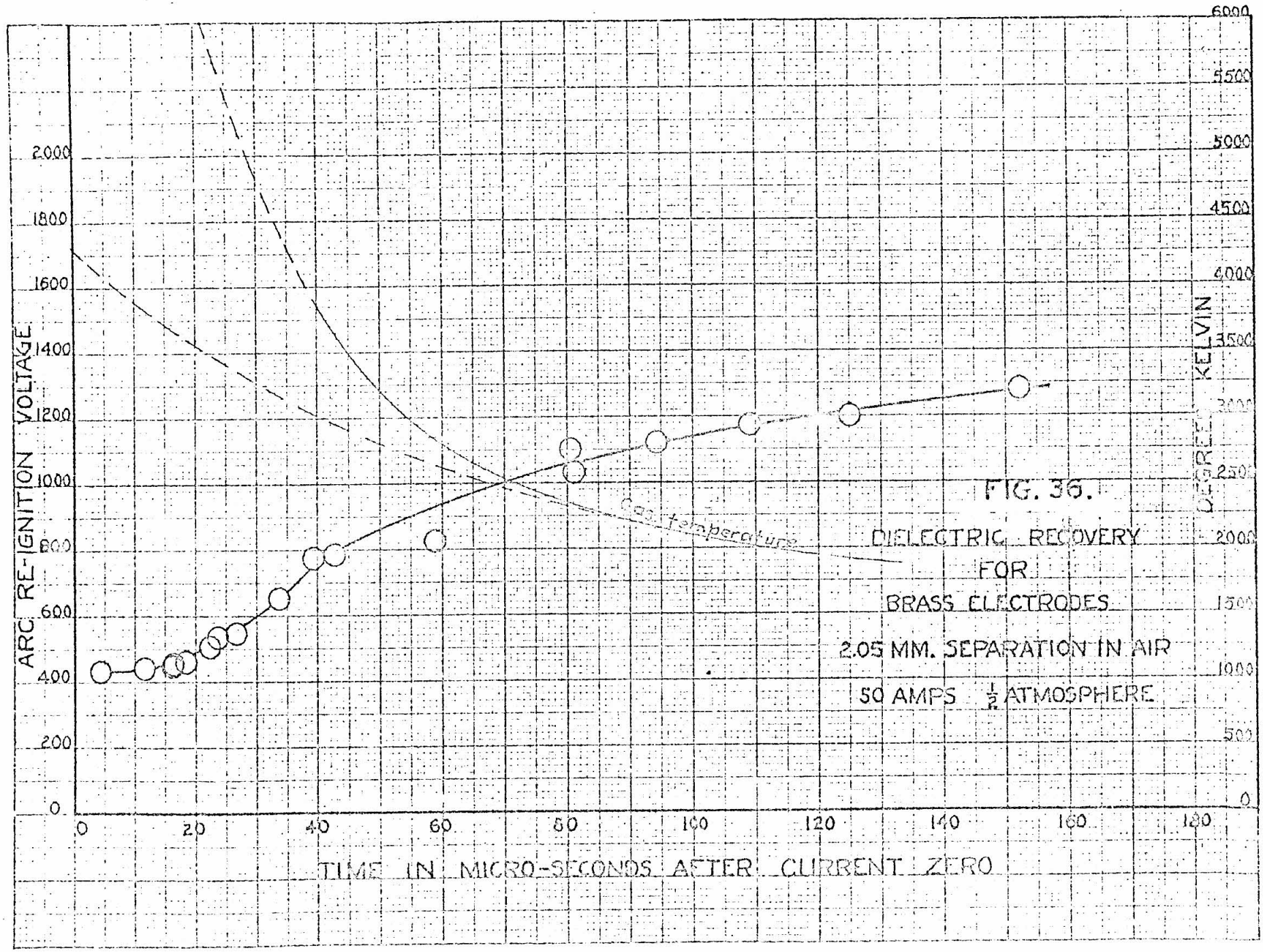

FIG. 36.

DIELECTRIC RECOVERY
FOR
BRASS ELECTRODES
2.05 MM. SEPARATION IN AIR
50 AMPS $\frac{1}{2}$ ATMOSPHERE

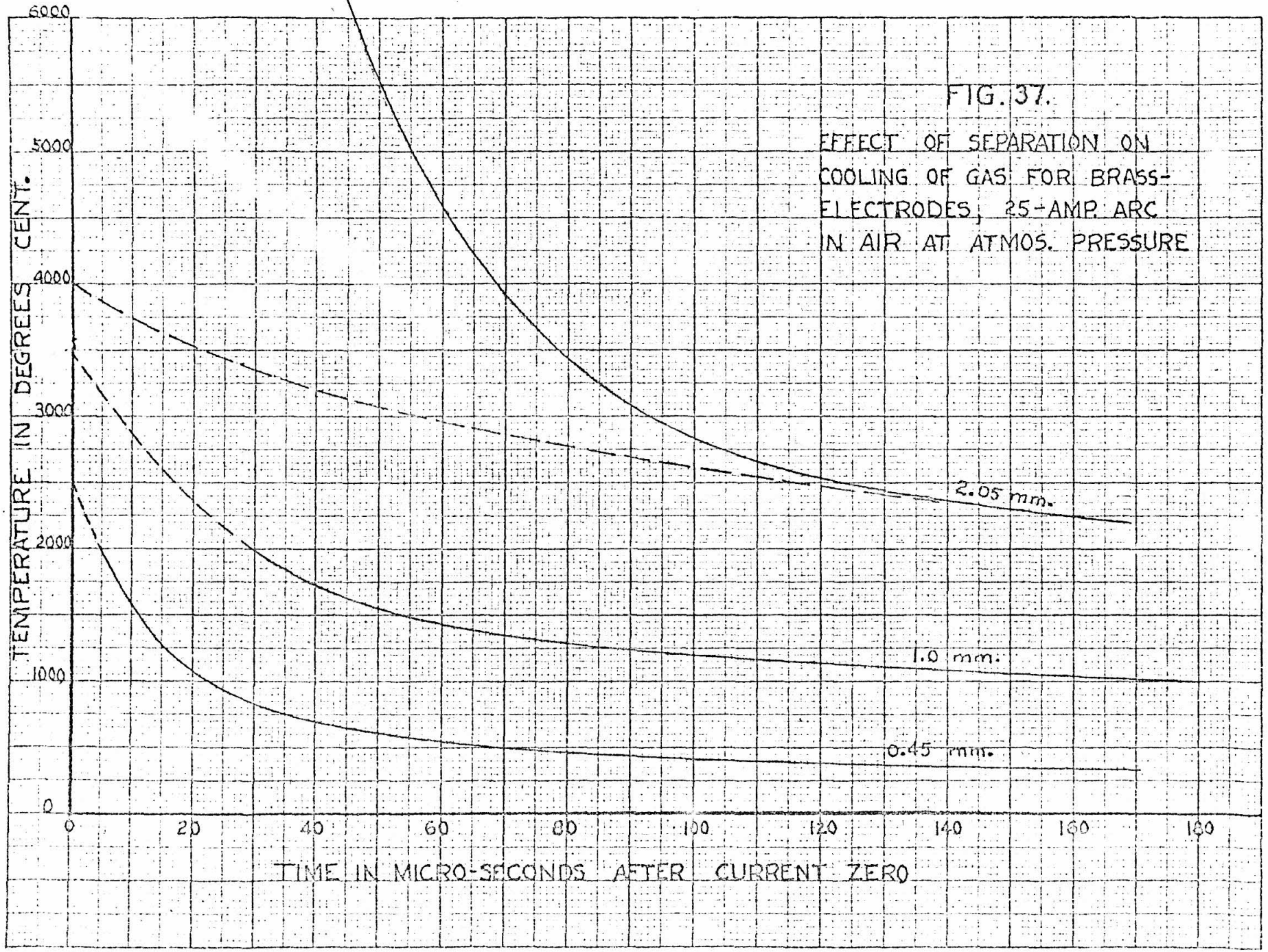
FIG. 37.
EFFECT OF SEPARATION ON COOLING OF GAS FOR BRASS-ELECTRODES, 25-AMP. ARC IN AIR AT ATMOS. PRESSURE
TEMPERATURE IN DEGREES CENT.
6000
5000
4000
3000
2000
1000
0
2.05 mm.
1.0 mm.
0.45 mm.
0
20
40
60
80
100
120
140
160
180
TIME IN MICRO-SECONDS AFTER CURRENT ZERO

FIG. 38.

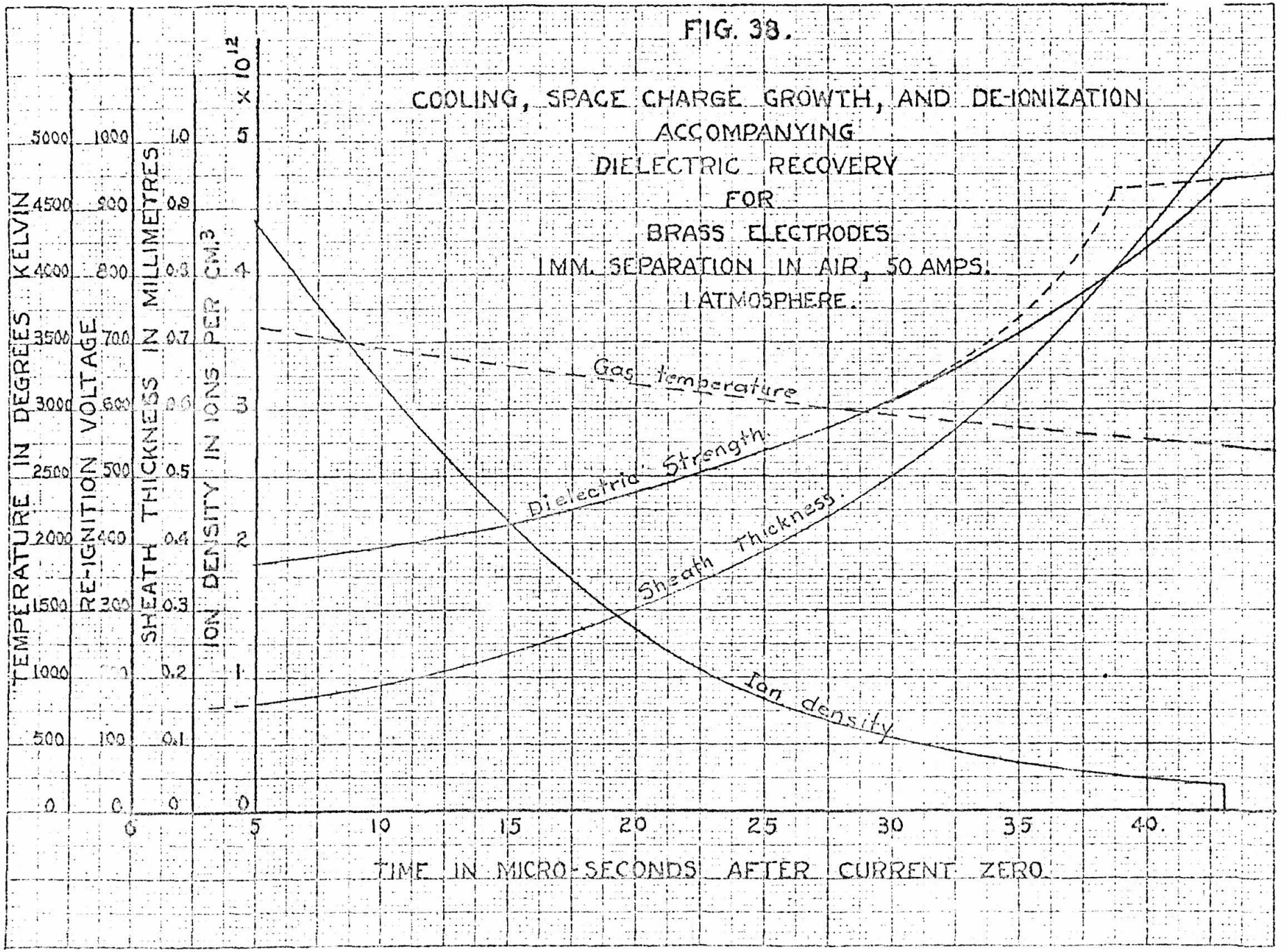
COOLING, SPACE CHARGE GROWTH, AND DE-IONIZATION ACCOMPANYING DIELECTRIC RECOVERY FOR BRASS ELECTRODES 1 MM. SEPARATION IN AIR, 50 AMPS. 1 ATMOSPHERE.
TEMPERATURE IN DEGREES KELVIN
RE-IGNITION VOLTAGE
SHEATH THICKNESS IN MILLIMETRES
ION DENSITY IN IONS PER CM.3 x 10^12
Gas temperature
Dielectric Strength
Sheath Thickness
Ion density
TIME IN MICRO-SECONDS AFTER CURRENT ZERO.

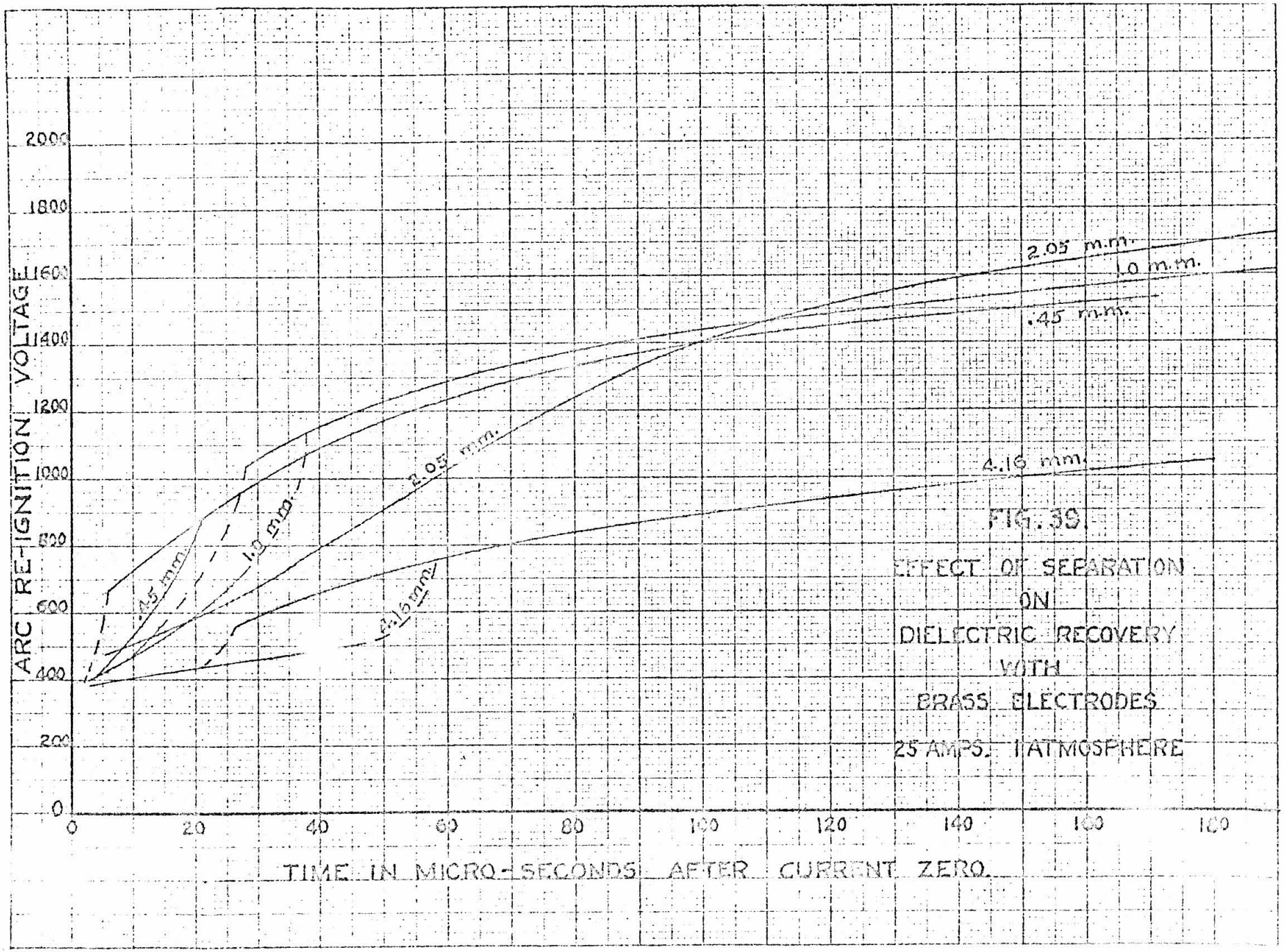

FIG. 39.

EFFECT OF SEPARATION ON DIELECTRIC RECOVERY WITH BRASS ELECTRODES 25 AMPS. 1 ATMOSPHERE

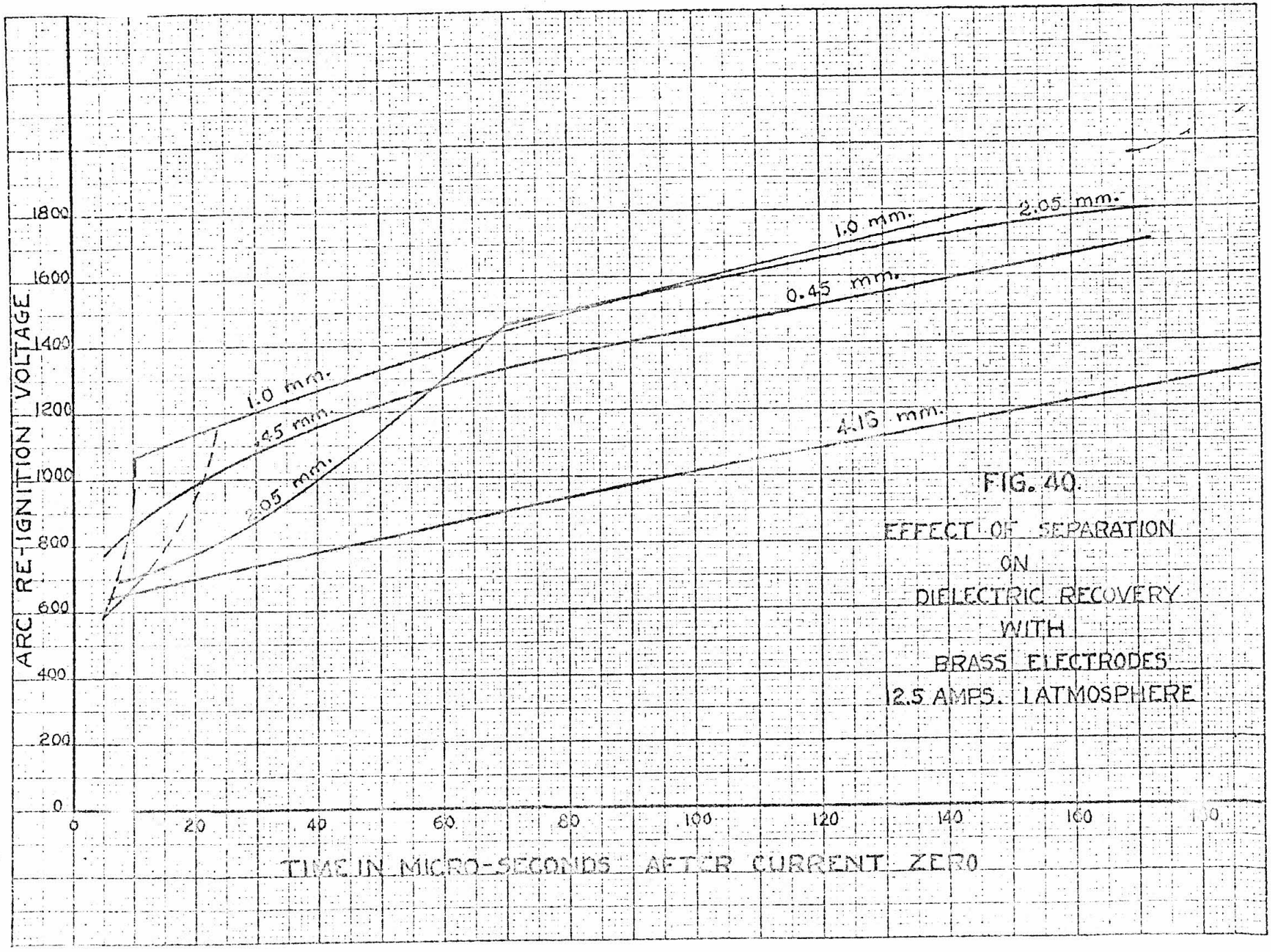

FIG. 40.

EFFECT OF SEPARATION
ON
DIELECTRIC RECOVERY
WITH
BRASS ELECTRODES
2.5 AMPS. IATMOSPHERE

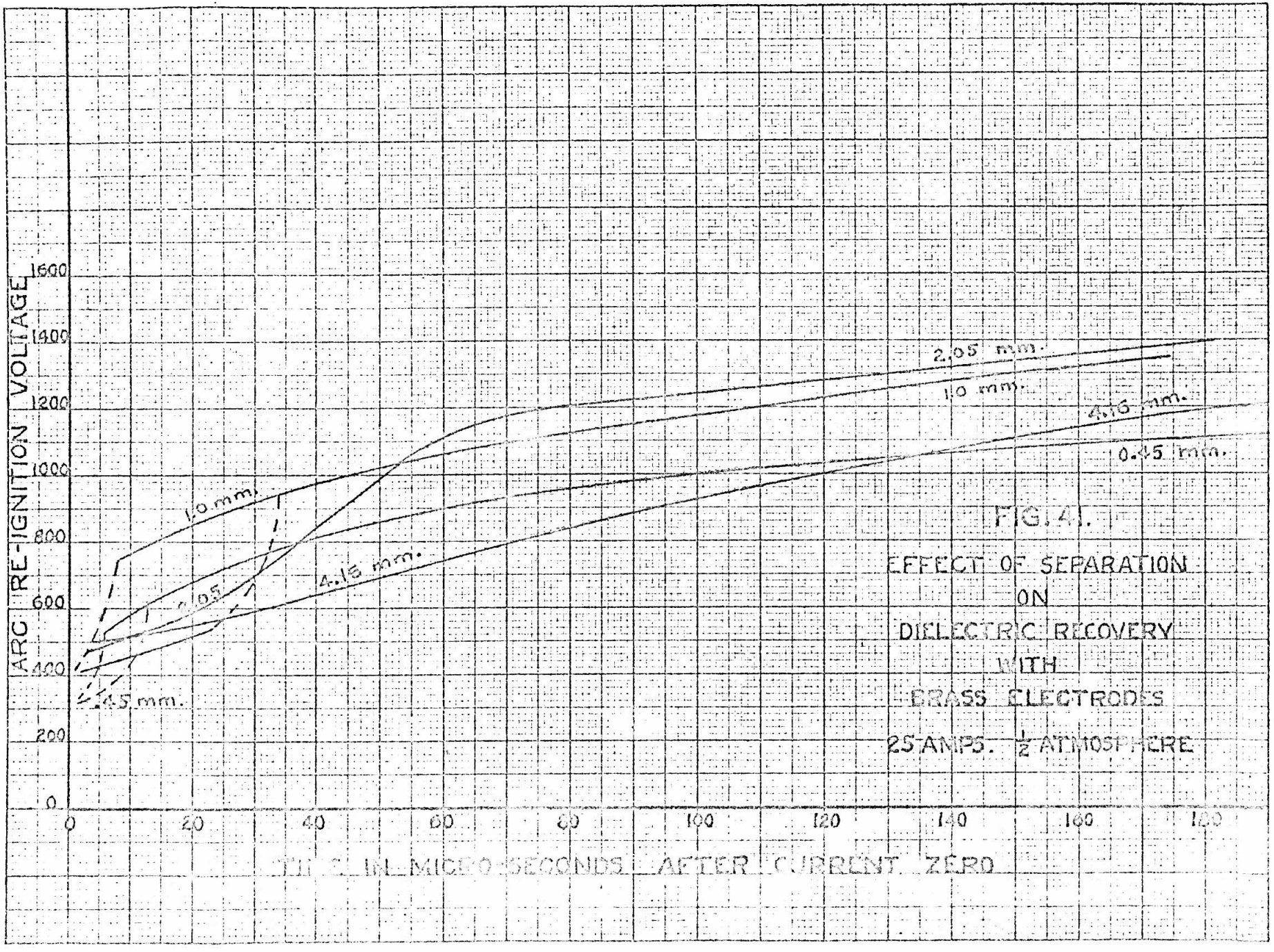

FIG. 41.

EFFECT OF SEPARATION ON DIELECTRIC RECOVERY WITH BRASS ELECTRODES 25 AMPS. ½ ATMOSPHERE

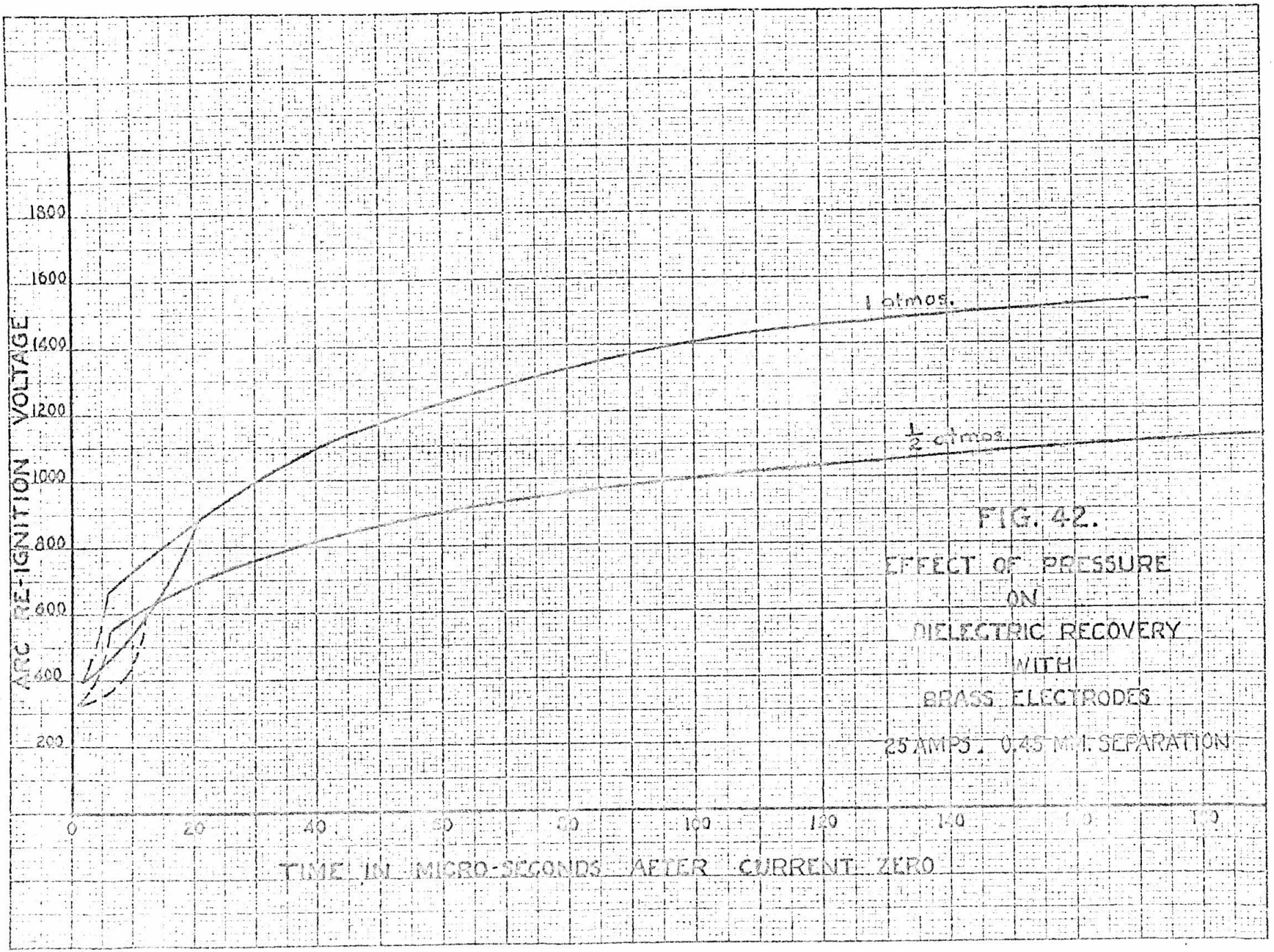

FIG. 42.

EFFECT OF PRESSURE ON DIELECTRIC RECOVERY WITH BRASS ELECTRODES

25 AMPS. 0.45 M.M. SEPARATION

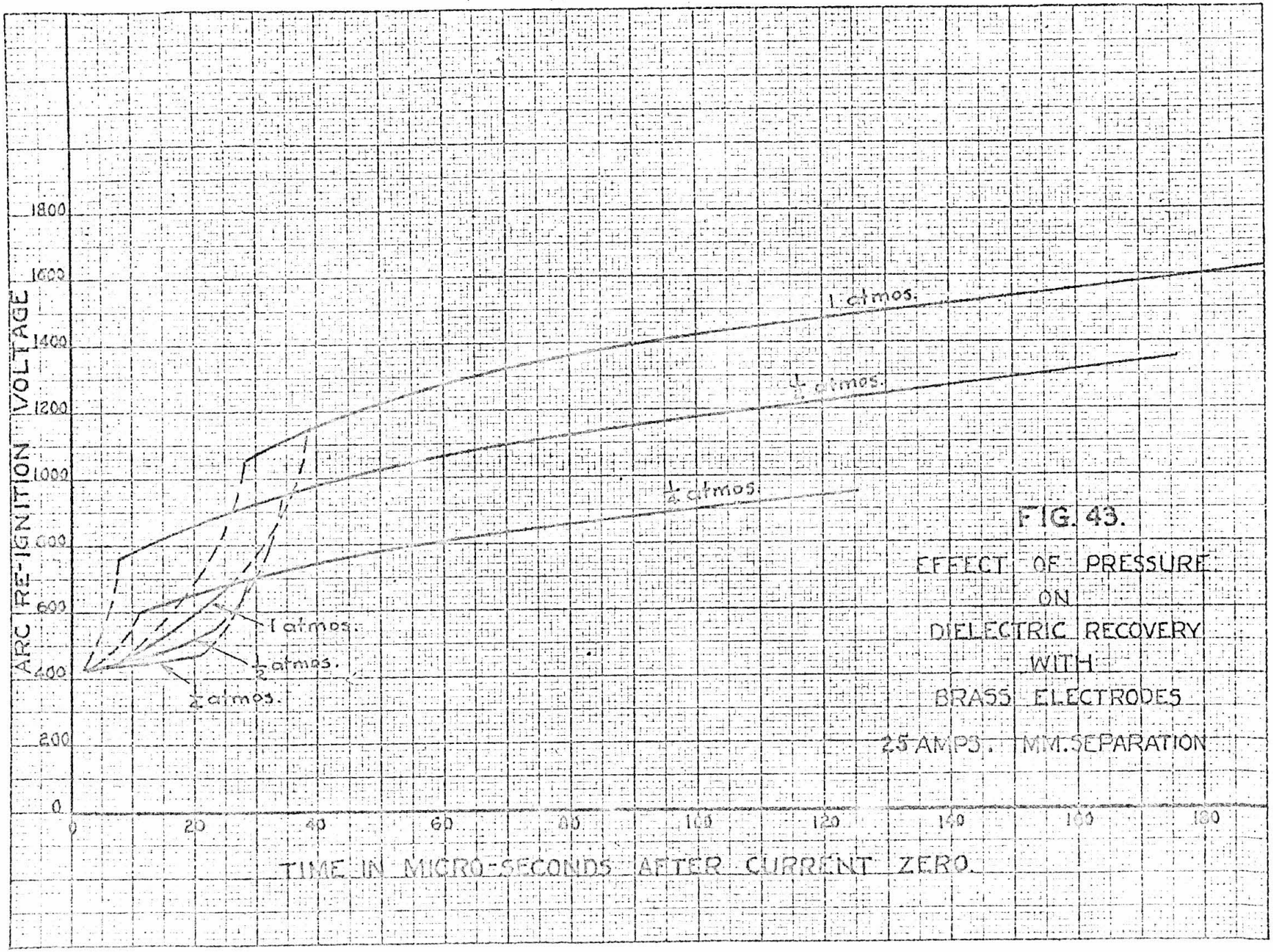

FIG. 43.

EFFECT OF PRESSURE ON DIELECTRIC RECOVERY WITH BRASS ELECTRODES

25 AMPS. MM. SEPARATION

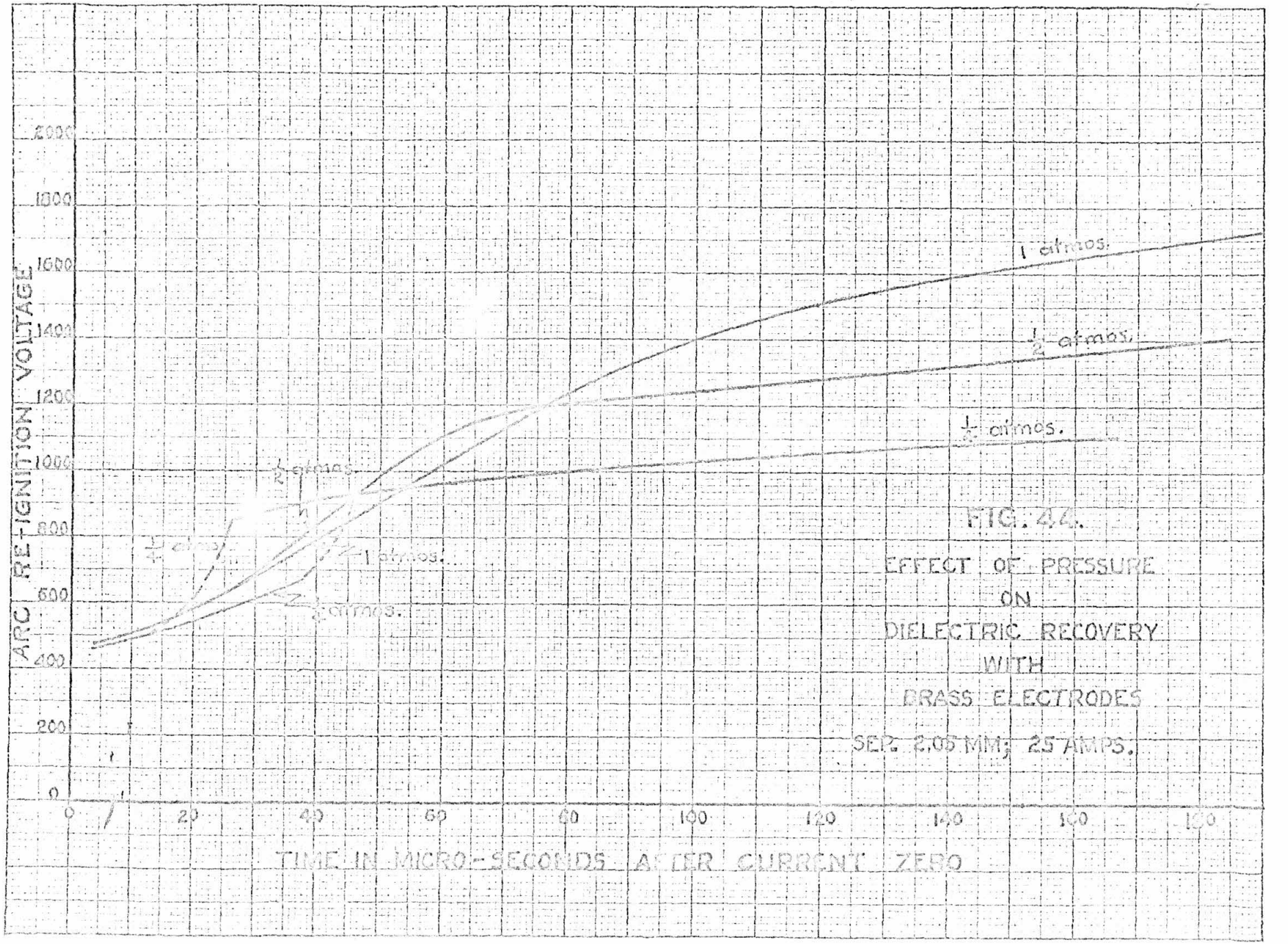

FIG. 44.

EFFECT OF PRESSURE ON DIELECTRIC RECOVERY WITH BRASS ELECTRODES

SEP. 2.05 MM; 25 AMPS.

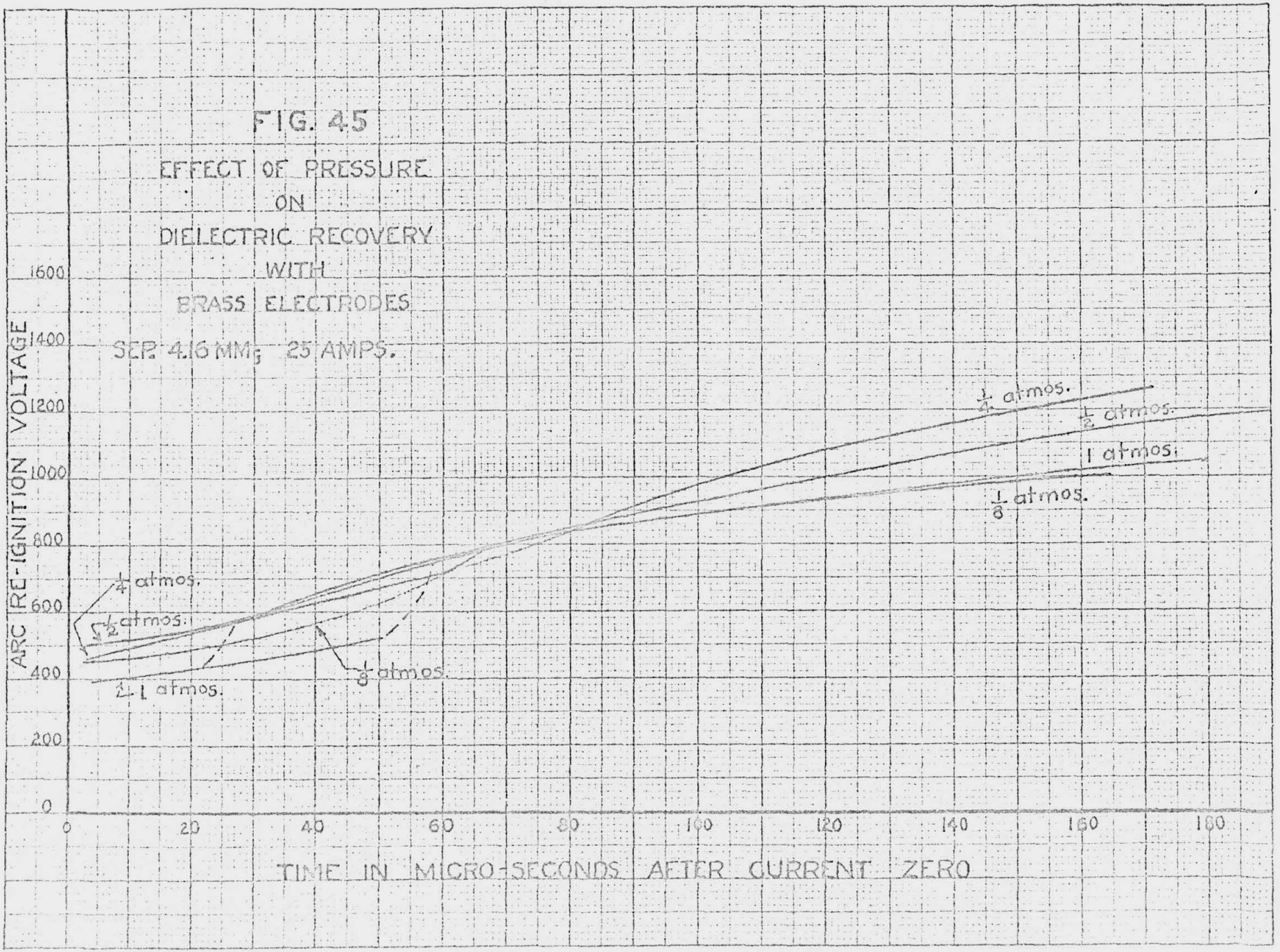
FIG. 45
EFFECT OF PRESSURE
ON
DIELECTRIC RECOVERY
WITH
BRASS ELECTRODES
SEP. 4.16 MM. 25 AMPS.
ARC RE-IGNITION VOLTAGE
1600
1400
1200
1000
800
600
400
200
0
0
20
40
60
80
100
120
140
160
180
TIME IN MICRO-SECONDS AFTER CURRENT ZERO
1/4 atmos.
1/2 atmos.
1 atmos.
1/8 atmos.
1/4 atmos.
1/2 atmos.
1 atmos.
1/8 atmos.

FIG. 46.

COMPARISON OF DIELECTRIC RECOVERY CURVES FOR BRASS ELECTRODES WITH

$p\ell = 0.25$

2.5 AMPS.

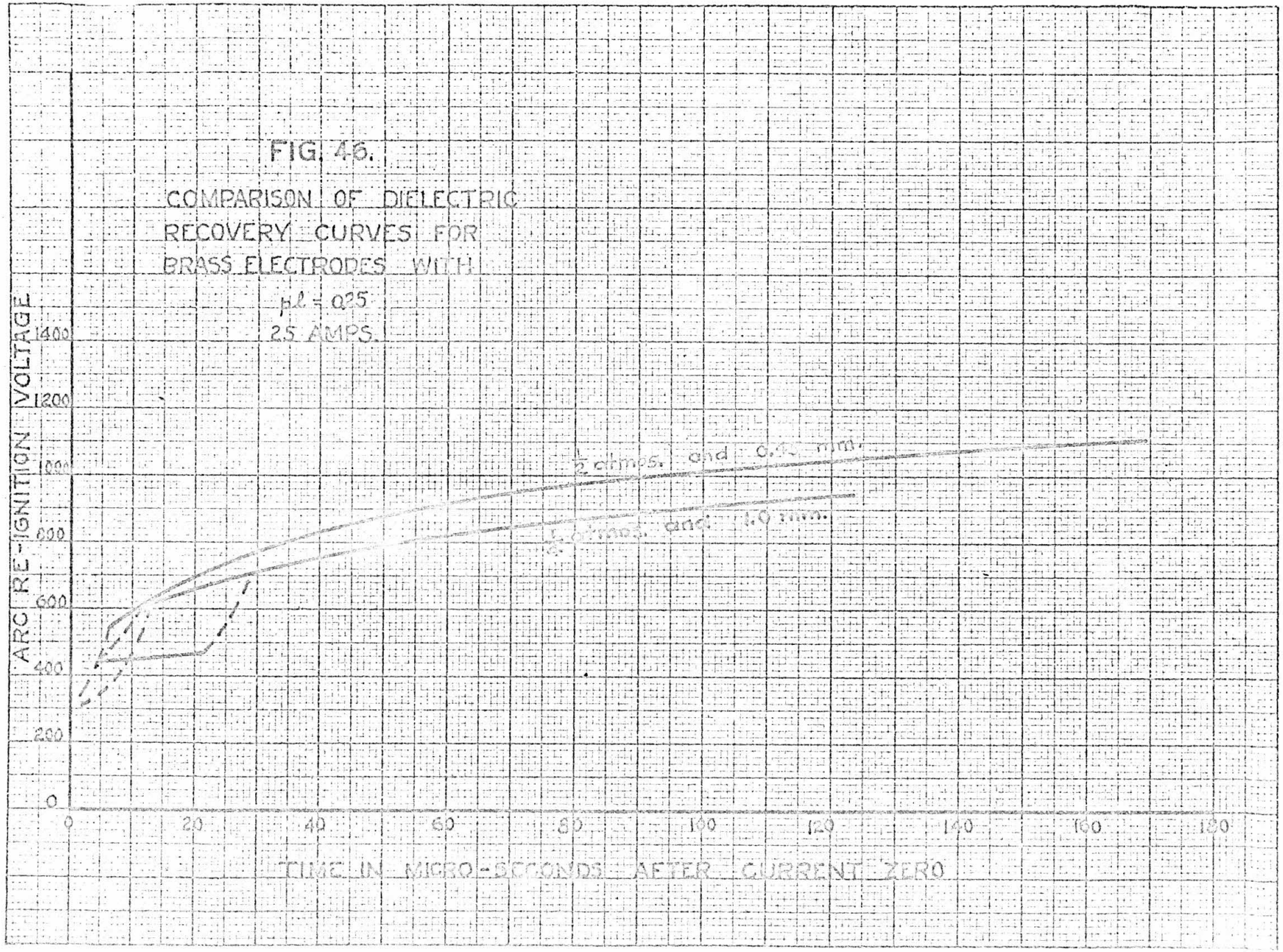

FIG. 47.

COMPARISON OF DIELECTRIC RECOVERY CURVES FOR BRASS ELECTRODES WITH

$p\ell = 0.5$

25 AMPS.

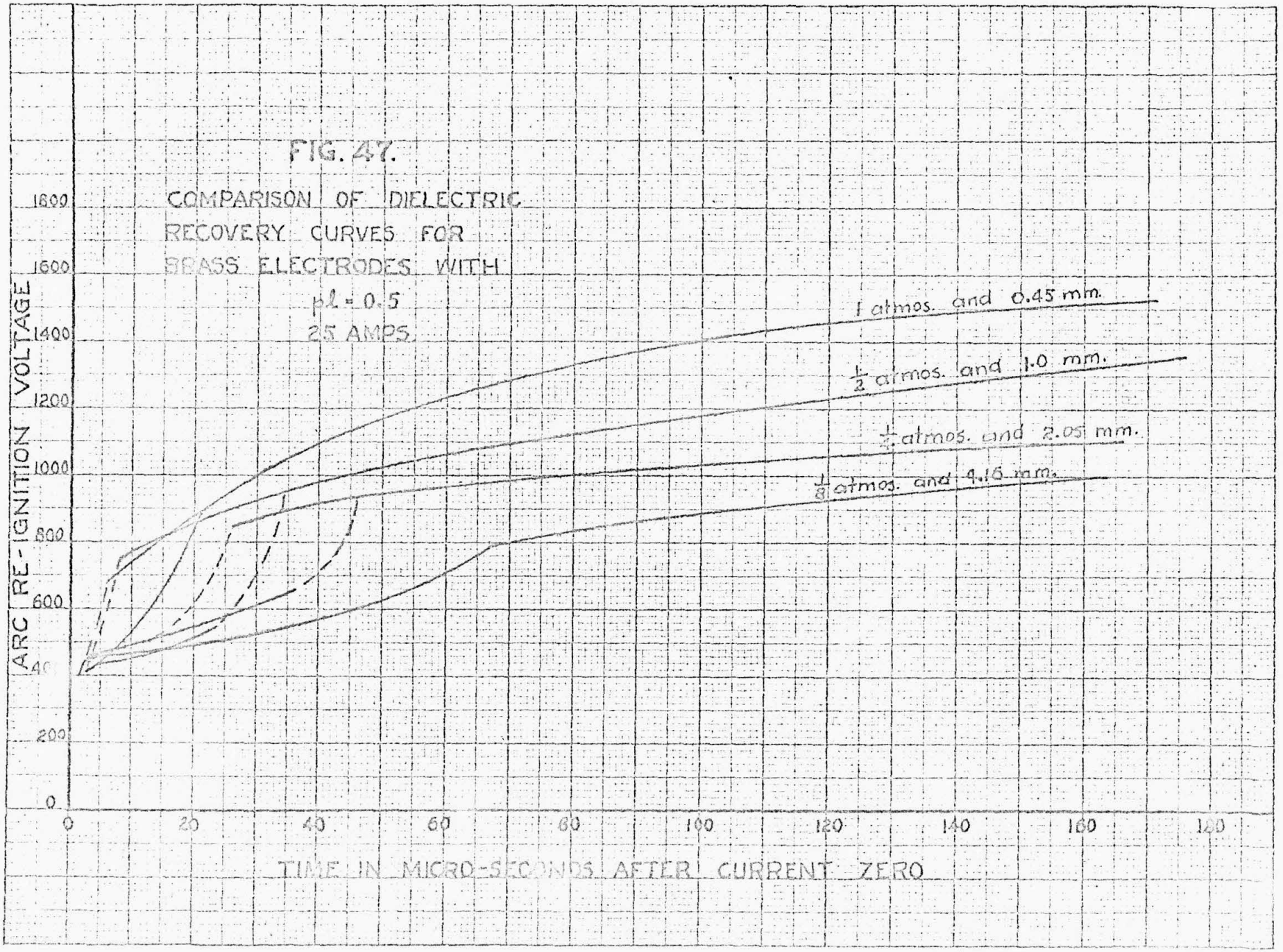

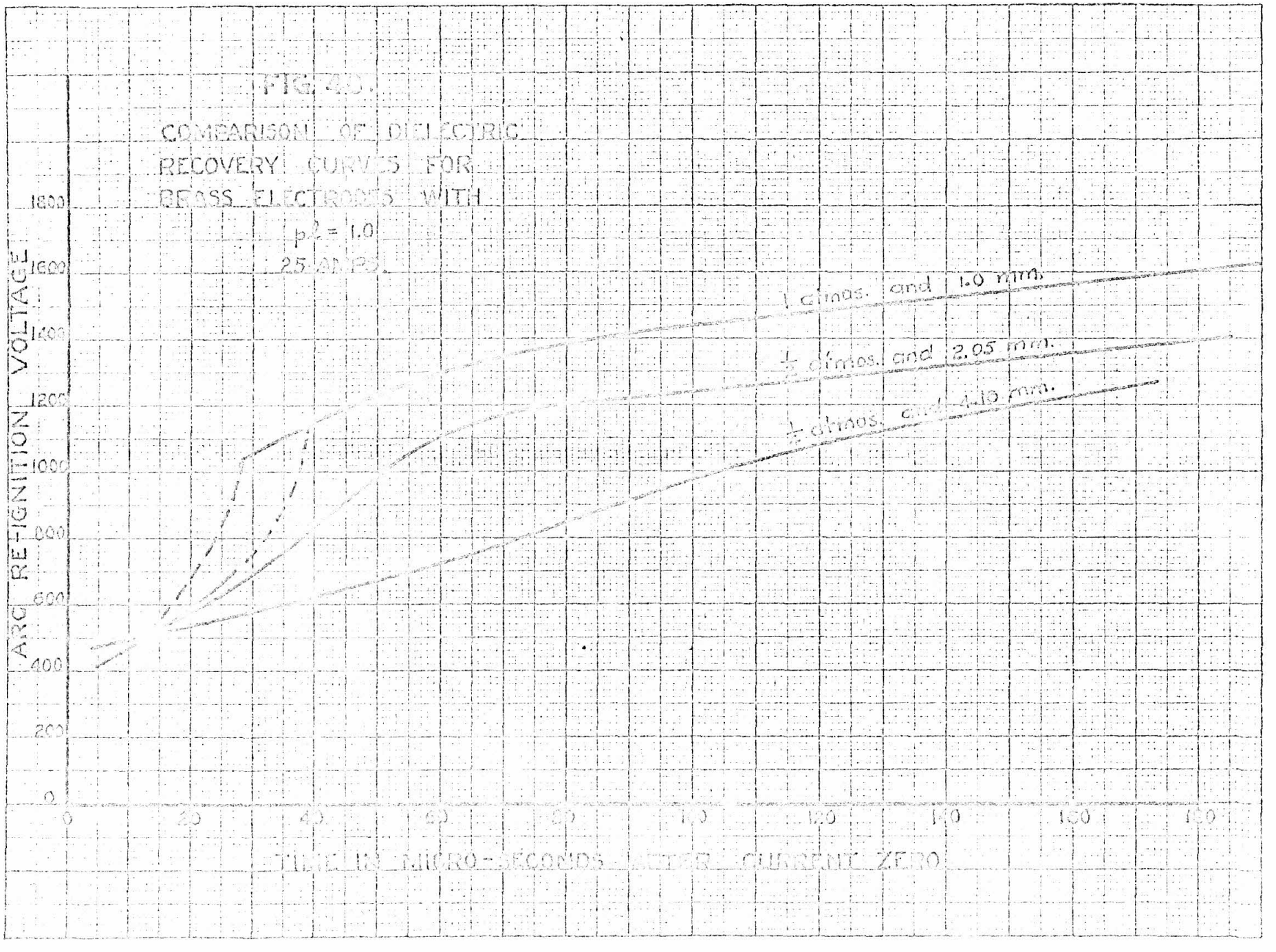
FIG. 20.
COMPARISON OF DIELECTRIC RECOVERY CURVES FOR BRASS ELECTRODES WITH
$p^2 = 1.0$
25 cm PSL
1 atmos. and 1.0 mm.
½ atmos. and 2.05 mm.
¼ atmos. and 4.10 mm.
ARC RE-IGNITION VOLTAGE
1800
1600
1400
1200
1000
800
600
400
200
0
0
20
40
60
80
100
120
140
160
180
TIME IN MICRO-SECONDS AFTER CURRENT ZERO

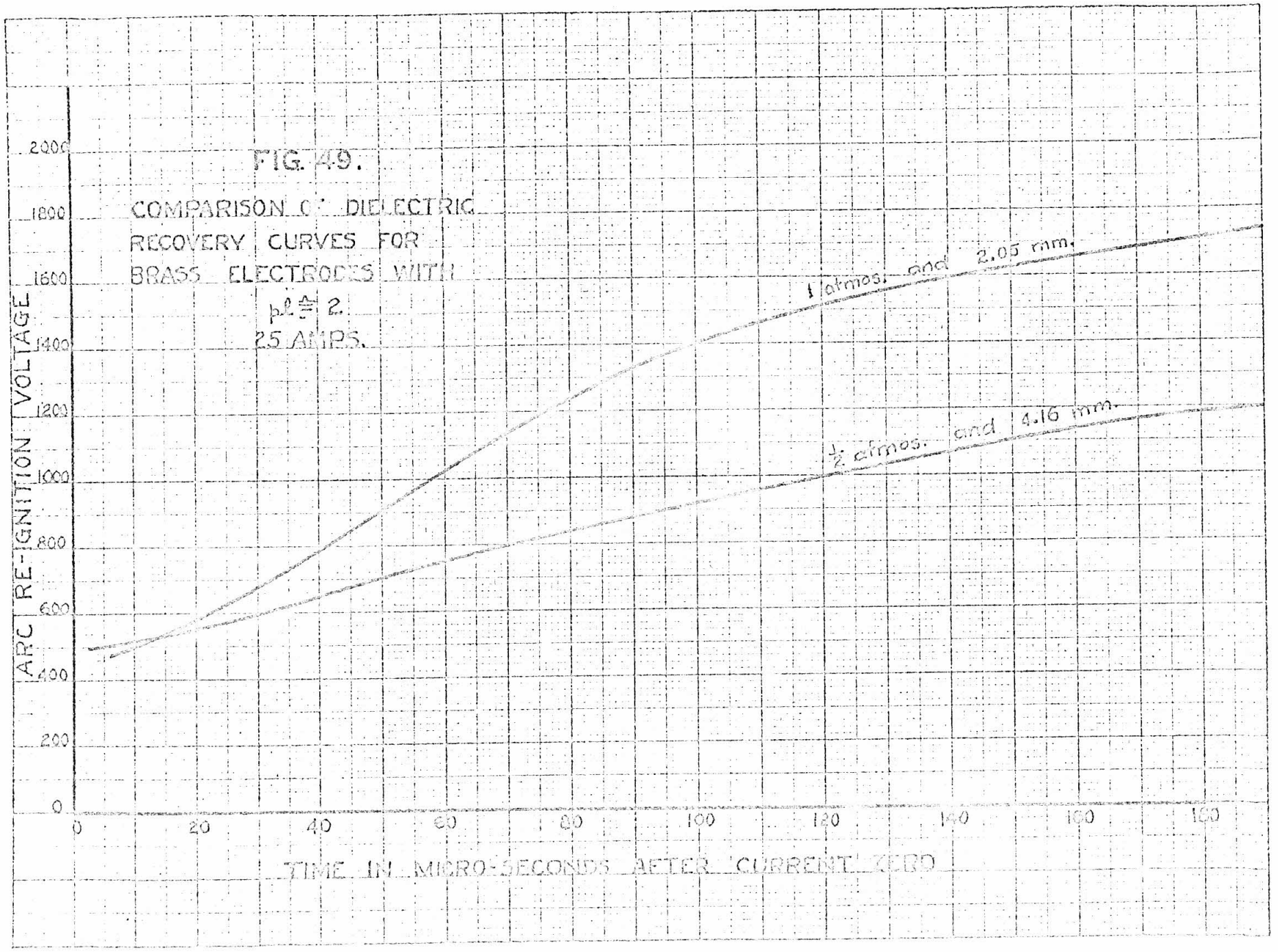
FIG. 49.
COMPARISON OF DIELECTRIC RECOVERY CURVES FOR BRASS ELECTRODES WITH
pl = 2.
2.5 AMPS.
1 atmos. and 2.05 mm.
½ atmos. and 4.16 mm.
ARC RE-IGNITION VOLTAGE
2000
1800
1600
1400
1200
1000
800
600
400
200
0
0
20
40
60
80
100
120
140
160
180
TIME IN MICRO-SECONDS AFTER CURRENT ZERO

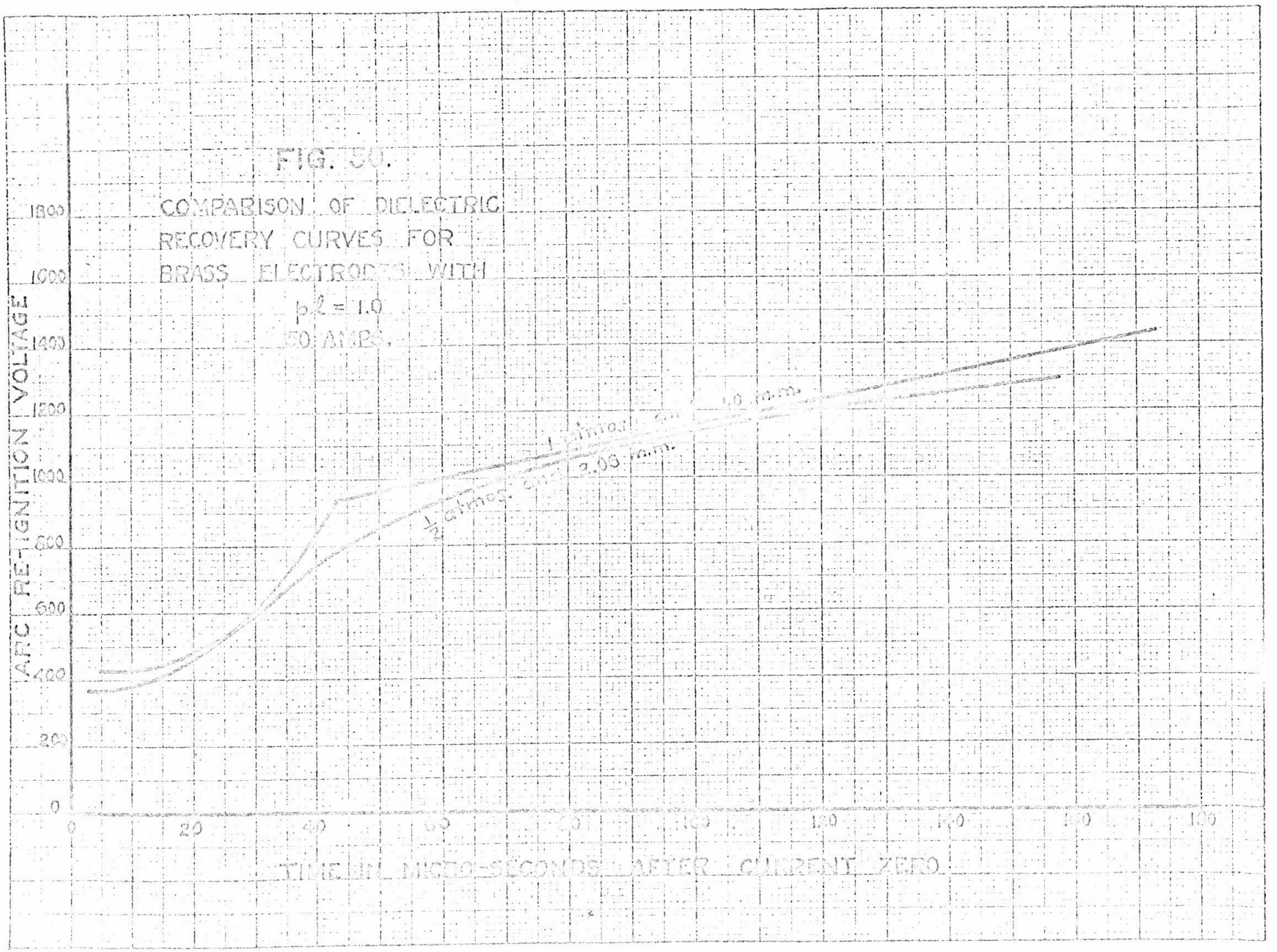
FIG. 50.
COMPARISON OF DIELECTRIC RECOVERY CURVES FOR BRASS ELECTRODES WITH
p.ℓ = 1.0
50 AMPS.
ARC RE-IGNITION VOLTAGE
1800
1000
1400
1200
1000
800
600
400
200
0
1 atmos. curve 1.0 mm.
½ atmos. curve 2.00 mm.
0
20
40
60
80
100
1.0
1.0
1.0
1.00
TIME IN MICRO-SECONDS AFTER CURRENT ZERO

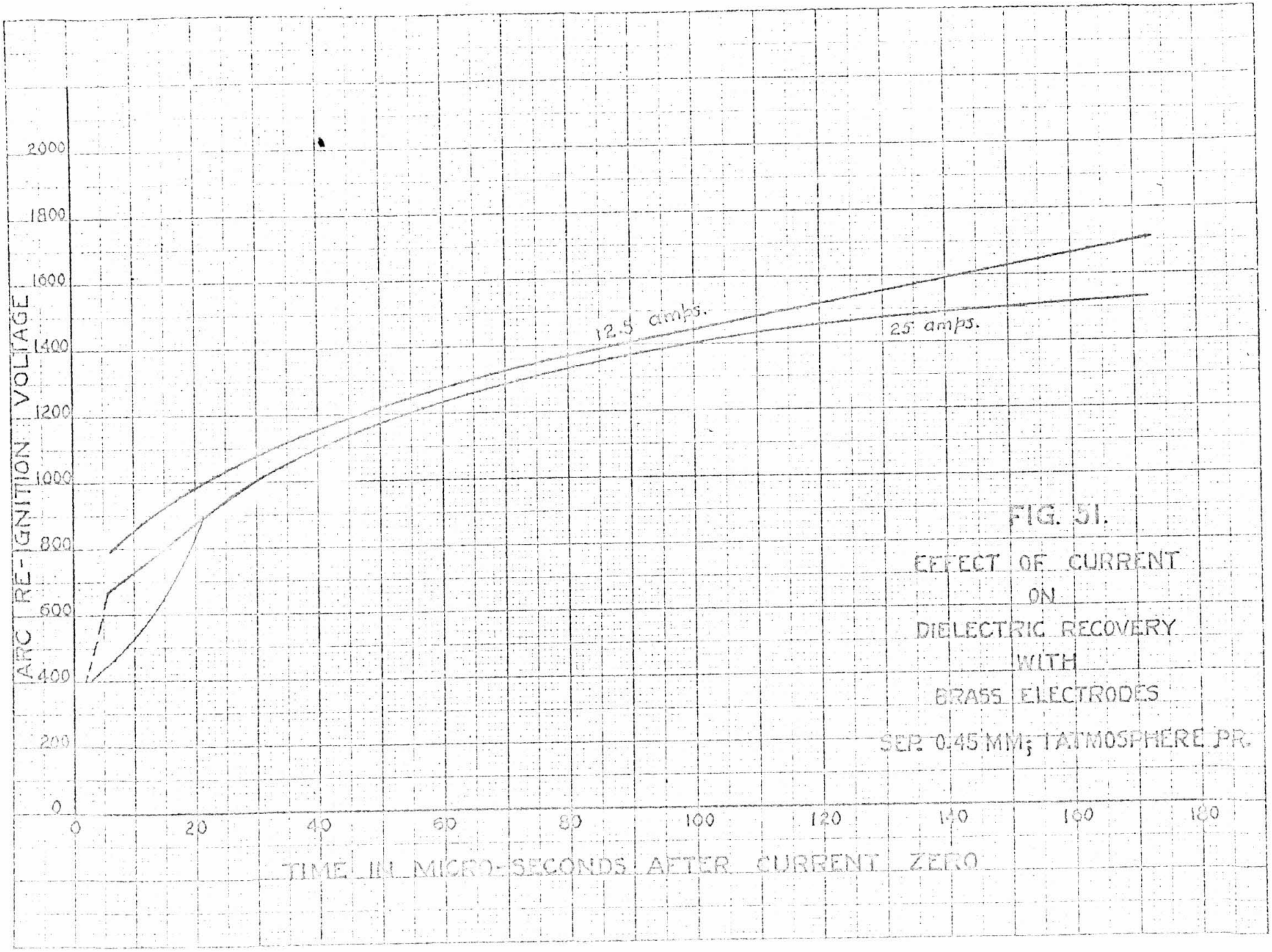

FIG. 51.

EFFECT OF CURRENT ON DIELECTRIC RECOVERY WITH BRASS ELECTRODES SEP. 0.45 MM; 1 ATMOSPHERE PR.

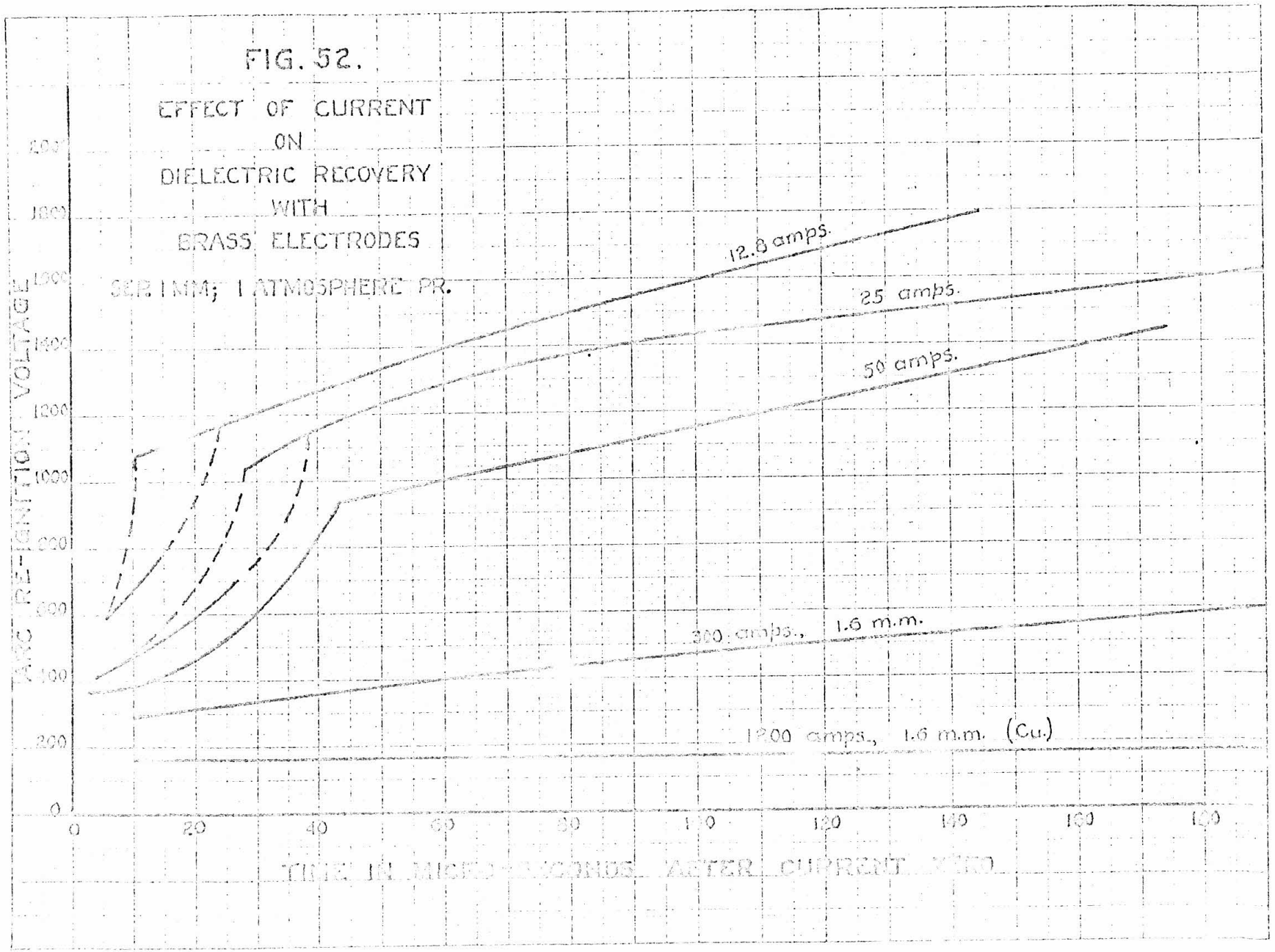
FIG. 52.
EFFECT OF CURRENT
ON
DIELECTRIC RECOVERY
WITH
BRASS ELECTRODES
SEP. 1 MM; 1 ATMOSPHERE PR.
ARC RE-IGNITION VOLTAGE
12.8 amps.
25 amps.
50 amps.
300 amps., 1.6 m.m.
1200 amps., 1.6 m.m. (Cu.)
0
200
400
600
800
1000
1200
1400
1600
1800
2000
0
20
40
60
80
100
120
140
160
180
TIME IN MICRO-SECONDS AFTER CURRENT ZERO

FIG. 53.

EFFECT OF CURRENT ON DIELECTRIC RECOVERY WITH BRASS ELECTRODES

SEP. 2.05 MM. 1 ATMOSPHERE PR.

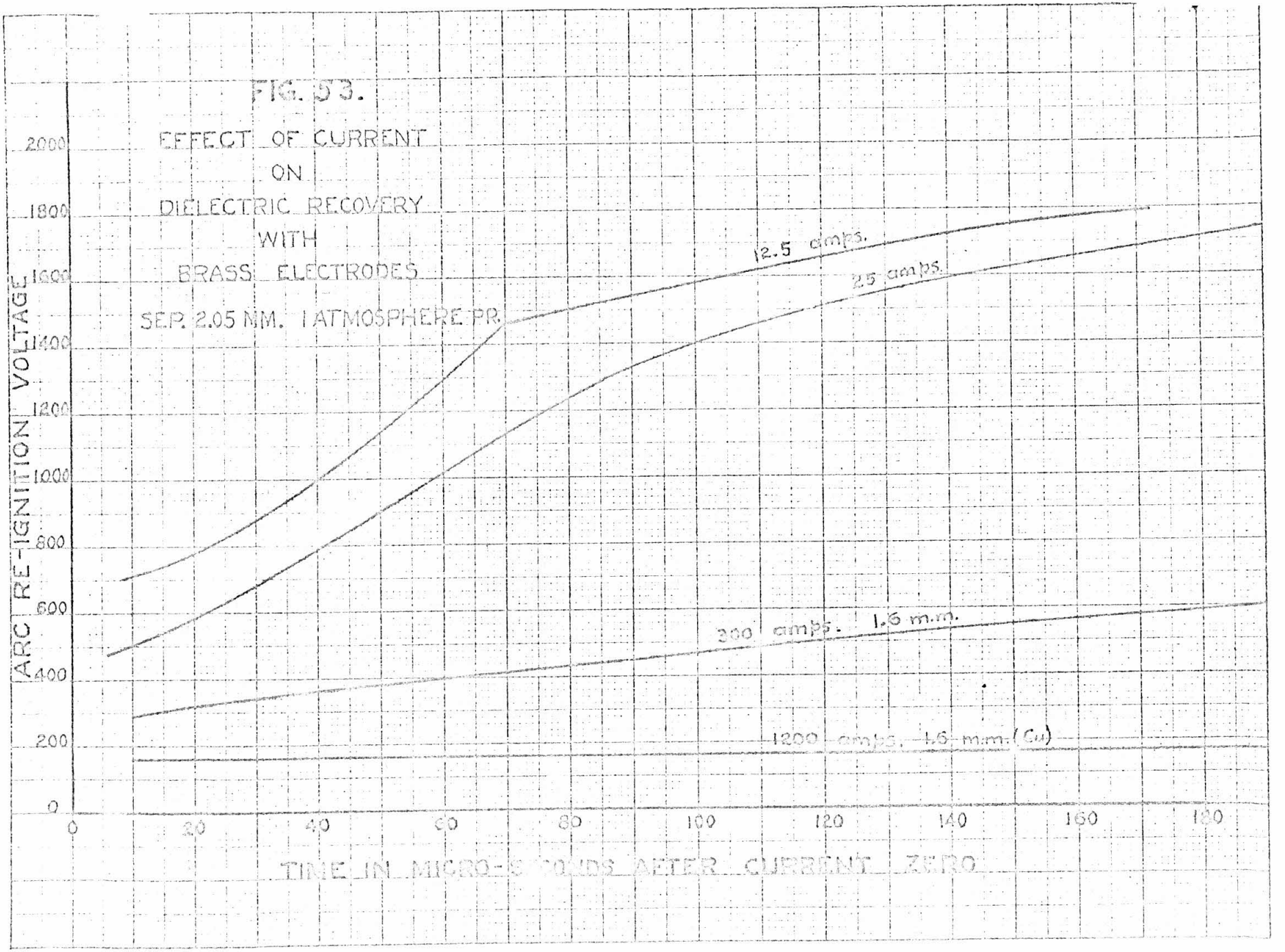

FIG. 54.

EFFECT OF CURRENT ON DIELECTRIC RECOVERY WITH BRASS ELECTRODES

SEP. 4.13 MM; 1 ATMOSPHERE PR.

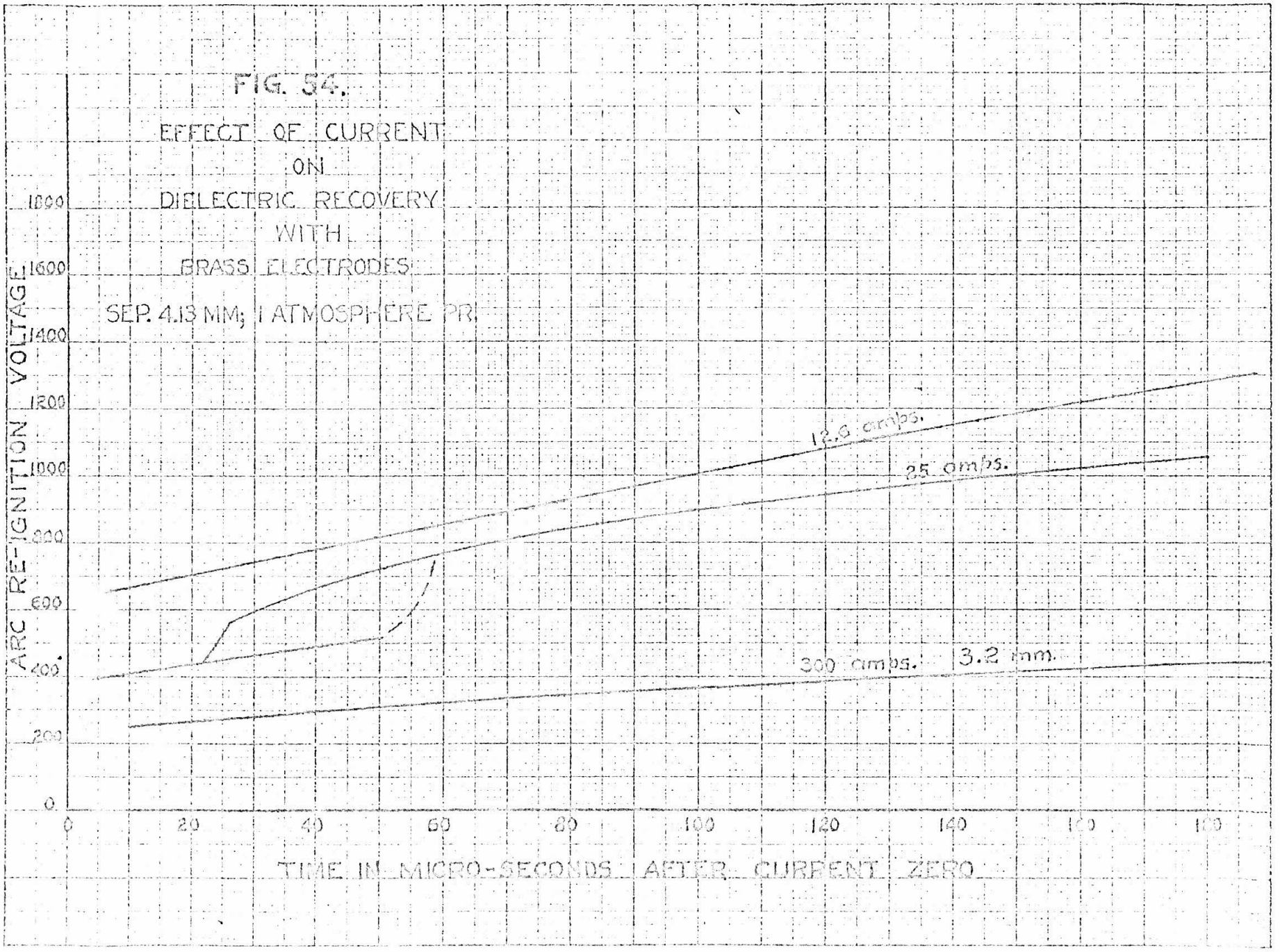

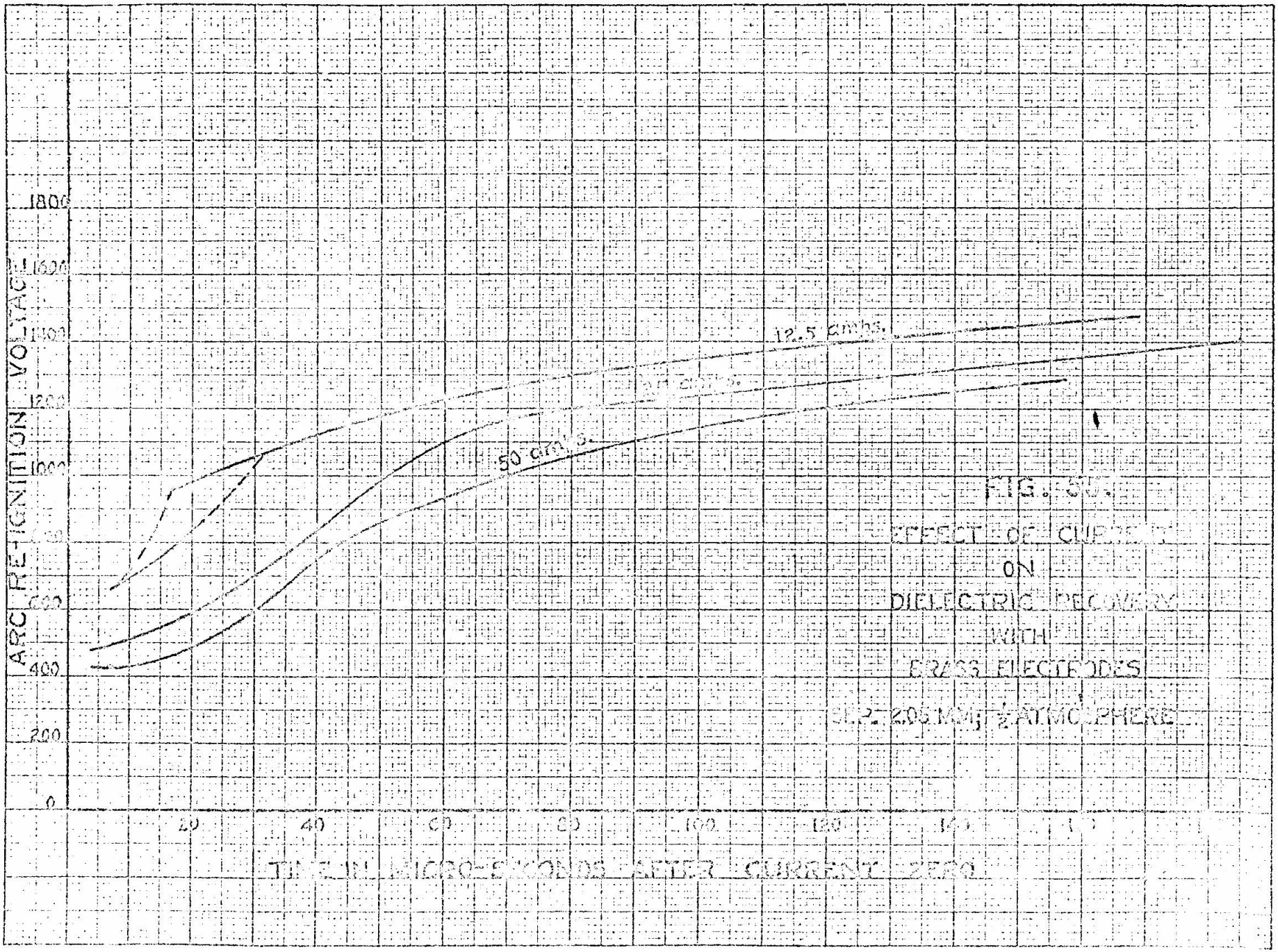

FIG. 5D.

EFFECT OF CURRENT
ON
DIELECTRIC RECOVERY
WITH
BRASS ELECTRODES
IN 2.2 MM. ARGON ATMOSPHERE.

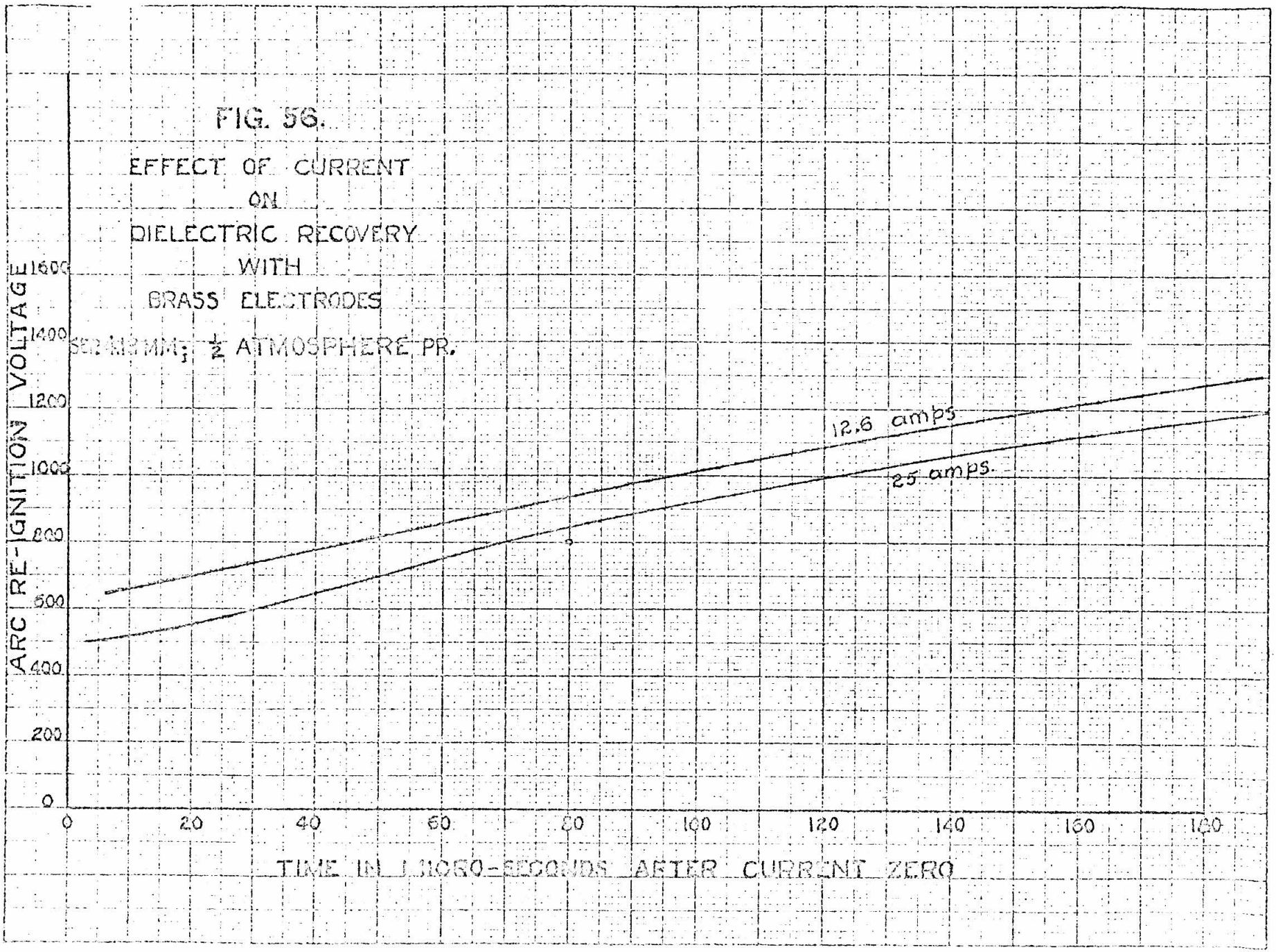
FIG. 56.
EFFECT OF CURRENT
ON
DIELECTRIC RECOVERY
WITH
BRASS ELECTRODES
5.82 M.M.; ½ ATMOSPHERE PR.
ARC RE-IGNITION VOLTAGE
1600
1400
1200
1000
800
600
400
200
0
12.6 amps
25 amps.
0
20
40
60
80
100
120
140
160
180
TIME IN MICRO-SECONDS AFTER CURRENT ZERO

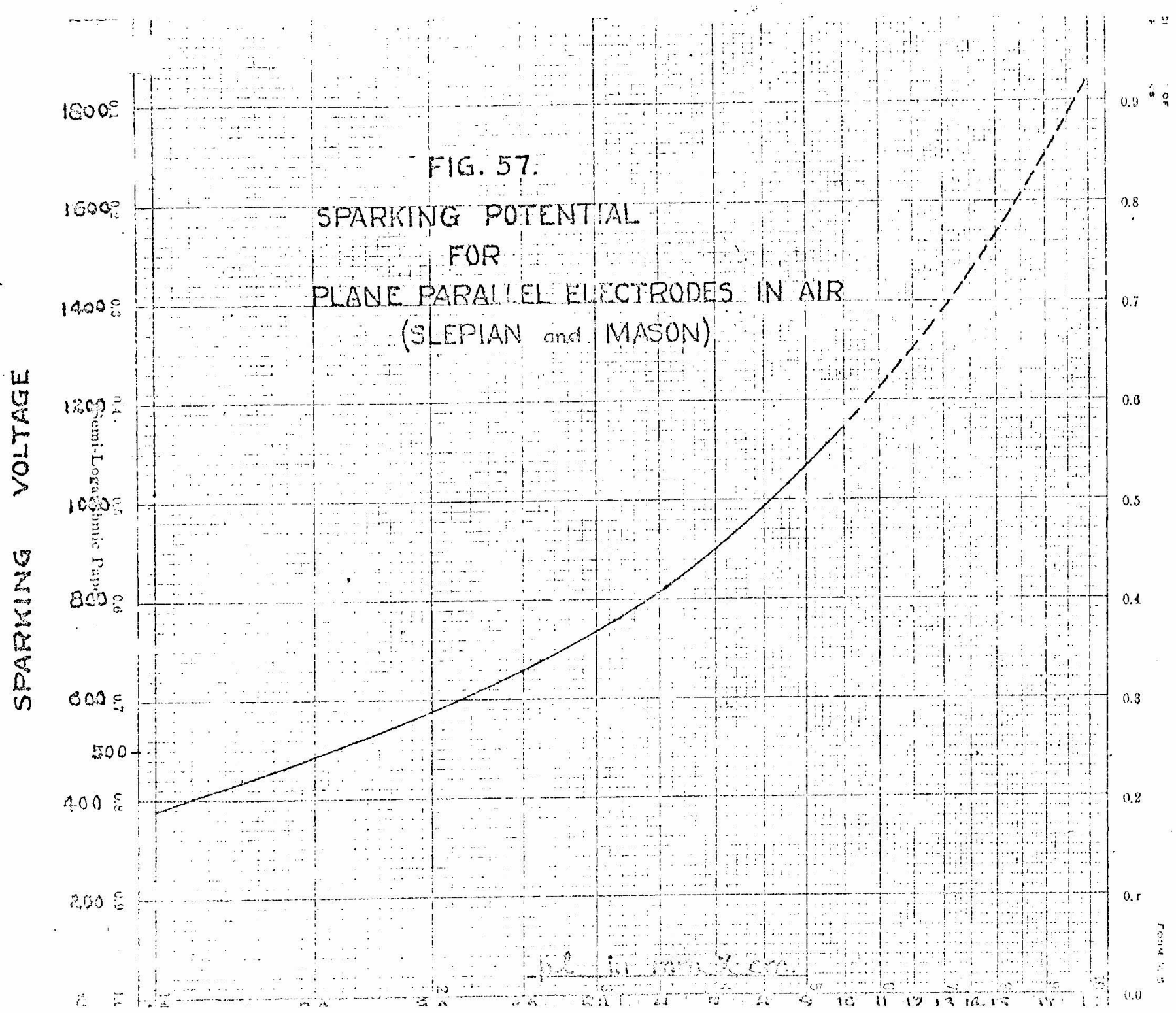
FIG. 57.
SPARKING POTENTIAL
FOR
PLANE PARALLEL ELECTRODES IN AIR
(SLEPIAN and MASON)
SPARKING VOLTAGE
1800
1600
1400
1200
1000
800
600
500
400
200
0.9
0.8
0.7
0.6
0.5
0.4
0.3
0.2
0.1
0.0

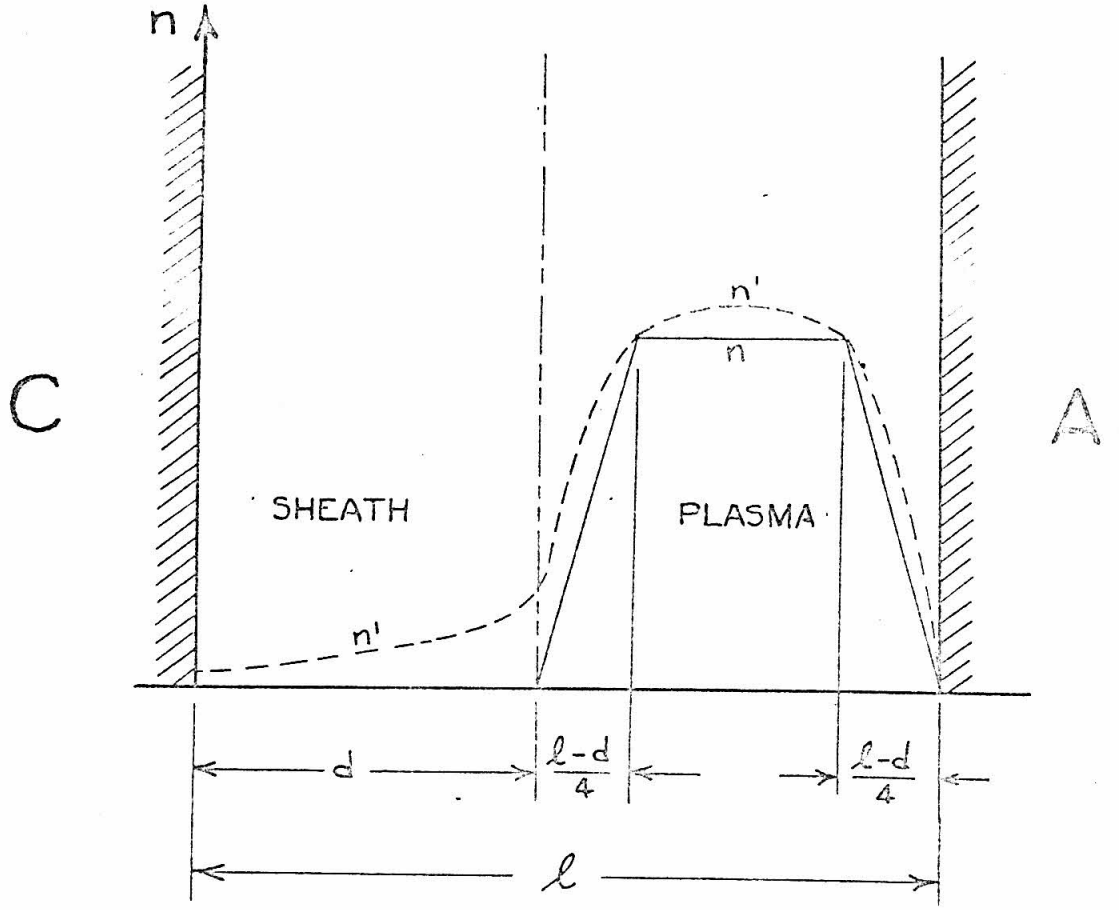

FIG. 58.

ASSUMED ION DISTRIBUTION
IN ARC SPACE

- FOR DIFFUSION CALCULATIONS